NASA CR-152319
BAC ER 14887

(NASA-CR-152319) PRSA HYDROGEN TANK THERMAL ACOUSTIC OSCILLATION STUDY Final Report (Beech Aircraft Corp.) 76 p HC A05/MF A01 CSCL 13G

N80-11470

Unclas
G3/37 40404

PRSA HYDROGEN TANK THERMAL ACOUSTIC OSCILLATION STUDY

Beechcraft

BEECH AIRCRAFT CORPORATION
BOULDER DIVISION

NASA CR-152319

BAC ER 14887

PRSA HYDROGEN TANK THERMAL ACOUSTIC OSCILLATION STUDY

September 1979

Prepared by
D. H. Riemer

Prepared for
NATIONAL AERONAUTICS AND SPACE ADMINISTRATION
AMES RESEARCH CENTER
MOFFETT FIELD
CALIFORNIA 94035

Prepared Under
Contract NAS 2-10229

Prepared by
Beech Aircraft Corporation
Boulder Division
Post Office Box 9631
Boulder, Colorado 80301

TABLE OF CONTENTS

PRECEDING PAGE BLANK NOT FILMED

LIST OF FIGURES

LIST OF FIGURES (Concluded)

LIST OF TABLES

FOREWORD

This study was performed by Beech Aircraft Corporation, Boulder Division, under NASA Contract NAS 2-10229. The funding of this contract was provided by NASA's Office of Aeronautics and Space Technology (OAST) through Ames Research Center (ARC). Mr. John Vorreiter was the ARC Technical Monitor.

Principal Investigator for this study was D. H. Riemer. W. L. Chronic assembled the test data on the Space Shuttle Power Reactant Storage Assembly Hydrogen Tank. G. L. Mills assisted in the reduction of the test data for use in the analytic model correlations.

All data are presented in the International System of Units as the primary system and English units as the secondary system. All calculations were done in English units and converted.

SUMMARY

The PRSA Thermal Acoustic Oscillation Study resulted in a review of existing test records, reduction of test data for use in the correlation of this data with the analytical predictions by Rott and Liburdy. The study presents 219 data points which are reduced to tabular form. Selected data points are compared to the prediction of the stability limit based on Rott's work.

The agreement between the analytical model and the test data was moderate for the supply line and poor for the fill and vent lines. The study points out some difficulties with attempting to utilize the idealized analytical model for a production supercritical hydrogen tank. The properties of supercritical hydrogen present problems in determining the appropriate values for the Prandtl number, the ratio of specific heats and the exponent for the power law viscosity curve used in the analytical model. Determining hot and cold fluid line lengths required for comparison with existing analytical models is a difficult task for a production cryogenic tank due to insufficient data on the line's temperature profile. The analytical models idealize the temperature profile as two constant temperature sections joined by a temperature jump where dT/dx is infinite. However, the relatively low steepness of the temperature jump existing in the PRSA fluid lines increases the uncertainty in predicting the stability limit. All of the above sources of difficulties contributed to the scatter in the data correlation.

NOMENCLATURE

a	Acoustic velocity
c	Kirchoff's constant
d	Kramer's constant
d^*	Stability constant
l_c	Tube length; cold end
L	Total tube length
P	Pressure
P_r	Prandtl number
r	Radial coordinate
r_o	Tube radius
S	Temperature profile steepness
t	Time
T	Temperature
u	Axial velocity component
v	Radial velocity component
X	Axial coordinate
Y	Magnitude of the ratio of tube radius to Stokes' boundary layer thickness

Greek Letters

α	Temperature ratio
β	Exponent in viscosity-temperature relationship
γ	Ratio of specific heats (C_p/C_v)
Γ	Mach number
ρ	Density
λ	Nondimensional frequency ($\frac{\omega l}{a}$)
μ	Dynamic viscosity
ν	Kinematic viscosity
ω	Frequency

Subscripts

c	Cold end value
h	Hot end value

1.0 INTRODUCTION

Thermally driven acoustic oscillations of the Space Shuttle Orbiter Power Reactant Storage Assembly (PRSA) Hydrogen Tank were first observed on September 27, 1977 during the first End-Item Acceptance Test (EIAT). The Beech Test Stop Notice (TSN) A02189 was written to document an out-of-tolerance condition involving a tank vent loss of 4.08 kg (8.99 lbs) for a 24-hour hold time. This loss was a factor of 10 greater than the allowable maximum of .36 kg (.81 lbs) for the 24-hour hold. The supply line oscillated at a frequency of 4.2 Hz with a pressure oscillation of 365 KPa (53 psia). The fill line was observed to oscillate predominately at 22 Hz at a pressure amplitude of 104 KPa (15 psia). The increased weight loss corresponds to an increased heat leak to the hydrogen tank of approximately 10 times the acceptable value.

This study was undertaken to review and assemble the test data that resulted from the three-month experimental investigation of the heat leak problem. The data presented in this study covers a period of time beginning September 29, 1977, when the pressure time histories were first recorded, through December 12, 1977. The final phase of the study was to correlate the reduced test data with current analytical models.

The PRSA Hydrogen Tank is a .32 m^3 (21.4 ft^3) spherical tank with one vapor-cooled shield (VCS) insulated from the outer shell and pressure vessel by multilayer insulation (MLI). Figure 1-1 contains a schematic of the PRSA Hydrogen Tank. A brief description of the flow paths for the fill, vent and supply lines is necessary for full appreciation of the thermal oscillation problem.

The supply line begins at the center of the pressure vessel and, upon exiting the pressure vessel, the supply line enters the line which makes up the VCS. The supply line passes through the VCS and exits the outer shell at the girth ring. The fill and vent lines are similar in flow path in that they both exit the top of the pressure vessel and exit the outer shell at the girth ring. The fill line extends from the top of the pressure vessel to the bottom while the vent line contains no significant line length internal to the pressure vessel. The external line configurations were varied throughout the testing and are discussed in Section 2.0.

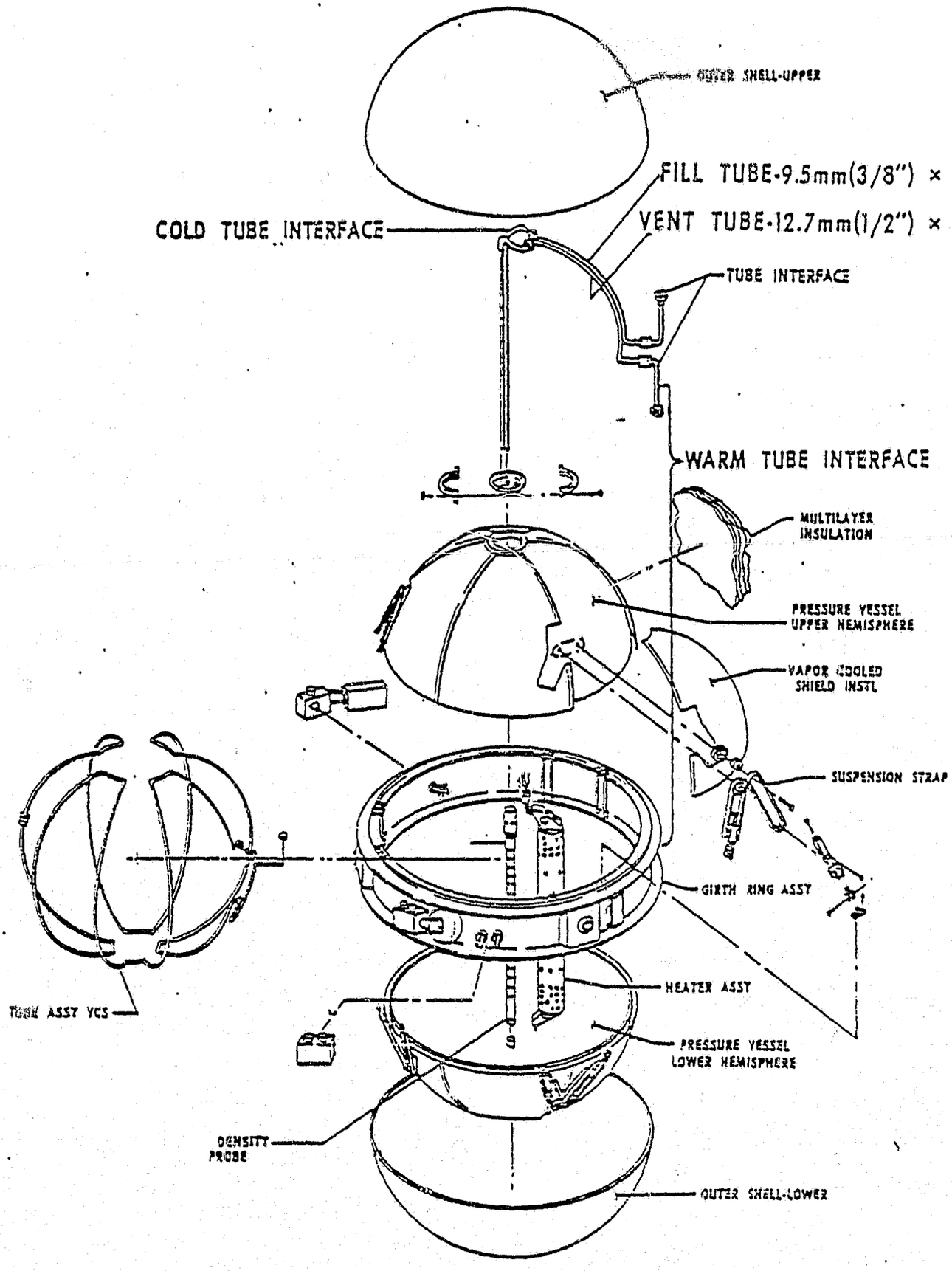

Figure 1-1 PRSA HYDROGEN TANK CONFIGURATION

2.0 TEST DATA REVIEW

In the course of determining a solution to the PRSA H_2 thermal acoustic oscillation problem, 17 hardware configurations have been identified. The configurations were examined under various operating conditions and tank orientations. All test data presented in Section 3.0 is related to these 17 configurations. Figures 2-1 through 2-17 contain the external flow diagrams for the 17 different configurations.

The test program covered approximately three months, beginning on September 28, 1977 and ending December 10, 1977. The objective of the test program was to determine a hardware fix to the thermal acoustic oscillation problem. This approach, which was proper at the time, creates several data gaps which represent significant problems in correlating this data. The data contains no information as to the temperature profile, a function of distance from the pressure vessel to the outer vacuum shell. In addition, the operating conditions do not vary sufficiently to allow for the determination of the effect of varying temperature ratios on the stability limit.

Beech and Rockwell technical advisors were monitoring the test efforts and directing flow network modifications. During the investigation, Rockwell personnel felt that a significant contribution to controlling the pressure oscillations could be made by insulating the flow lines and tank surfaces. Various insulation systems were tried but no significant, positive results could be observed. Calculations, at the time, indicated that a significant improvement in the oscillation problem could be realized by insulating the girth ring flow line interface. This interface was insulated during December 1977 and the current tank configuration still includes this insulation, while the fill line was always insulated to allow for tank loading. The vent and supply lines were not always insulated.

A positive control observation was made in the positioning of the fill, vent and supply valves. The valves can be adjusted either closed or open to effect a change in oscillation. By successive steps of experimental control, a determination was made that some restriction in the fill or supply line external to the tank would probably reduce the ill effects of thermal acoustic oscillation. Restrictions in the lines, in the form of washer-type orifices, were installed in various locations in the system. Some of the orifices caused such restriction that filling the tank could not be accomplished through the simulated Rockwell-insulated lines. A certain amount of control was apparent when alternate sized restrictions were installed in any one configuration and operating

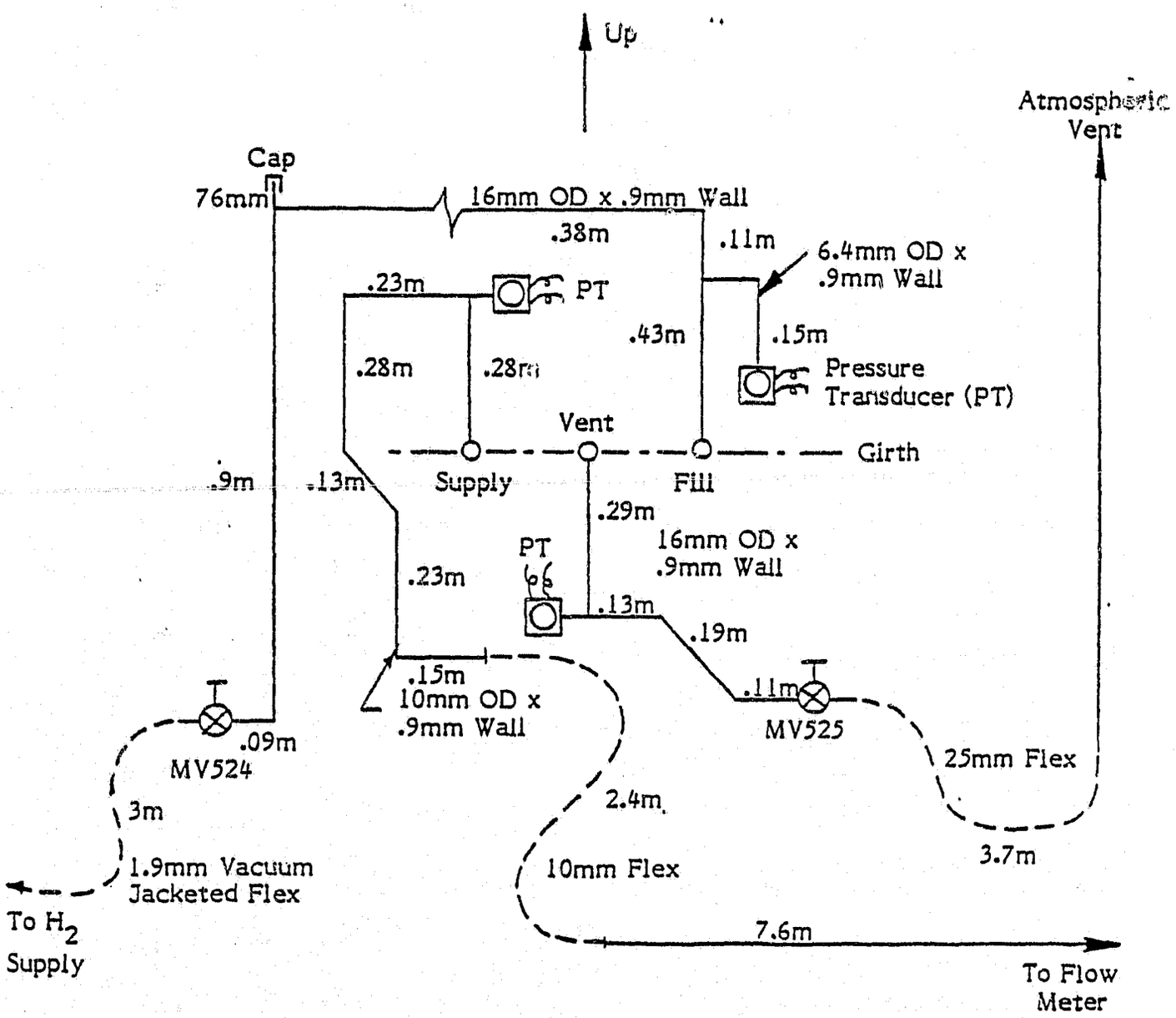

Figure 2-1 END-ITEM ACCEPTANCE TEST (EIAT) FOR SEPTEMBER 28 TO OCTOBER 3, 1977

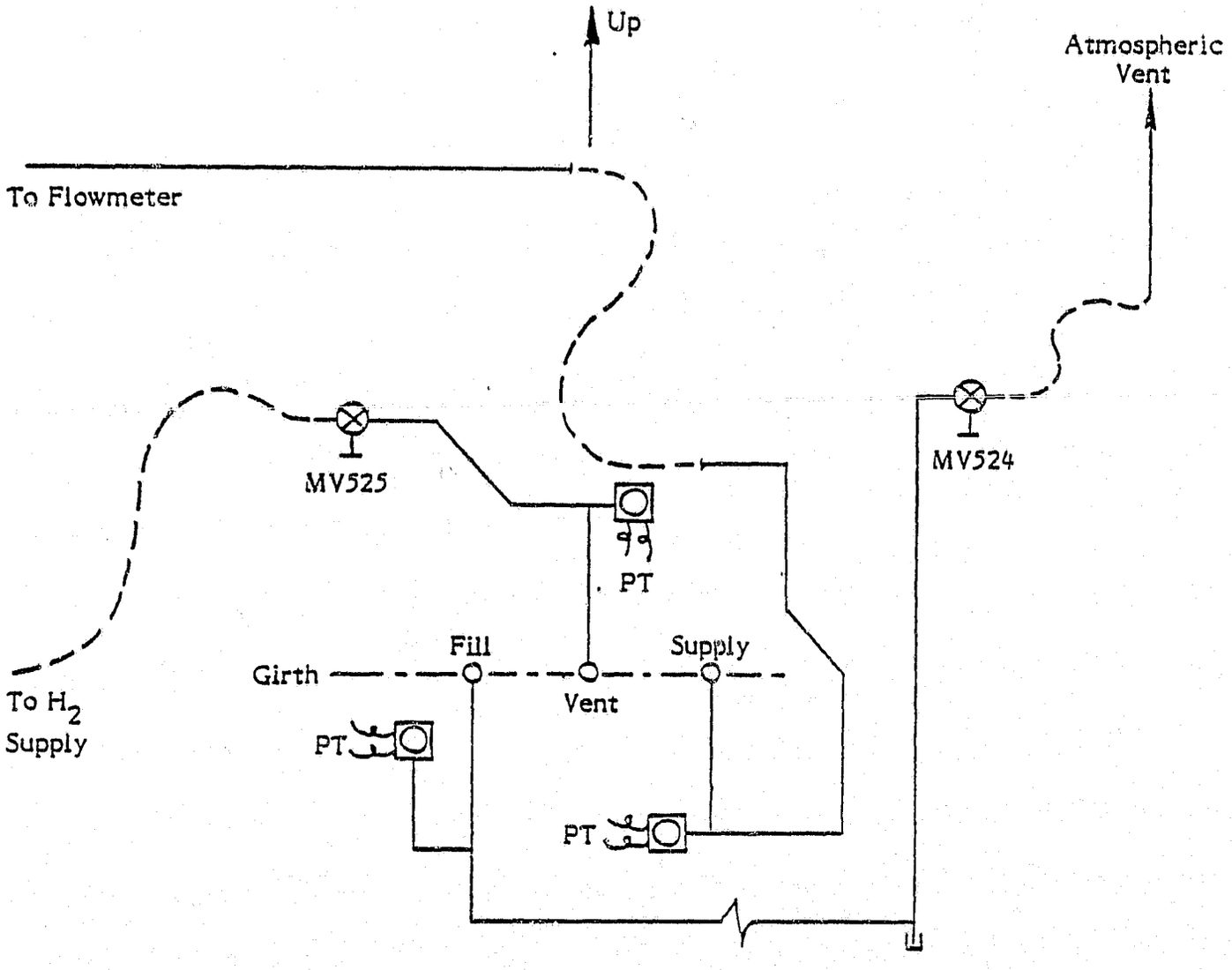

NOTE: Line lengths are given in Figure 2-1

Figure 2-2 INVERTED END-ITEM ACCEPTANCE TEST FOR OCTOBER 4 TO OCTOBER 10, 1977

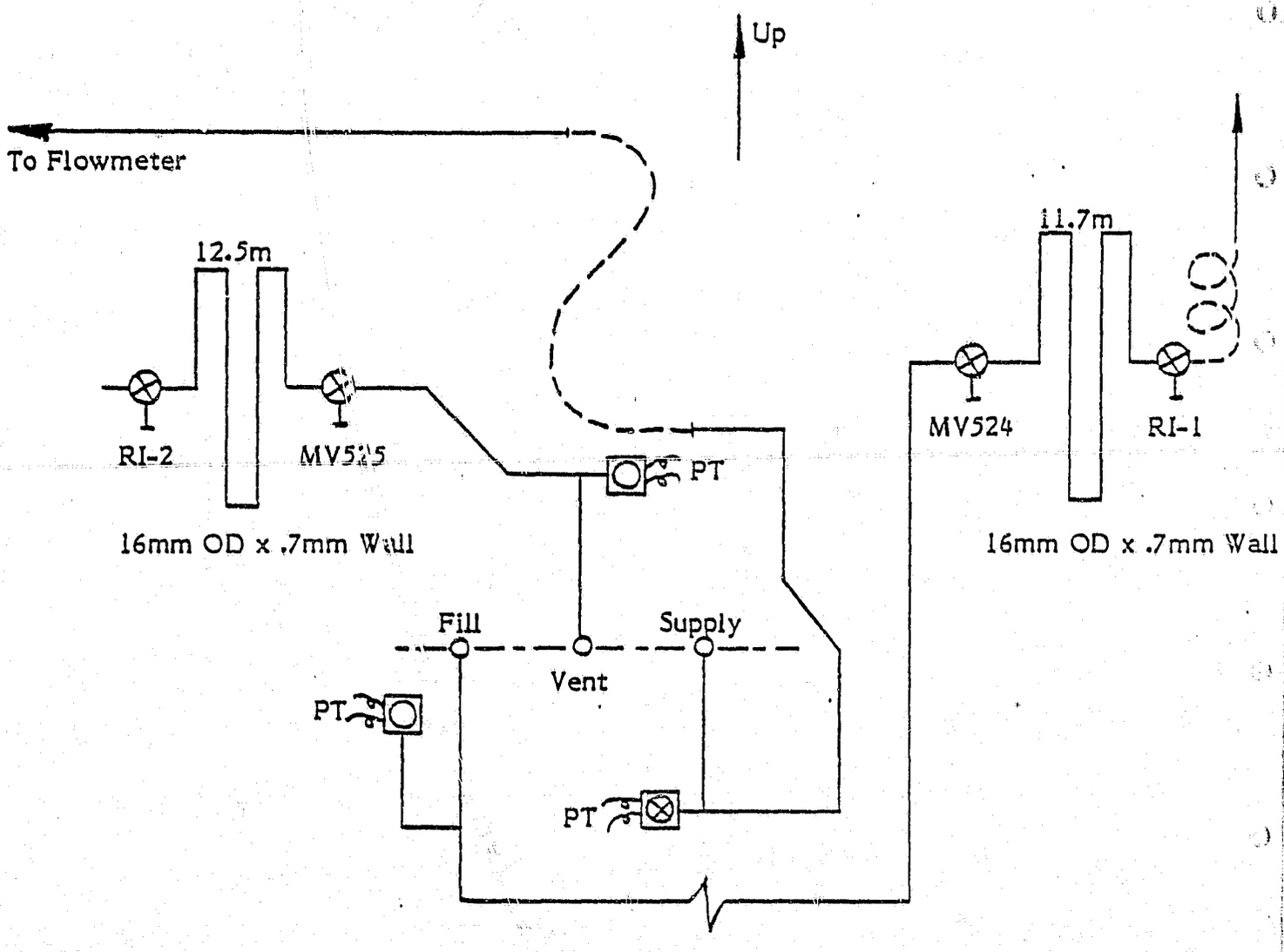

NOTE: Line lengths are given in Figure 2-1

Figure 2-3 INVERTED END-ITEM ACCEPTANCE TEST FOR OCTOBER 11 TO OCTOBER 17, 1977

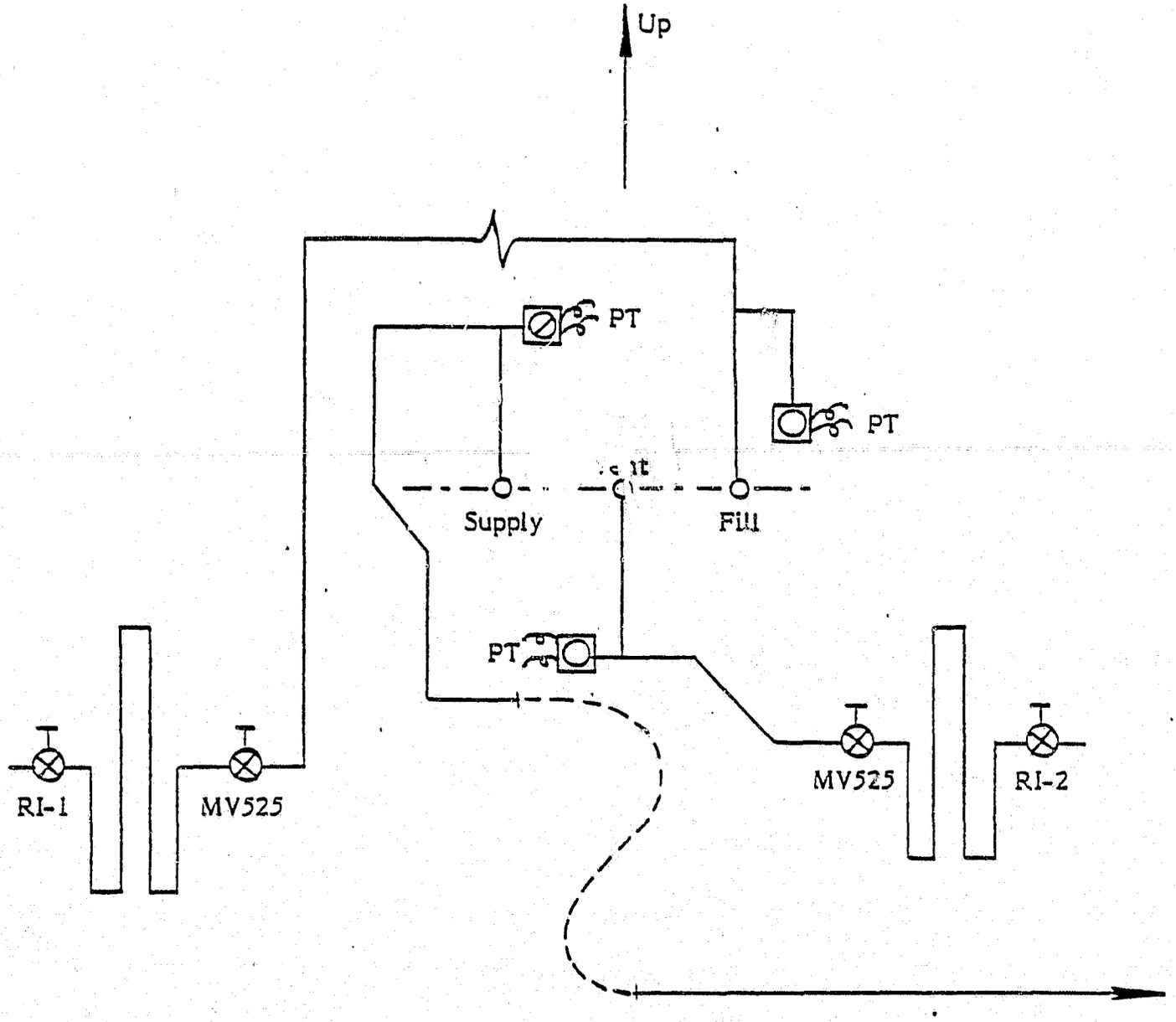

NOTE: Line lengths are given in Figure 2-1

Figure 2-4 ROCKWELL INSULATED LINES, OCTOBER 17, 1977

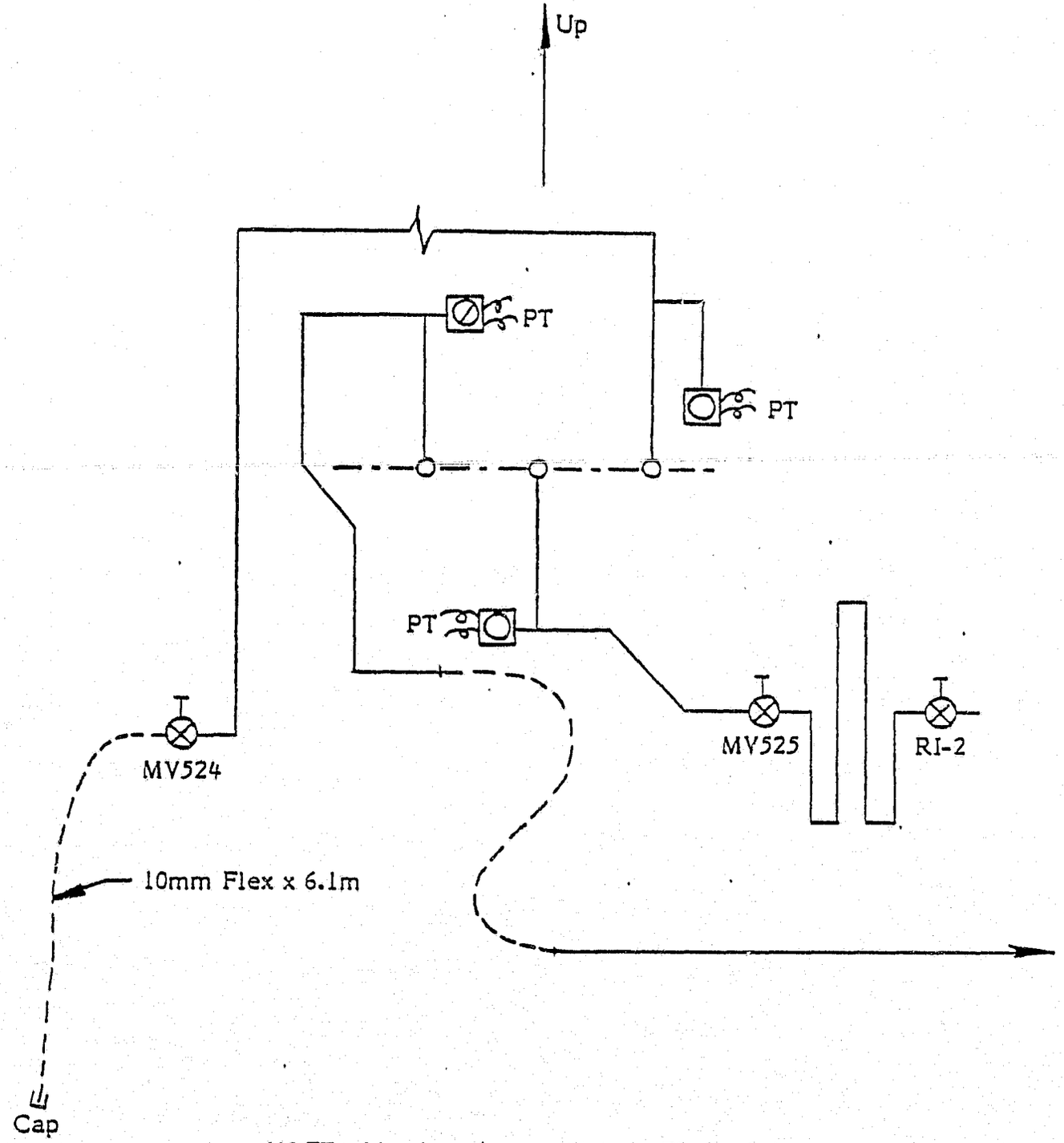

NOTE: Line lengths are given in Figure 2-1

Figure 2-5 PRSA TANK CONFIGURATION FOR OCTOBER 18, 1977 AT 1500 HOURS, 6m FLEX LINE ON FILL

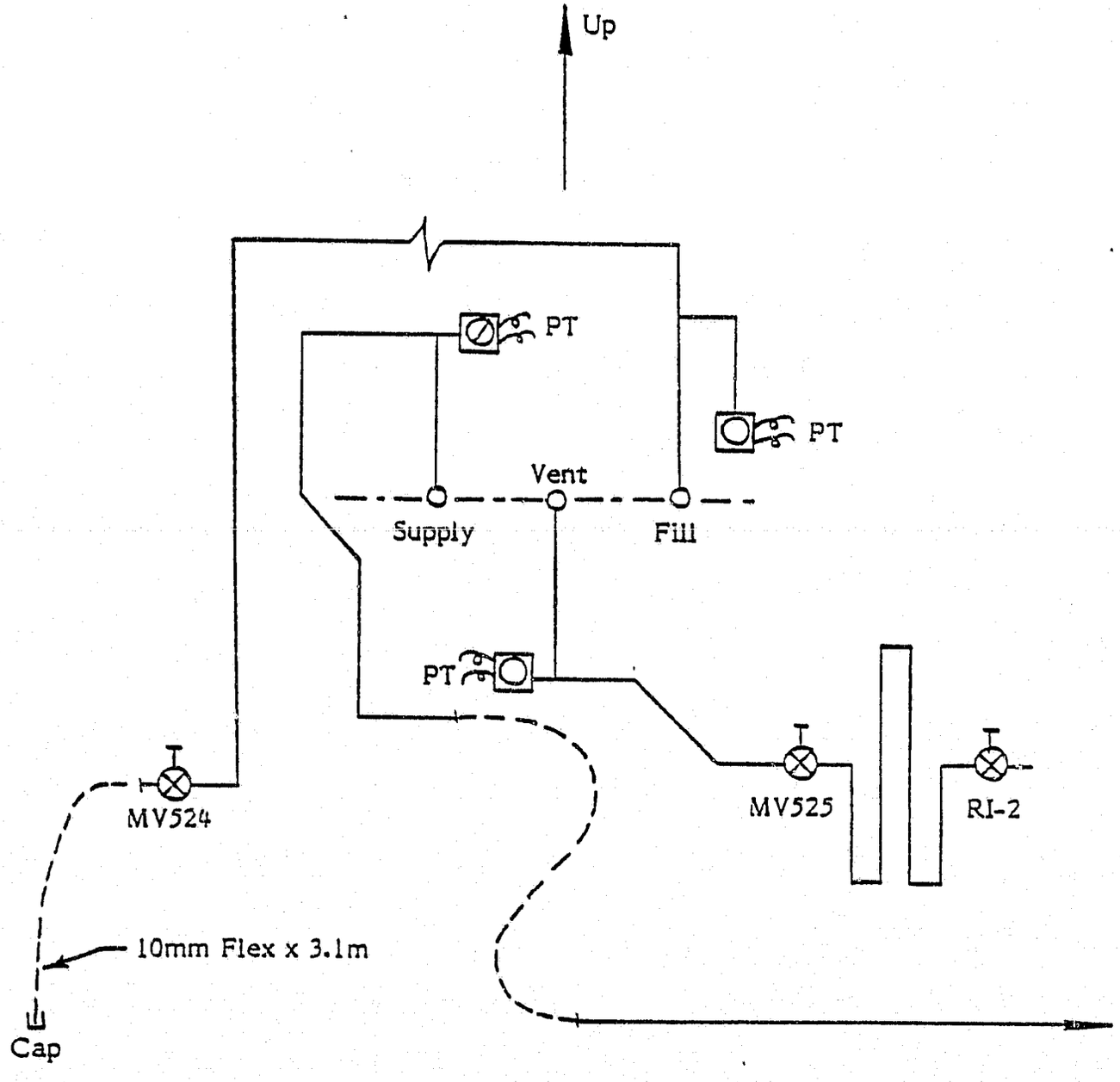

NOTE: Line lengths are given in Figure 2-1

Figure 2-6 PRSA TANK CONFIGURATION FOR OCTOBER 18, 1977 AT 2230 HOURS, 3m FLEX LINE ON FILL

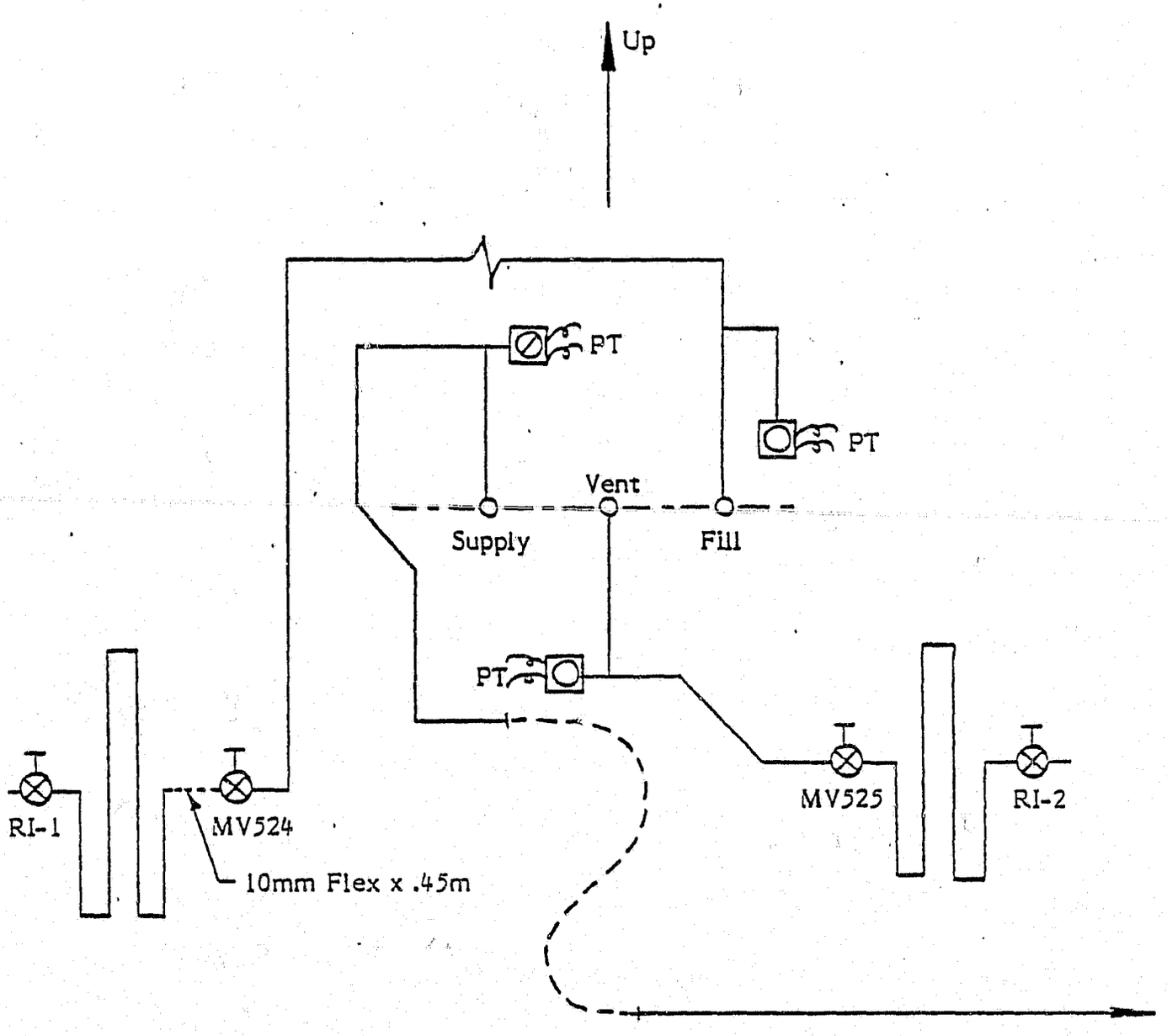

NOTE: Line lengths are given in Figure 2-1

Figure 2-7 PRSA TANK CONFIGURATION FOR OCTOBER 20, 1977, .46m FLEX LINE BETWEEN ROCKWELL LINE AND FILL LINE

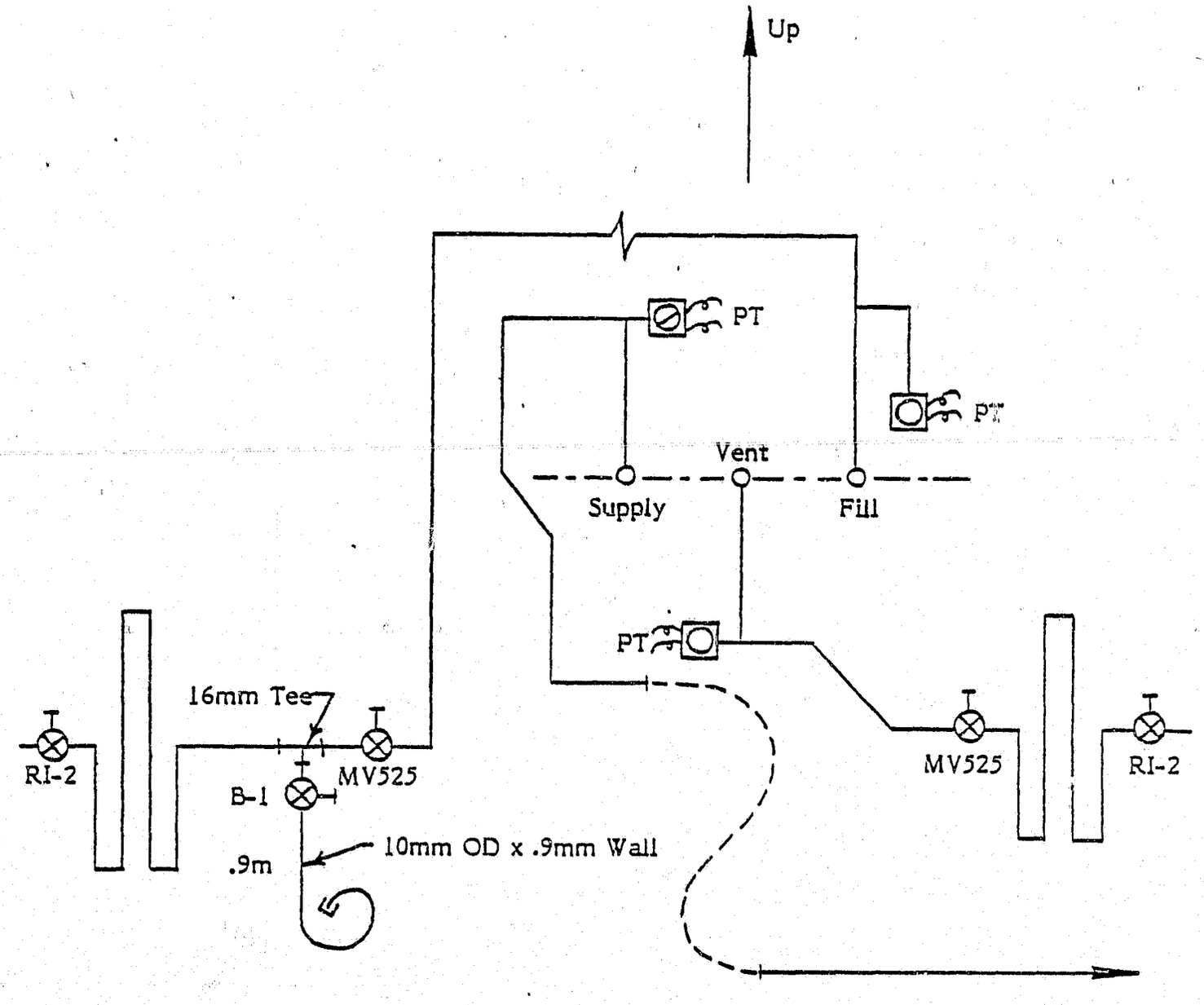

Figure 2-8 PRSA TANK CONFIGURATION FOR OCTOBER 21, 1977 AT 1500 HOURS WITH 10mm x .9m EXTERNAL VOLUME IN FILL LINE

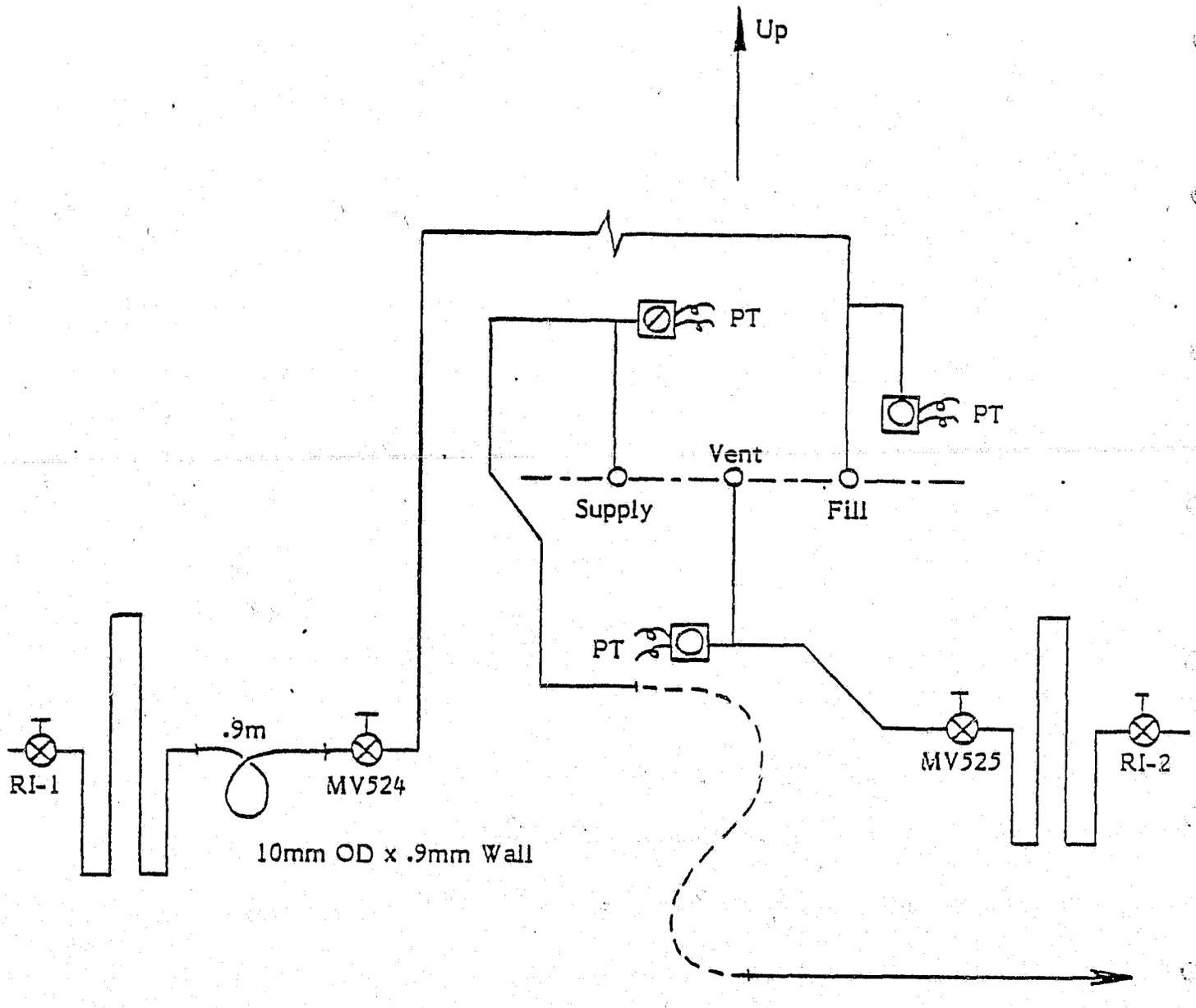

Figure 2-9 PRSA TANK CONFIGURATION FOR OCTOBER 22, 1977 AT 1500 HOURS, 10mm x .9m ADDITIONAL VOLUME IN FILL LINE

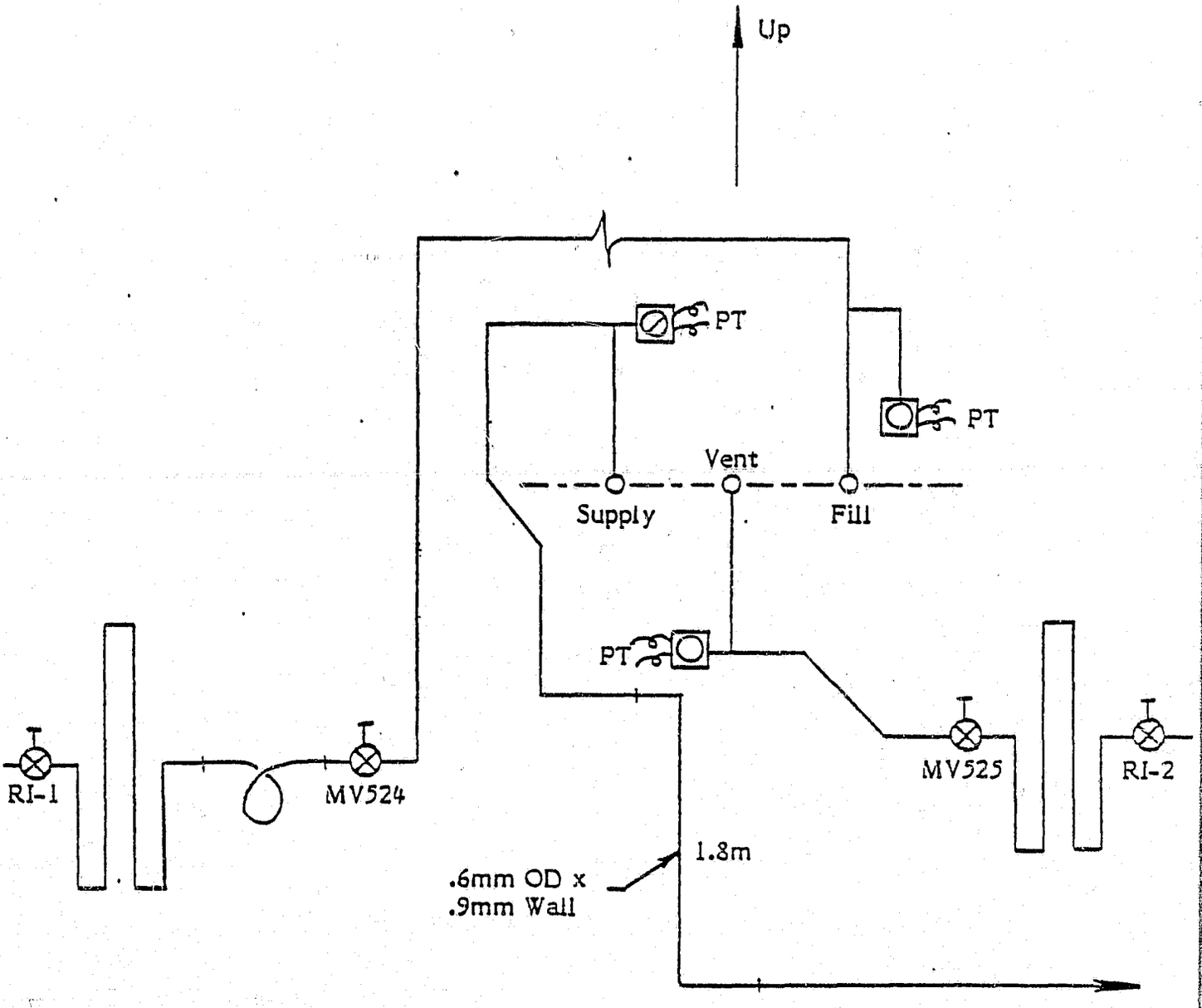

NOTE: Line lengths are given in Figure 2-1

Figure 2-10 PRSA TANK CONFIGURATION FOR OCTOBER 25, 1977 AT 1241 HOURS, HARD LINE REPLACES FLEX TUBE IN SUPPLY LINE

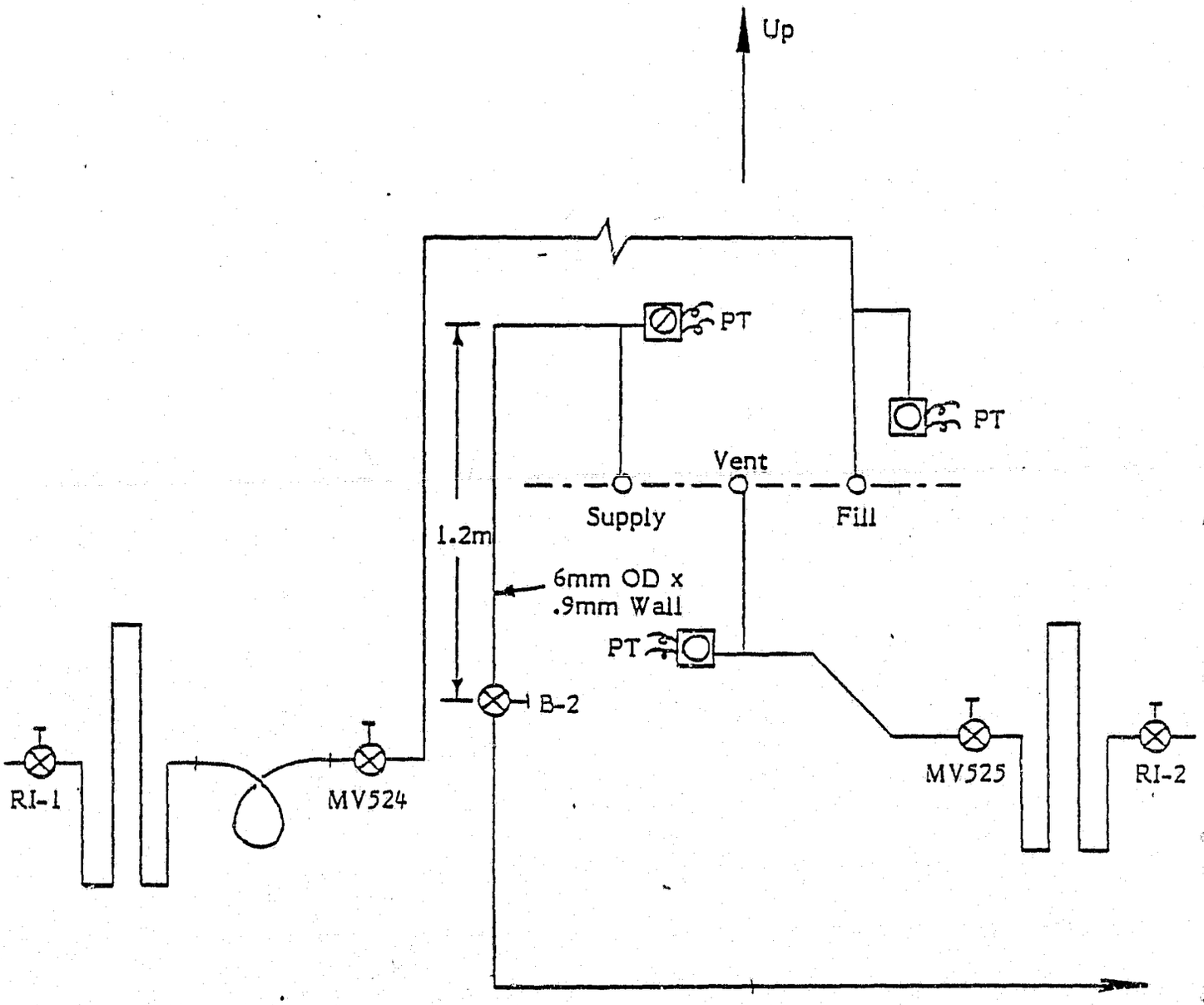

NOTE: Line lengths are given in Figure 2-1

Figure 2-11 PRSA TANK CONFIGURATION FOR OCTOBER 26, 1977 AT 2205 HOURS, ADDITIONAL VALVE PLACED IN SUPPLY LINE

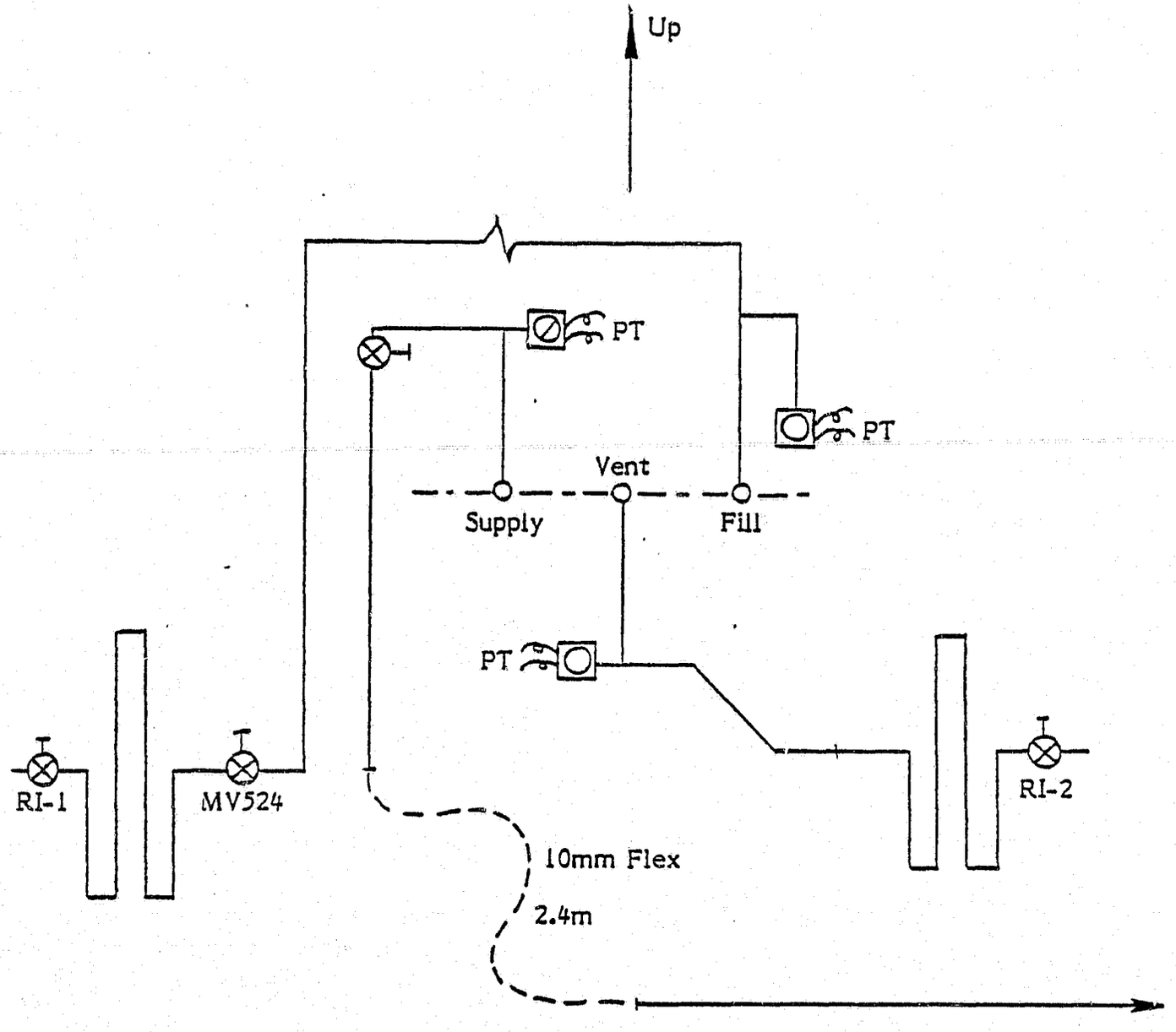

NOTE: Line lengths are given in Figure 2-1

Figure 2-12 PRSA TANK CONFIGURATION FOR OCTOBER 31, 1977 AT 1600 HOURS, REMOVED MV525 FROM VENT LINE AND ADDED FLEX LINE TO SUPPLY

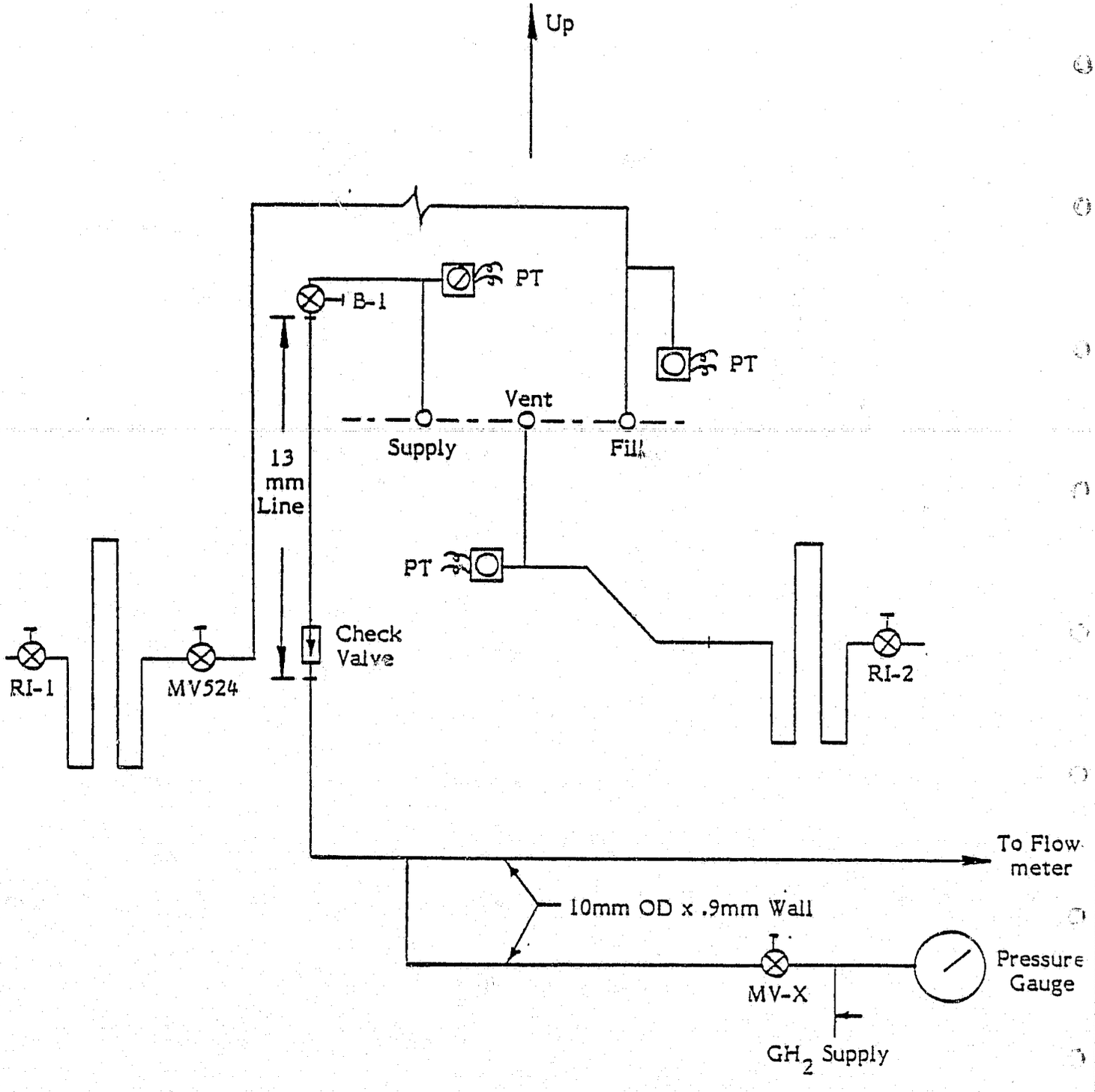

Figure 2-13 PRSA TANK CONFIGURATION FOR NOVEMBER 2, 1977, ROCKWELL INSULATED LINES

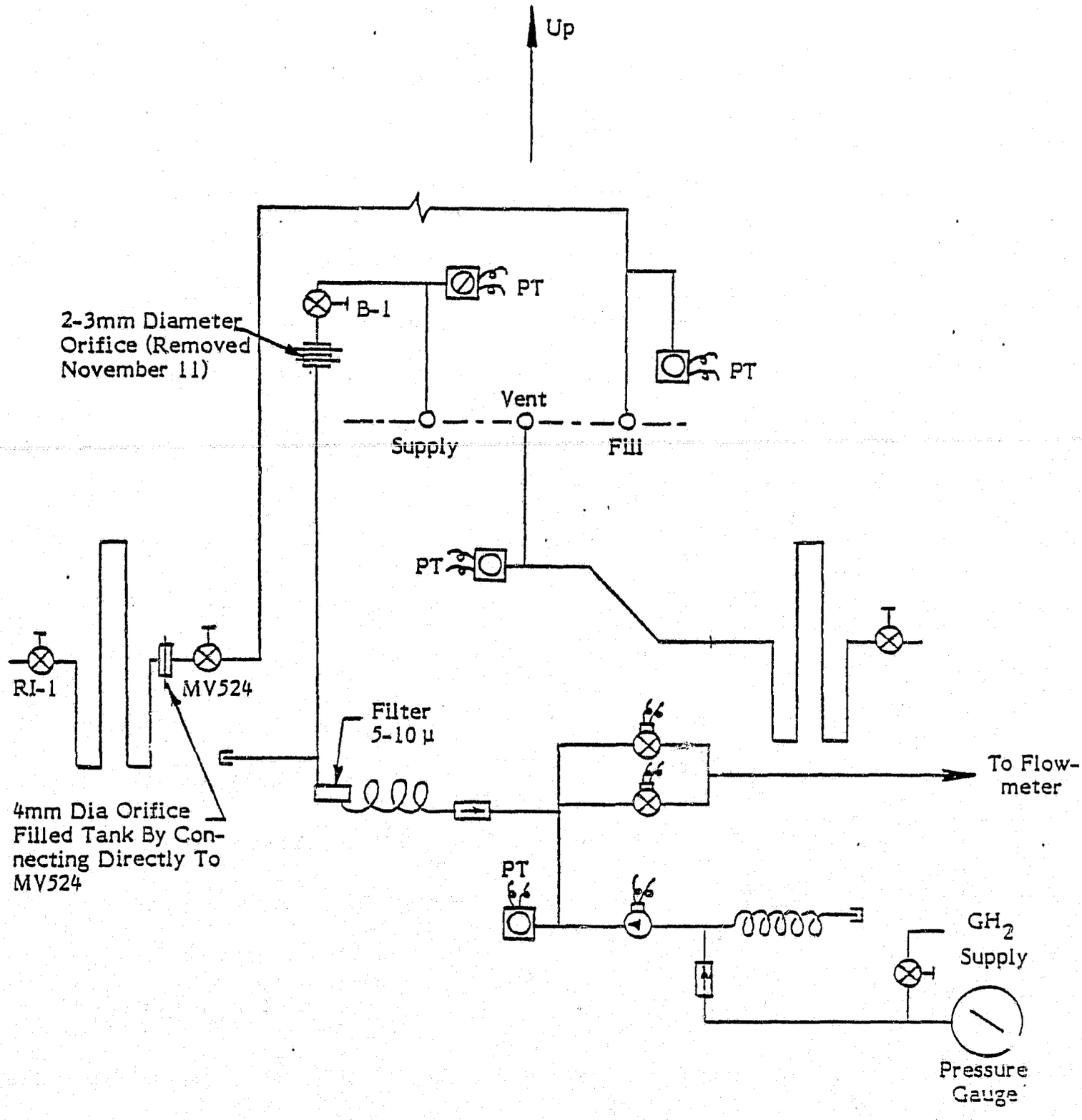

Figure 2-14 PRSA TANK CONFIGURATION FOR NOVEMBER 5 TO NOVEMBER 11, 1977

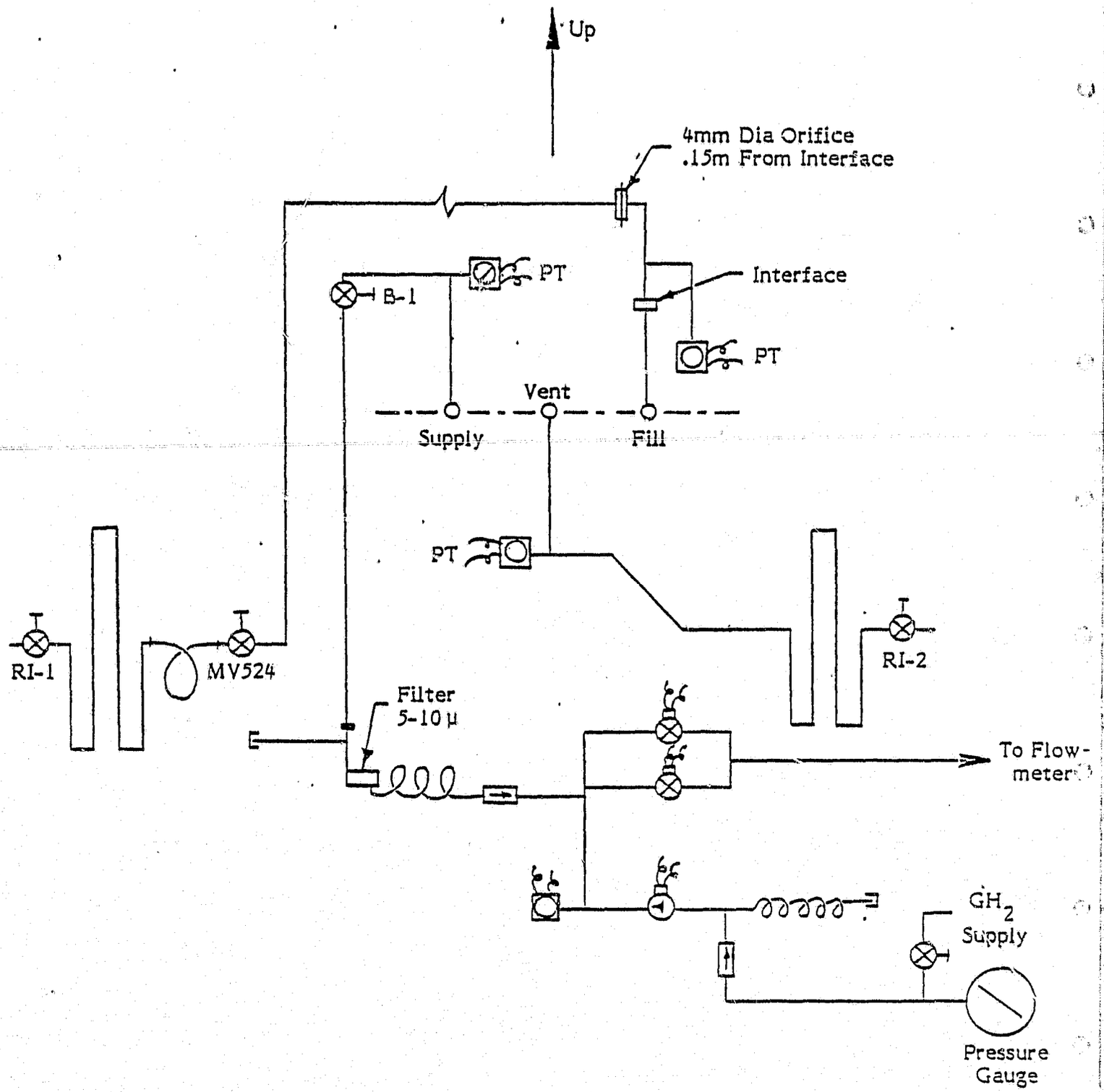

Figure 2-15 PRSA TANK CONFIGURATION FOR NOVEMBER 21, 1977

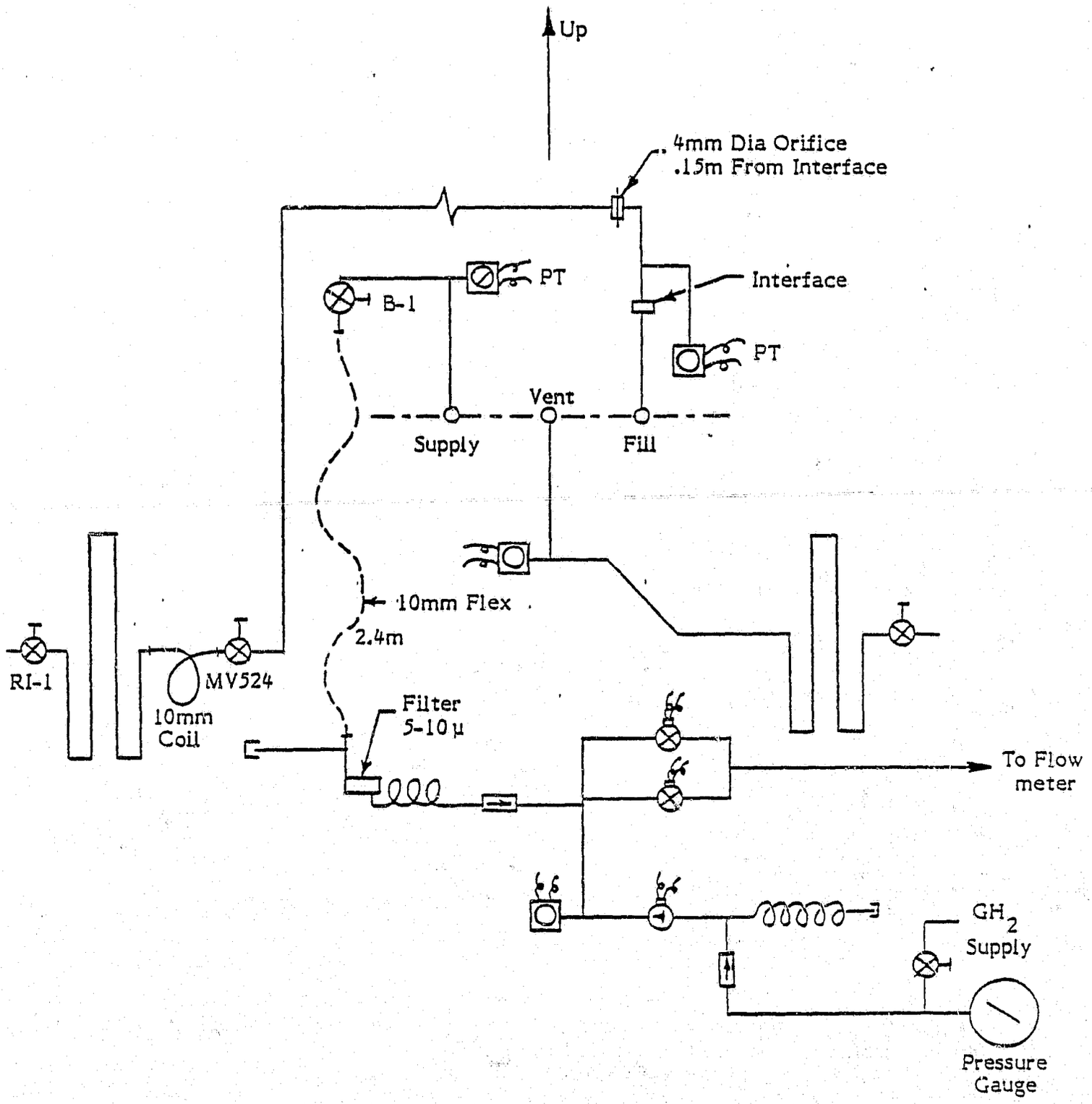

Figure 2-16 PRSA TANK CONFIGURATION FOR NOVEMBER 22, 1977

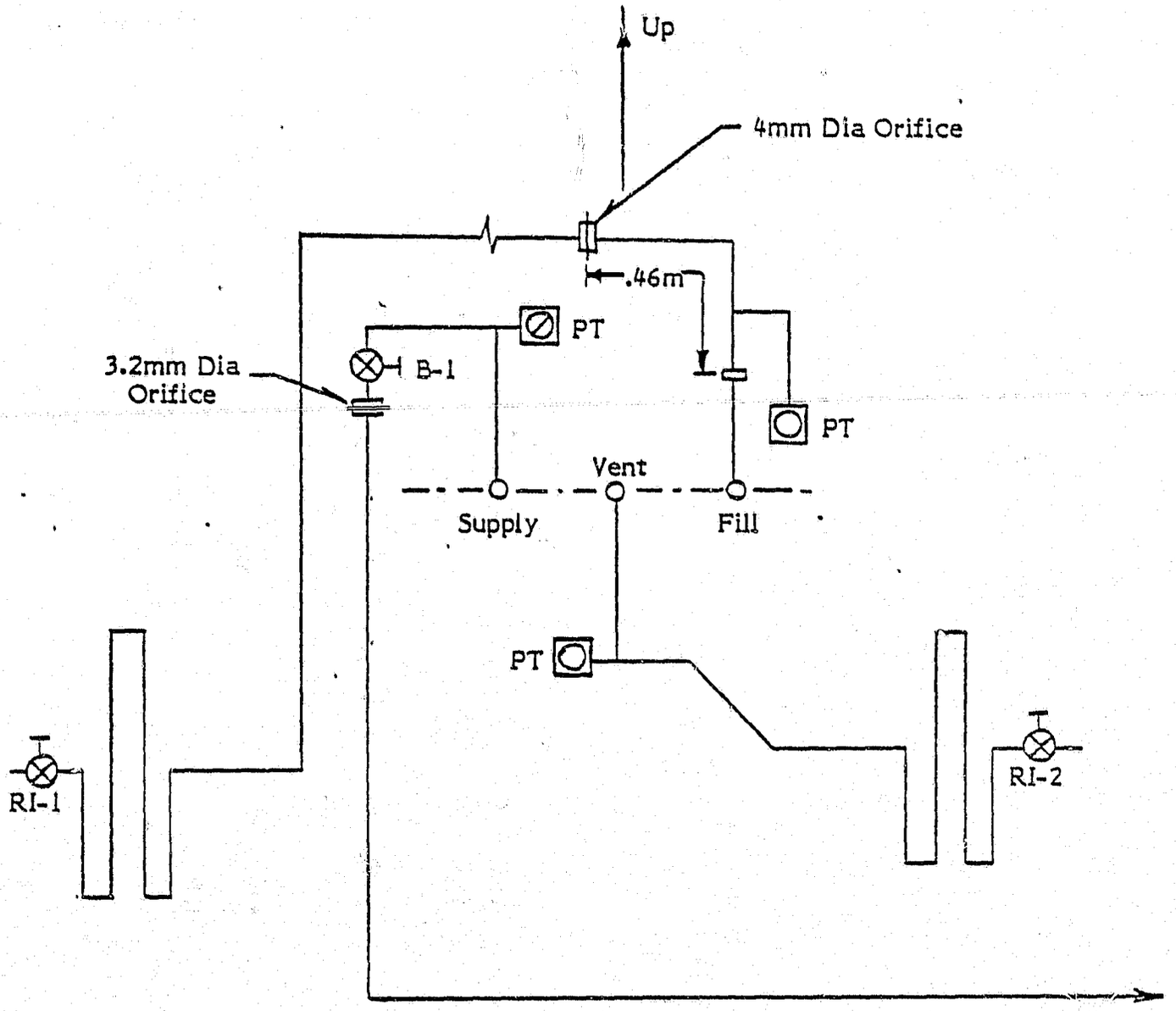

Dec. 7 3mm dia replaced with 3.6mm - 3.8mm, which increased the oscillating pressure. Installed 2mm dia (1251 - 1615 hours).
Dec. 9 (0345 hours) Installed 5mm dia in fill line.
Dec. 13 Fill line orifice changed to 4.4mm dia → 3.8mm dia.

Figure 2-17 PRSA TANK CONFIGURATION FOR DECEMBER 6 TO DECEMBER 13, 1977

condition. The most successful restriction appeared to be a 4.39 mm (0.173 in.) diameter orifice in the fill line close to the tank interface. However, this has not proved to be a definite solution. It should be noted that the line with the greatest tendency toward oscillation was the fill line, even though at times it could be stopped completely. The fill line oscillated predominately in the range of frequencies from 20 Hz to 30 Hz at a pressure amplitude of 20 KPa (3 psia) to 50 KPa (7 psia). The supply line displayed a different frequency of between 1.6 Hz and 4.6 Hz and amplitude. The vent line rarely displayed any oscillation.

The test data review consisted of collecting pressure trace data records and the corresponding test data log entries. The data for this study was selected in an attempt to collect a number of various tank operating conditions. It must be realized that the tests were conducted to find a solution to the thermal oscillation problem. This results in very limited tank operating conditions. The ratio of hot to cold temperatures only vary from 7.0 to 12.2, while flow rates varied in general from 0. kg/sec to 1.7 kg/sec. This limited variance on the critical thermal acoustic oscillation parameters is unfortunate. The test data was chosen to show the effect of valve opening and closing. The opening or closing of a valve generates a change in the fluid velocity from the steady state condition. This velocity change is accompanied by pressure change proportional to the velocity change. This effect is known as "waterhammer." This pressure transient which travels at the acoustic velocity of the fluid is damped by fluid viscous forces. This pressure perturbation was, in most cases, followed by the steady pressure oscillations attributed to thermal acoustic effects.

3.0 TEST DATA REDUCTION

As discussed in Section 2.0, 17 different hardware configurations were identified. The data collected for these configurations resulted in 219 data points. These data points represent different flow rates, internal or external temperatures, valve positions and orifice location and size. The data was collected from the pressure traces and Beech Engineering Test Log data contained in Beech Memorandum Report 14895. The pressure traces supplied the oscillation frequency and amplitude. In addition, tank temperature, environmental temperature, mass flow rate, configuration and valve positions were also determined from test logs. The reduced data is presented in Table 3-I for all 219 data points. Table 3-I contains the test purpose, configuration correlated to Figures 2-1 through 2-17, line (supply, fill or vent), environmental temperature, internal tank temperature, and oscillation frequency and amplitude. In addition, the acoustic velocity (a_c) and kinematic viscosity (ν_c) for the internal tank temperature are given. The thermal acoustic oscillation parameter Y_c, which is defined as $r_o (\omega/\nu_c)^{1/2}$ has been calculated for all data points. The meaning of Y_c with regard to predicting thermal acoustic oscillations is saved for Section 4.2. Table 3-I also contains notes indicating valve positions. In general, the valve is closed unless otherwise indicated. The last column of Table 3-I was used to indicate secondary modes of oscillation by including the secondary frequency and amplitude. This table contains the data necessary to correlate the PRSA Hydrogen Tank data with existing analytical models.

The effect on several critical parameters of thermal acoustic oscillations may be seen from Table 3-I. The first set of points of interest are points 7 and 8 of Table 3-I. Data point 7 indicates that the supply line oscillates at a frequency of 24 Hz for a temperature ratio of 9.6. This oscillation occurs with valve MV-525 (see Figure 2-2) closed while data point 8 indicates no oscillations for similar operating conditions, with the exception of valve MV-525 in the open position. While the oscillation is occurring in the fill line, MV-525 is located in the vent line.

A similar effect is illustrated by data points 11 and 12. In this case, the fill line is stable when oscillations occur. For thermal acoustic oscillation to begin, some small perturbation is required. In the first example, it is thought that the opening of MV-525 provided the required perturbation. In the second example, some small change in tank operating conditions may have initiated the oscillations.

TABLE 3-I PRSA HYDROGEN TANK THERMAL ACOUSTIC OSCILLATION DATA

Data Point	Purpose of Test	Tank, Line and Valve Configuration (See Figure 2-)	Tank Pressure (KPa)	Line	Mass Flow (Kg/hr)	T_{hot} (^{o}K)	T_{cold} (^{o}K)	α	ν_c m^2/sec x10^{-7}	a_c (m/sec)	Y_c	Oscillation Frequency (Hz)	Oscillation Peak-to-Peak Pressure (KPa)	Notes
1	Preparation for Minimum dQ/dM	1	1947	Supply	0.0637	317.2	41.61	7.6	1.70	504	48.0	4.2	365*	
2	Minimum dQ/dM	1	1951	Supply	0.0582	319.4	40.81	7.8	1.57	492	49.0	4.0	365*	
3	24-Hour Hold, Inverted	2	1931	Supply	0.0786	317.2	28.89	11.0	1.36	926	38.0	2.1	104	
4	24-Hour Hold, Inverted	2	1931	Fill	0.0	317.2	28.89	11.0	1.36	926	223.0	21.6	104	†.0519 Hz 282 KPa
5	24-Hour Hold, inverted	2	1931	Vent	0.0	317.2	28.89	11.0	1.36	926	-	0.0	-	
6	Heater Depletion, Inverted	2	1931	Supply	1.6627	317.5	33.22	9.6	1.16	683	44.0	2.4	21	
7	Heater Depletion, Inverted	2	1931	Fill	0.0	317.5	33.22	9.6	1.16	683	254.0	24.0	103	
8	Heater Depletion, Inverted	2, MV-525 Opened	1931	Fill	0.0	317.5	33.22	9.6	1.16	683	-	0.0	-	
9	Heater Depletion, Inverted	2	1931	Vent	0.0	317.5	33.22	9.6	1.16	683	-	0.0	-	
10	Preparation for Minimum dQ/dM	2	1913	Supply	.0116	316.6	36.95	8.6	1.21	456	-	0.0	-	
11	Preparation for Minimum dQ/dM	2	1913	Fill	0.0	316.6	36.95	8.6	1.21	456	-	0.0	-	
12	Preparation for Minimum dQ/dM	2	1913	Fill	0.0	316.6	36.95	8.6	1.21	456	291.7	32.9	100	
13	Preparation for Minimum dQ/dM	2	1913	Vent	0.0	316.6	36.95	8.6	1.21	456	-	0.0	-	
14	24-Hour Hold	3	1448	Supply	0.0	314.3	25.67	12.2	1.55	1048	40.7	4.0	91	
15	24-Hour Hold	3	1448	Fill	0.0	314.3	25.67	12.2	1.55	1048	189.9	17.9	191	
16	24-Hour Hold	3	1448	Fill	0.0	314.3	25.67	12.2	1.55	1048	195.6	19.1	114	†.06 Hz 245 KPa
17	24-Hour Hold	3	1448	Vent	0.0	314.3	25.67	12.2	1.55	1048	-	0.0	-	
18	24-Hour Hold	3	1931	Supply	.3445	315.7	33.22	9.5	1.16	683	47.6	2.8	77	
19	24-Hour Hold	3	1931	Fill	0.0	315.7	33.22	9.5	1.16	683	247.8	22.9	128	
20	24-Hour Hold	3, MV-525 Opened	1931	Fill	0.0	315.7	33.22	9.5	1.16	683	-	0.0	-	
21	24-Hour Hold	3	1931	Vent	0.0	315.7	33.22	9.5	1.16	683	-	0.0	-	
22	Heater Depletion	3	1931	Supply	1.2427	319.4	35.43	9.0	1.32	461	41.4	2.3	46	
23	Heater Depletion	3	1931	Fill	0.0	319.4	35.43	9.0	1.32	461	147.6	9.2	46	
24	Heater Depletion	3	1931	Vent	0.0	319.4	35.43	9.0	1.32	461	-	0.0	-	

*On Pressure Gauge † Secondary oscillation at this frequency and peak pressure.

TABLE 3-I PRSA HYDROGEN TANK THERMAL ACOUSTIC OSCILLATION DATA (Continued)

Data Point	Purpose of Test	Tank, Line and Valve Configuration (See Figure 2-)	Tank Pressure (KPa)	Line	Mass Flow (Kg/hr)	T_{hot} (^{o}K)	T_{cold} (^{o}K)	α	ν_c m^2/sec $x10^7$	a_c (m/sec)	γ_c	Oscillation Frequency (Hz)	Oscillation Peak-to-Peak Pressure (KPa)	Notes
25	Minimum dQ/dM	3	1916	Supply	0.618	315.7	37.91	8.3	1.30	468	55.2	4.2	41	
26	Minimum dQ/dM	3	1916	Fill	0.0	315.7	37.91	8.3	1.30	468	-	0.0	-	
27	Minimum dQ/dM	3, MV-525 Closed	1916	Fill	0.0	315.7	37.91	8.3	1.30	468	283.0	33.3	100	
28	Minimum dQ/dM	3	1916	Vent	0.0	315.7	37.91	8.3	1.30	468	-	0.0	-	
29	24-Hour Hold	3	1930	Supply	.1757	313.7	27.62	11.4	1.42	971	38.0	2.2	100	
30	24-Hour Hold	3	1930	Fill	0.0	313.7	27.62	11.4	1.42	971	218.0	21.7	105	†.0535 Hz 323 KPa
31	24-Hour Hold	3	1930	Vent	0.0	313.7	27.62	11.4	1.42	971	-	0.0	-	
32	24-Hour Hold	4	1930	Supply	.288	316.2	38.32	8.3	1.37	467	40.0	2.3	46	
33	24-Hour Hold	4	1930	Fill	0.0	316.2	38.32	8.3	1.37	467	138.0	8.3	46	
34	24-Hour Hold	4	1930	Vent	0.0	316.2	38.32	8.3	1.37	467	-	0.0	-	
35	24-Hour Hold	4	1930	Supply	.1136	315.1	32.03	9.8	1.21	467	52.0	3.4	55	
36	24-Hour Hold	4	1930	Fill	0.0	315.1	32.03	9.8	1.21	757	243.0	22.9	109	
37	24-Hour Hold	4	1930	Vent	0.0	315.1	32.03	9.8	1.21	757	-	0.0	-	
38	24-Hour Hold	5	1930	Supply	.099	315.8	31.30	10.1	1.26	820	43.0	2.5	100	
39	24-Hour Hold	5	1930	Fill	0.0	315.8	31.30	10.1	1.26	820	238.0	22.9	73	†.0347 Hz 157.9 KPa
40	24-Hour Hold	5, MV-524 Open	1930	Fill	0.0	315.8	31.30	10.1	1.26	820	-	0.0	-	
41	24-Hour Hold	5	1930	Vent	0.0	315.8	31.30	10.1	1.26	820	-	0.0	-	
42	24-Hour Hold	5	1930	Supply	.0538	315.3	31.54	10.0	1.26	788	51.0	3.5	48	
43	24-Hour Hold	5	1930	Fill	0.0	315.3	31.54	10.0	1.26	788	227.0	20.8	46	
44	24-Hour Hold	5, MV-524 Open With Flex Line	1930	Fill	0.0	315.3	31.54	10.0	1.26	788	-	0.0	-	
45	24-Hour Hold	5	1930	Vent	.0	315.3	31.54	10.0	1.26	788	-	0.0	-	

†Secondary oscillation at this frequency and peak pressure.

TABLE 3-I PRSA HYDROGEN TANK THERMAL ACOUSTIC OSCILLATION DATA (Continued)

Data Point	Purpose of Test	Tank, Line and Valve Configuration (See Figure 2-)	Tank Pressure (KPa)	Line	Mass Flow (Kg/hr)	T_{hot} (^{o}K)	T_{cold} (^{o}K)	α	ν_c m^2/sec $x10^7$	a_c (m/sec)	Y_c	Oscillation Frequency (Hz)	Oscillation Peak-to-Peak Pressure (KPa)	Notes
46	24-Hour Hold	6	1930	Supply	0.118	313.9	33.35	9.4	1.16	683	47.0	2.7	59	
47	24-Hour Hold	6	1930	Fill	0.0	313.9	33.35	9.4	1.16	683	249	23.0	90	
48	24-Hour Hold	6, MV-524 Open	1930	Fill	0.0	313.9	33.35	9.4	1.16	683	-	0.0	-	
49	24-Hour Hold	6	1930	Vent	0.0	313.9	33.35	9.4	1.16	683	-	0.0	-	
50	24-Hour Hold	7	1930	Supply	0.374	317.6	34.60	9.2	1.14	595	53.0	3.4	91	
51	24-Hour Hold	7	1930	Fill	0.0	317.6	34.60	9.2	1.14	595	251.0	23.0	41	
52	24-Hour Hold	7	1930	Fill	0.0	317.6	34.60	9.2	1.14	595	-	0.0	-	
53	24-Hour Hold	7	1930	Vent	0.0	317.6	34.60	9.2	1.14	595	-	0.0	-	
54	24-Hour Hold	8	1930	Supply	.0307	315.4	35.43	8.9	1.12	498	55.0	3.6	46	
55	24-Hour Hold	8	1930	Fill	0.0	315.4	35.43	8.9	1.12	498	-	0.0	-	
56	24-Hour Hold	8	1930	Vent	0.0	315.4	35.43	8.9	1.12	498	-	0.0	-	
57	24-Hour Hold	8, MV-524 Closed	1923	Supply	N/A	316.8	26.40	12.0	1.48	1011	31.9	1.6	48	
58	24-Hour Hold	8, MV-524 Closed	1923	Fill	0.0	316.8	26.40	12.0	1.48	1011	129.9	8.0	48	
59	24-Hour Hold	8, MV-524 Closed	1923	Vent	0.0	316.8	26.40	12.0	1.48	1011	-	0.0	-	
60	24-Hour Hold	8, B-1 Closed	1930	Supply	0.1852	317.5	31.79	10.0	1.27	788	37.6	1.9	32	
61	24-Hour Hold	8, B-1 Closed	1930	Fill	0.0	317.5	31.79	10.0	1.27	788	141.1	8.1	32	
62	24-Hour Hold	8, B-1 Closed	1930	Vent	0.0	317.5	31.79	10.0	1.27	788	-	0.0	-	
63	24-Hour Hold	8, B-1 Open	1927	Supply	0.207	315.7	31.79	10.0	1.27	788	36.6	1.8	37	
64	24-Hour Hold	8, B-1 Open	1927	Fill	0.0	315.7	31.79	10.0	1.27	788	141.1	8.1	37	
65	24-Hour Hold	8, B-1 Open	1927	Vent	0.0	315.7	31.79	10.0	1.27	788	-	0.0	-	

TABLE 3-I PRSA HYDROGEN TANK THERMAL ACOUSTIC OSCILLATION DATA (Continued)

Data Point	Purpose of Test	Tank, Line and Valve Configuration (See Figure 2-)	Tank Pressure (KPa)	Line	Mass Flow (Kg/hr)	T_{hot} (^{o}K)	T_{cold} (^{o}K)	α	ν_c m^2/sec $x10^7$	a_c (m/sec)	Y_c	Oscillation Frequency (Hz)	Oscillation Peak-to-Peak Pressure (KPa)	Notes
66	24-Hour Hold	8, MV-524 Closed	1930	Supply	0.0409	315.5	29.33	10.8	1.33	948	43.7	2.7	55	
67	24-Hour Hold	8, MV-524 Closed	1930	Fill	0.0	315.5	29.33	10.8	1.33	948	-	0.0	-	
68	24-Hour Hold	8, MV-524 Open	1930	Fill	0.0	315.5	29.33	10.8	1.33	948	141.6	8.54	55	
69	24-Hour Hold	8, MV-524 Closed	1930	Vent	0.0	315.5	29.33	10.8	1.33	948	-	0.0	-	
70	24-Hour Hold	8	1930	Supply	0.0409	315.3	32.03	9.8	1.21	757	37.4	1.8	46	
71	24-Hour Hold	8	1930	Fill	0.0	315.3	32.03	9.8	1.21	757	148.0	8.04	46	
72	24-Hour Hold	8	1930	Fill	0.0	315.3	32.03	9.8	1.21	757	-	0.0	-	
73	24-Hour Hold	8	1930	Vent	0.0	315.3	32.03	9.8	1.21	757	-	0.0	-	
74	24-Hour Hold	9	1930	Supply	0.0420	316.3	29.53	10.7	1.33	901	46.1	3.0	32	
75	24-Hour Hold	9	1930	Fill	0.0	316.3	29.53	10.7	1.33	901	-	0.0	-	
76	24-Hour Hold	9	1930	Vent	0.0	316.3	29.53	10.7	1.33	901	-	0.0	-	
77	24-Hour Hold	9	1932	Supply	0.1484	315.8	30.07	10.5	1.31	876	40.7	2.3	63	
78	24-Hour Hold	9	1932	Fill	0.0	315.8	30.07	10.5	1.31	876	231.5	22.5	91	†† N/A † 268.2 KPa
79	24-Hour Hold	9	1932	Vent	0.0	315.8	30.07	10.5	1.31	876	-	0.0	-	
80	24-Hour Hold	9	1930	Supply	0.1303	315.9	30.07	10.5	1.31	876	40.7	2.3	64	
81	24-Hour Hold	9	1930	Fill	0.0	315.9	30.07	10.5	1.31	876	189.1	15.0	100	
82	24-Hour Hold	9	1930	Fill	0.0	315.9	30.07	10.5	1.31	876	-	0.0	0.0	
83	24-Hour Hold	9	1930	Vent	0.0	315.9	30.07	10.5	1.31	8.76	-	0.0	0.0	
84	24-Hour Hold	9	1930	Supply	0.0524	317.0	31.79	10.0	1.24	788	50.8	3.4	46	
85	24-Hour Hold	9	1930	Fill	0.0	317.0	31.79	10.0	1.24	788	-	0.0	0.0	
86	24-Hour Hold	9	1930	Vent	0.0	317.0	31.79	10.0	1.24	788	-	0.0	-	

† Secondary oscillation at this frequency and peak pressure. †† Secondary frequency unavailable.

TABLE 3-I PRSA HYDROGEN TANK THERMAL ACOUSTIC OSCILLATION DATA (Continued)

Data Point	Purpose of Test	Tank, Line and Valve Configuration (See Figure 2-)	Tank Pressure (KPa)	Line	Mass Flow (Kg/hr)	T_{hot} (^{o}K)	T_{cold} (^{o}K)	α	ν_c m^2/sec $x10^7$	a_c (m/sec)	Y_c	Oscillation Frequency (Hz)	Oscillation Peak-to-Peak Pressure (KPa)	Notes
87	24-Hour Hold	10	1930	Supply	0.0	318.5	28.61	11.1	1.41	937	-	0.0	-	
88	24-Hour Hold	10	1930	Fill	0.0	318.5	28.61	11.1	1.41	937	-	0.0	-	
89	24-Hour Hold	10	1930	Vent	0.0	318.5	28.61	11.1	1.41	937	-	0.0	-	
90	24-Hour Hold	10	1930	Supply	0.0205	317.6	29.09	10.9	1.48	926	-	0.0	-	
91	24-Hour Hold	10	1931	Supply	0.0743	318.1	30.57	10.4	1.29	848	53.4	3.9	68	
92	24-Hour Hold	10	1931	Fill	0.0	318.1	30.57	10.4	1.29	848	-	0.0	-	
93	24-Hour Hold	10	1931	Vent	0.0	318.1	30.57	10.4	1.29	848	-	0.0	-	
94	24-Hour Hold	10	1930	Supply	0.0420	317.3	29.33	10.8	1.35	901	52.2	3.9	72.8	
95	24-Hour Hold	10	1930	Fill	0.0	317.3	29.33	10.8	1.35	901	-	-	-	
96	24-Hour Hold	10	1930	Vent	0.0	317.3	29.33	10.8	1.35	901	-	-	-	
97	24-Hour Hold	10	1868	Supply	100	319.1	29.58	10.8	1.35	901	47.3	3.2	141.1	
98	24-Hour Hold	10	1868	Fill	0.0	319.1	29.58	10.8	1.35	901	-	0.0	-	
99	24-Hour Hold	10	1868	Vent	0.0	319.1	29.58	10.8	1.35	901	-	0.0	-	
100	24-Hour Hold	10, MV-530 Opened	1853	Supply	0.0	316.9	29.58	10.7	1.43	901	-	0.0	-	
101	24-Hour Hold	10, MV-530 Opened	1853	Fill	0.0	316.9	29.58	10.7	1.43	901	-	0.0	-	
102	24-Hour Hold	10, MV-530 Opened	1853	Vent	0.0	316.9	29.58	10.7	1.43	901	-	0.0	-	
103	24-Hour Hold	10	1912	Supply	0.0	316.0	24.80	10.4	1.32	862	-	0.0	-	
104	24-Hour Hold	10	1912	Fill	0.0	316.0	24.80	10.4	1.32	862	-	0.0	-	
105	24-Hour Hold	10	1912	Vent	0.0	316.0	24.80	10.4	1.32	862	-	0.0	-	
106	24-Hour Hold	11	1930	Supply	0.020	316.2	29.83	10.6	1.31	876	-	0.0	-	
107	24-Hour Hold	11	1930	Supply	0.0	316.2	29.83	10.6	1.31	876	55.6	4.3	46	
108	24-Hour Hold	11	1930	Fill	0.0	316.2	29.83	10.6	1.31	876	-	0.0	-	
109	24-Hour Hold	11	1930	Vent	0.0	316.2	29.83	10.6	1.31	876	-	0.0	-	
110	24-Hour Hold	11	1930	Supply	0.0	318.9	30.57	10.4	1.30	848	-	0.0	-	

TABLE 3-I PRSA HYDROGEN TANK THERMAL ACOUSTIC OSCILLATION DATA (Continued)

Data Point	Purpose of Test	Tank, Line and Valve Configuration (See Figure 2-)	Tank Pressure (KPa)	Line	Mass Flow (Kg/hr)	T_{hot} (^{o}K)	T_{cold} (^{o}K)	α	ν_c m^2/sec $x10^7$	a_c (m/sec)	Y_c	Oscillation Frequency (Hz)	Oscillation Peak-to-Peak Pressure (KPa)	Notes
111	24-Hour Hold	11, MV-532 Opened	1930	Supply	0.1853	318.9	30.57	10.4	1.30	848	48.2	3.2	68	
112	24-Hour Hold	11	1930	Fill	0.0	318.9	30.57	10.4	1.30	848	137.7	7.9	28	
113	24-Hour Hold	11	1930	Vent	0.0	318.9	30.57	10.4	1.30	848	-	0.0	-	
114	24-Hour Hold	11	1929	Supply	0.0919	315.7	29.58	10.7	1.34	901	45.9	3.0	86	
115	24-Hour Hold	11	1929	Fill	0.0	315.7	29.58	10.7	1.34	901	135.7	7.9	9.0	
116	24-Hour Hold	11	1929	Vent	0.0	315.7	29.58	10.7	1.34	901	-	0.0	-	
117	24-Hour Hold	11, B-2 Open	1923	Supply	0.0127	316.3	34.46	9.1	1.13	595	56.3	3.8	6.6	
118	24-Hour Hold	11, B-2 Open	1923	Fill	0.0	316.3	34.46	9.2	1.13	595	-	0.0	-	
119	24-Hour Hold	11, B-2 Open	1923	Vent	0.0	316.3	34.46	9.2	1.13	595	-	0.0	-	
120	24-Hour Hold	11, B-1 Closed	1925	Supply	0.0291	317.6	32.77	9.7	1.24	738	53.0	3.7	41	
121	24-Hour Hold	11, B-1 Closed	1925	Fill	0.0	317.6	32.77	9.7	1.24	738	-	0.0	-	
122	24-Hour Hold	11, B-1 Closed	1925	Vent	0.0	317.6	32.77	9.7	1.24	738	-	0.0	-	
123	24-Hour Hold	11	1927	Supply	0.0209	315.4	30.57	10.3	1.30	848	-	0.0	-	
124	24-Hour Hold	11	1927	Fill	0.0	315.4	30.57	10.3	1.30	848	-	0.0	-	
125	24-Hour Hold	11	1927	Vent	0.0	315.4	30.57	10.3	1.30	848	-	0.0	-	
126	24-Hour Hold	12	1937	Supply	0.1495	314.7	36.82	9.1	1.21	456	79.4	8.1	9.0	
127	24-Hour Hold	12	1937	Fill	0.0	314.7	36.82	9.1	1.21	456	144.6	8.1	37.0	
128	24-Hour Hold	12	1937	Vent	0.0	314.7	36.82	9.1	1.21	456	-	0.0	-	
129	24-Hour Hold	12, MV-524 Closed 9 Turns	1917	Supply	0.0	315.0	34.73	9.1	1.22	571	-	0.0	-	
130	24-Hour Hold	12, MV-524 Closed 9 Turns	1917	Fill	0.0	315.0	34.73	9.1	1.22	571	-	0.0	-	

TABLE 3-I PRSA HYDROGEN TANK THERMAL ACOUSTIC OSCILLATION DATA (Continued)

Data Point	Purpose of Test	Tank, Line and Valve Configuration (See Figure 2-)	Tank Pressure (KPa)	Line	Mass Flow (Kg/hr)	T_{hot} (^{o}K)	T_{cold} (^{o}K)	α	ν_c m^2/sec $x10^7$	a_c (m/sec)	γ_c	Oscillation Frequency (Hz)	Oscillation Peak-to-Peak Pressure (KPa)	Notes
131	24-Hour Hold	12, MV-524 Closed 9 Turns	1917	Vent	0.0	315.0	34.73	9.1	1.22	571	-	0.0	-	
132	EIAT Heater Depletion	12	1923	Supply	1.24	316.1	32.52	9.7	1.24	738	39.0	2.0	7.0	
133	EIAT Heater Depletion	12	1923	Fill	0.0	316.1	32.52	9.7	1.24	738	-	0.0	-	
134	EIAT Heater Depletion	12	1923	Vent	0.0	316.1	32.52	9.7	1.24	738	-	0.0	-	
135	EIAT Heater Depletion	12	1929	Supply	1.0355	313.8	44.59	7.0	1.98	530	36.5	2.8	28.0	
136	EIAT Heater Depletion	12	1929	Fill	0.0	313.8	44.59	7.0	1.98	530	-	0.0	0.0	
137	EIAT Heater Depletion	12	1929	Vent	0.0	313.8	44.59	7.0	1.98	530	-	0.0	0.0	
138	EIAT Preparation for Minimum dQ/dM	12, B-1 Closed	1928	Supply	0.0069	314.1	44.59	7.0	1.98	530	46.3	4.5	9.0	
139	EIAT Preparation for Minimum dQ/dM	12, B-1 Closed	1928	Fill	0.0	314.1	44.59	7.0	1.98	530	-	0.0	0.0	
140	EIAT Preparation for Minimum dQ/dM	12, B-1 Closed	1928	Vent	0.0	314.1	44.59	7.0	1.98	530	-	0.0	0.0	
141	EIAT Preparation for Minimum dQ/dM	12, B-1 Open	1930	Supply	0.0172	314.78	44.59	7.1	1.98	530	-	0.0	-	
142	EIAT Preparation for Minimum dQ/dM	12, B-1 Open	1930	Fill	0.0	314.78	44.59	7.1	1.98	530	-	0.0	-	
143	EIAT Preparation for Minimum dQ/dM	12, B-1 Open	1930	Vent	0.0	314.78	44.59	7.1	1.98	530	-	0.0	-	
144	EIAT Preparation for Minimum dQ/dM	13, B-1 Open	1930	Supply	0.0287	315.85	42.05	7.5	1.69	504	-	0.0	-	
145	EIAT Preparation for Minimum dQ/dM	13, B-1 Open	1930	Fill	0.0	315.85	42.05	7.5	1.69	504	-	0.0	-	
146	EIAT Preparation for Minimum dQ/dM	13, B-1 Open	1930	Vent	0.0	315.85	42.05	7.5	1.69	504	-	0.0	-	
147	EIAT Preparation for Minimum dQ/dM	13, B-1 Open, MV-524 Opened 3 Turns	1930	Supply	0.0280	316.38	42.06	7.5	1.69	504	49.5	4.4	46	

TABLE 3-I PRSA HYDROGEN TANK THERMAL ACOUSTIC OSCILLATION DATA (Continued)

Data Point	Purpose of Test	Tank, Line and Valve Configuration (See Figure 2-)	Tank Pressure (KPa)	Line	Mass Flow (Kg/hr)	T_{hot} (^{o}K)	T_{cold} (^{o}K)	α	ν_c m^2/sec $x10^7$	a_c (m/sec)	Y_c	Oscillation Frequency (Hz)	Oscillation Peak-to-Peak Pressure (KPa)	Notes
148	EIAT Preparation for Minimum dQ/dM	13, B-1 Open, MV-524 Opened 3 Turns	1930	Fill	0.0	316.38	42.06	7.5	1.69	504	-	0.0	-	
149	EIAT Preparation for Minimum dQ/dM	13, B-1 Open, MV-524 Opened 3 Turns	1930	Vent	0.0	316.38	42.06	7.5	1.69	504	-	0.0	-	
150	24-Hour Hold	13	1933	Supply	0.1565	314.07	31.79	9.9	1.26	788	-	0.0	-	
151	24-Hour Hold	13	1933	Fill	0.0	314.07	31.79	9.9	1.26	788	140.8	8.0	48	
152	24-Hour Hold	13	1933	Vent	0.0	314.07	31.79	9.9	1.26	788	126.8	8.0	21	
153	24-Hour Hold	13, MV-524 Open	1930	Supply	0.0856	315.39	35.57	8.9	1.12	498	-	0.0	-	
154	24-Hour Hold	13, MV-524 Closed 8 Turns	1930	Fill	0.0	315.39	35.57	8.9	1.12	498	148.4	7.9	46	
155	24-Hour Hold	13, MV-524 Open	1930	Fill	0.0	315.39	35.57	8.9	1.12	498	-	0.0	-	
156	24-Hour Hold	13, MV-524 Open	1930	Vent	0.0	315.39	35.57	8.9	1.12	498	-	0.0	-	
157	24-Hour Hold	13	1929	Supply	0.1514	318.11	35.29	9.0	1.12	498	-	0.0	-	
158	24-Hour Hold	13	1929	Fill	0.0	318.11	35.29	9.0	1.12	498	150.3	8.1	46	
159	24-Hour Hold	13	1929	Vent	0.0	318.11	35.29	9.0	1.12	498	-	0.0	-	
160	24-Hour Hold	13	1929	Supply	0.1514	318.11	35.29	9.0	1.12	498	62.2	4.6	136	
161	24-Hour Hold	13	1929	Fill	0.0	318.11	35.29	9.0	1.12	498	150.3	8.1	50	
162	24-Hour Hold	13	1929	Vent	0.0	318.11	35.29	9.0	1.12	498	-	0.0	-	
163	24-Hour Hold	13	1930	Supply	0.0144	317.75	36.53	8.7	1.21	456	42.3	2.3	91	
164	24-Hour Hold	13	1930	Fill	0.0	317.75	36.53	8.7	1.21	456	-	0.0	-	

TABLE 3-I PRSA HYDROGEN TANK THERMAL ACOUSTIC OSCILLATION DATA (Continued)

Data Point	Purpose of Test	Tank, Line and Valve Configuration (See Figure 2-)	Tank Pressure (KPa)	Line	Mass Flow (Kg/hr)	T_{hot} (^{o}K)	T_{cold} (^{o}K)	α	ν_c m^2/sec $x10^{7}$	a_c (m/sec)	Y_c	Oscillation Frequency (Hz)	Oscillation Peak-to-Peak Pressure (KPa)	Notes
165	24-Hour Hold	13	1930	Vent	0.0	317.75	36.53	8.7	1.21	456	-	0.0	-	
166	24-Hour Hold	13	1930	Supply	0.0144	317.75	36.53	8.7	1.21	456	40.4	2.1	50	
167	24-Hour Hold	13	1930	Fill	0.0	317.75	36.53	8.7	1.21	456	150.7	8.8	41	
168	24-Hour Hold	13	1930	Vent	0.0	317.75	36.53	8.7	1.21	456	118.4	6.7	68	
169	24-Hour Hold	13	1909	Supply	0.0	316.10	28.11	11.2	1.39	948	-	0.0	-	
170	24-Hour Hold	13	1909	Fill	0.0	316.10	28.11	11.2	1.39	948	-	0.0	-	
171	24-Hour Hold	13	1909	Vent	0.0	316.10	28.11	11.2	1.39	948	-	0.0	-	
172	24-Hour Hold	14, B-1 Open, 3.2 mm Orifice	1930	Supply	0.2323	315.20	28.11	11.2	1.39	948	-	0.0	-	
173	24-Hour Hold	14, MV-524 Open, 4.4 mm Orifice	1930	Fill	0.0	315.20	28.11	11.2	1.39	948	-	0.0	-	
174	24-Hour Hold	14	1930	Vent	0.0	315.20	28.11	11.2	1.39	948	-	0.0	-	
175	24-Hour Hold	14, B-1 Open, 3.2 mm Orifice	1868	Supply	N/A	316.03	29.09	10.9	1.39	926	-	0.0	-	
176	24-Hour Hold	14, MV-524 Open, 4.4 mm Orifice	1868	Fill	0.0	316.03	29.09	10.9	1.38	926	-	0.0	-	
177	24-Hour Hold	14	1868	Vent	0.0	316.03	29.09	10.9	1.38	926	-	0.0	-	
178	24-Hour Hold	14	1847	Supply	N/A	317.27	30.32	10.5	1.35	876	33.4	1.6	21	
179	24-Hour Hold	14	1847	Fill	0.0	317.27	30.32	10.5	1.35	876	-	0.0	-	
180	24-Hour Hold	14	1847	Vent	0.0	317.27	30.32	10.5	1.35	876	-	0.0	-	
181	24-Hour Hold	14, B-1 Open, No Orifice	1933	Supply	N/A	316.68	30.71	10.3	1.30	848	-	0.0	-	

TABLE 3-I PRSA HYDROGEN TANK THERMAL ACOUSTIC OSCILLATION DATA (Continued)

Data Point	Purpose of Test	Tank, Line and Valve Configuration (See Figure 2-)	Tank Pressure (KPa)	Line	Mass Flow (Kg/hr)	T_{hot} (^{o}K)	T_{cold} (^{o}K)	α	ν_c m^2/sec $\times 10^7$	a_c (m/sec)	γ_c	Oscillation Frequency (Hz)	Oscillation Peak-to-Peak Pressure (KPa)	Notes
182	24-Hour Hold	14, MV-524 Open, 4.4 mm Orifice	1933	Fill	0.0	316.68	30.71	10.3	1.30	848	-	0.0	-	
183	24-Hour Hold	14	1933	Vent	0.0	316.68	30.71	10.3	1.30	848	-	0.0	-	
184	24-Hour Hold Remove Insula-	14, MV-524 Open	1881	Supply	0.0	318.41	27.13	11.7	1.46	991	-	0.0	-	
185	24-Hour Hold tion on Girth	14, MV-524 Open	1881	Fill	0.0	318.41	27.13	11.7	1.46	991	-	0.0	-	
186	24-Hour Hold and Fill Line,	14, MV-524 Closed	1881	Fill	0.0	318.41	27.13	11.7	1.46	991	185.0	16.0	200	
187	24-Hour Hold Open B-1	14, MV-524 Open	1881	Vent	0.0	318.41	27.13	11.7	1.46	991	-	0.0	-	
188	24-Hour Hold	14	1930	Supply	0.2641	314.72	27.37	11.5	1.46	991	-	0.0	-	
189	24-Hour Hold	14	1930	Fill	0.0	314.72	27.37	11.5	1.46	991	-	0.0	-	
190	24-Hour Hold	14	1930	Vent	0.0	314.72	27.37	11.5	1.46	991	-	0.0	-	
191	EIAT Preparation for Minimum dQ/dM	14	1937	Supply	0.800	318.28	44.17	7.2	1.98	530	-	0.0	-	
192	EIAT Preparation for Minimum dQ/dM	14, Htr No. 1 Turned On	1937	Supply	0.800	318.28	44.17	7.2	1.98	530	51.2	5.5	46	
193	EIAT Preparation for Minimum dQ/dM	14	1937	Fill	0.0	318.28	44.17	7.2	1.98	530	-	0.0	-	
194	EIAT Preparation for Minimum dQ/dM	14	1937	Vent	0.0	318.28	44.17	7.2	1.98	530	-	0.0	-	
195	EIAT Preparation for Minimum dQ/dM	14	1923	Supply	0.0218	316.74	29.33	10.8	1.40	901	-	0.0	-	
196	EIAT Preparation for Minimum dQ/dM	14	1923	Supply	0.0218	316.74	29.33	10.8	1.40	901	36.7	2.0	68	
197	EIAT Preparation for Minimum dQ/dM	14	1923	Fill	0.0	316.74	29.33	10.8	1.40	901	-	0.0	-	
198	EIAT Preparation for Minimum dQ/dM	14	1923	Vent	0.0	316.74	29.33	10.8	1.40	901	-	0.0	-	
199	24-Hour Hold	17	1930	Supply	0.0064	315.73	28.35	11.1	1.39	948	-	0.0	-	

TABLE 3-I PRSA HYDROGEN TANK THERMAL ACOUSTIC OSCILLATION DATA (Concluded)

Data Point	Purpose of Test	Tank, Line and Valve Configuration (See Figure 2-)	Tank Pressure (KPa)	Line	Mass Flow (Kg/hr)	T_{hot} (^{o}K)	T_{cold} (^{o}K)	α	ν_c m^2/sec $x10^7$	a_c (m/sec)	Y_c	Oscillation Frequency (Hz)	Oscillation Peak-to-Peak Pressure (KPa)	Notes
200	24-Hour Hold	17	1930	Fill	0.0	315.73	28.35	11.1	1.39	948	-	0.0	-	
201	24-Hour Hold	17	1930	Vent	0.0	315.73	28.35	11.1	1.39	948	-	0.0	-	
202	24-Hour Hold	17	1930	Supply	0.0277	315.37	27.37	11.5	1.46	991	-	0.0	-	
203	24-Hour Hold 5.1 mm Orifice	17	1930	Fill	0.0	315.37	27.37	11.5	1.46	991	-	0.0	-	
204	24-Hour Hold in Fill Line	17	1930	Vent	0.0	315.37	27.37	11.5	1.46	991	-	0.0	-	
205	24-Hour Hold	17	1930	Supply	0.0400	315.56	27.13	11.6	1.46	991	-	0.0	-	
206	24-Hour Hold	17	1930	Fill	0.0	315.56	27.13	11.6	1.46	991	122.3	7.0	46	
207	24-Hour Hold	17	1930	Vent	0.0	315.56	27.13	11.6	1.46	991	110.2	7.0	46	
208	24-Hour Hold	17	1930	Supply	0.0	317.99	28.61	11.1	1.39	948	58.2	5.0	90	
209	24-Hour Hold	17	1930	Fill	0.0	317.99	28.61	11.1	1.39	948	-	0.0	-	
210	24-Hour Hold	17	1930	Vent	0.0	317.99	28.61	11.1	1.39	948	-	0.0	-	
211	24-Hour Hold	17	1930	Supply	0.0545	314.90	22.80	11.3	1.42	971	-	0.0	-	
212	24-Hour Hold 3.8 mm Orifice	17	1930	Fill	0.0	314.90	22.80	11.3	1.42	971	-	0.0	-	
213	24-Hour Hold in Fill Line	17	1930	Vent	0.0	314.90	22.80	11.3	1.42	971	-	0.0	-	
214	24-Hour Hold	17	1930	Supply	0.0045	314.18	45.12	7.0	1.98	530	48.8	5.0	60	
215	24-Hour Hold	17	1930	Fill	0.0	314.18	45.12	7.0	1.98	530	-	0.0	-	
216	24-Hour Hold	17	1930	Vent	0.0	314.18	45.12	7.0	1.98	530	-	0.0	-	
217	24-Hour Hold	17	1933	Supply	0.0	314.78	43.98	7.2	1.98	530	57.7	7.0	55	
218	24-Hour Hold	17	1933	Fill	0.0	314.78	43.98	7.2	1.98	530	-	0.0	-	
219	24-Hour Hold	17	1933	Vent	0.0	314.788	43.98	7.2	1.98	530	-	0.0	-	

The initial proposal indicated that a correlation of test data and the analytical model by Liburdy would be completed. This model allows for a mean fluid flow term and, due to this term, one goal of this study was to determine the effect of flow on the thermal acoustic oscillation stability limit. Test data points 106 and 107 are of particular interest. Data point 106 indicates that, for a flow rate of .020 kg/hr, the supply line is stable at a temperature ratio of 10.6. The supply line oscillates for data point 107 at a freqency of 4.3 Hz for a similar temperature ratio with no flow. This is in the direction as predicted by Liburdy; that is that flow increases stability. However, test data points 87 and 94 contradict this trend. Data point 87 is stable with no flow for a temperature ratio of 11. For a flow rate of .042 kg/hr, the supply line oscillates at a frequency of 3.9 Hz at a temperature ratio of 10.8; this condition is described by data point 94. While the temperature ratios are not equal, the stable point, data point 87, has the higher temperature ratio and therefore should be the least stable.

Some observations were made while reducing the test data concerning the onset of oscillations. In several instances, the fluid line would be stable when, for no apparent reason, oscillations would begin. The opening and closing of valves would in general effect the oscillations in both a positive and negative manner. Valve opening in general would initiate oscillation if the line had previously been stable. The steady oscillations may have been prompted by the transient effect of valve opening. However, if the line was initially oscillating when the valve was opened, the trend was toward stability. The effect of opening the valve, in this case, may be to disrupt the oscillation pattern.

4.0 TEST DATA COMPARISON

This section presents the test data comparison with current analytical models. In order to understand the development of the current models, a historical background is presented in Section 4.1. Section 4.2 contains the test data correlation and a description of the analytical model used.

4.1 Historical Background. Thermally driven pressure oscillations are known to occur spontaneously in tubes subjected to large temperature gradients. Thermal oscillations were first noticed in glass blowing where audible sound was produced by heating the tube end. Thermal acoustic oscillations can occur in cryogenic lines leading from room temperature to the cryogenic reservoir temperature. These oscillations cause pressure fluctuations and are generally accompanied by large heat inputs to the cryogenic reservoir.

A qualitative explanation of thermal acoustic oscillations is based upon the physical mechanism that oscillations are encouraged if heat is added to the air at the point of greatest compression and heat is taken out at the point of greatest expansion. Under these conditions, a small perturbation can grow and become a self-sustaining oscillation due to the heating and cooling effects. This heating and cooling results from the large temperature gradient that exists between the warm and cold ends of the tube. During the pressure rise portion of an oscillation cycle, there is movement of the gas from the open cold end toward the closed warm end of the tube. As the gas elements travel, their pressure increases and, from adiabatic compression, their temperature rises. However, the gas temperature rise due to compression is less than the wall temperature increase due to the cold-to-warm end temperature gradient. Therefore, there is a temperature difference which transfers heat from the wall to the adjacent gas elements. As the gas elements continue moving toward the warm end, pressure increases and heat is transferred from the wall to the gas. After the pressure in the element has peaked, the process is reversed. As the gas elements move toward the cold open end, their pressure drops, they come into contact with colder sections of the tube wall and heat is transferred from the gas to the wall. It is the net heat flux into the gas that is the driving force for the existence of thermal oscillations. The opposing or dissipating forces are the gas viscosity and the kinetic energy expelled into the cold reservoir. This energy (heat flux) pumped into the cold reservoir is the difference between the heat transferred to the gas

during the pressure rise portion of a cycle and the heat transferred from the gas during the pressure drop portion of a cycle. When the net heat flux into the gas exactly balances the dissipative forces, the criteria for sustained thermal oscillations are met.

The following paragraphs contain a review of the pertinent literature on thermal acoustic oscillation phenomenon. The following summaries start with the initial observations of Sondhass in 1850 of heat-generated sound produced by glass blowers to the present where the emphasis on this phenomenon is almost exclusively confined to the storage of cryogens. Included in the summaries is a brief elaboration of any pertinent technical information. This may consist of observational data, design information, methods of analysis or correlation of experimental data with analyses.

C. Sondhaus (1850) (Reference 1). Sondhaus observed that audible sound was produced from the tubes used by glass blowers. When a gas flame applied to the bulb end caused the air in the tube to oscillate producing a sound which was characteristic of the dimensions of the tube.

H. V. Helmholtz (1863) (Reference 2) and G. Kirchhoff (1868) (Reference 3). The first calculation of the damping of acoustic waves in long tubes due to friction at the side walls was made by Helmholtz.

Lord Rayleigh (1878) (Reference 4). Lord Rayleigh provided an explanation for the spontaneous occurrence of thermally driven oscillations. He explained that the oscillations occur if heat is added to the gas at the point of greatest compression and heat is taken out at the point of greatest expansion. This explanation has become known as the "Rayleigh criterion."

K. W. Taconis (1949) (Reference 5). The first reported observation of thermal acoustic oscillations in low temperature apparatus was made by Taconis.

H. A. Kramers (1949) (Reference 6). Kramers was the first to develop a theoretical analysis of the thermal acoustic oscillation problem and investigate the stability limits (with limited success) under which the oscillations can exist. He used the framework of Kirchhoff's theory in explaning that tubes which are room temperature at their closed end and liquid helium temperature at their open end may experience spontaneous acoustic oscillations. His investigation of the stability limit was carried out under the assumption

that the Stokes boundary layer thickness is small compared to the tube radius which would yield only one branch of the stability curve. He assumed the amplitude of the acoustic wave was small and therefore could use a linearized first order approximation of the hydrodynamic equations.

J. R. Clement and J. Gaffney (1954) (Reference 7). Clement and Gaffney experimentally studied thermal oscillations which occurred in small diameter tubes having one end at room temperature and the other end in a dewar filled with liquid helium.

They investigated the effects of varying degrees of closure at the hot and cold ends of the oscillating tubes. A tube completely open at the hot end could not be made to oscillate unless its inside diameter was less than about one millimeter. Simple tubes completely closed at the cold end could not be made to oscillate, either filled with gas only or with some condensed liquid at the cold end. However, only a very small opening at the cold end was required for oscillations to occur. They also observed oscillations in the annular space between the double wall of a liquid helium transfer-siphon tube which were damped by placing a snug fitting brass ring in the annulus near the cold end to block the gas motion.

L. Trilling (1955) (Reference 8). Trilling conducted an analytical study of heat generated pressure waves. By linearizing the hydrodynamic equations, he showed that sharp increases in boundary temperature can cause pressure waves to propagate in the same manner as pushing a piston through a gas-filled pipe.

K. T. Feldman (1966) (Reference 9). Feldman conducted extensive experimental and theoretical studies of the Sondhauss oscillation. A physical analysis of the heat exchange mechanism driving the Sondhauss oscillation was presented treating the Sondhauss oscillator as a heat engine. In order for the amplitude of the oscillation to grow to a steady-state condition, heat input had to be properly phased so that a net increase occurred in the total energy of the gas system after each cycle of oscillation.

J. D. Bannister (1966) (Reference 10). Bannister conducted experiments for measuring thermal acoustic oscillations in tubes connecting liquid helium reservoirs to room temperature environments. He measured oscillation pressure amplitudes and frequencies together with longitudinal temperature profiles and heat pumping rates for different tube sizes. He found a linear correlation between the pressure amplitude and the slenderness

ratio (length to diameter) of the tube and that the heat pumping rate is directly proportional to oscillation intensity (amplitude times frequency), Figures 4-1 and 4-2.

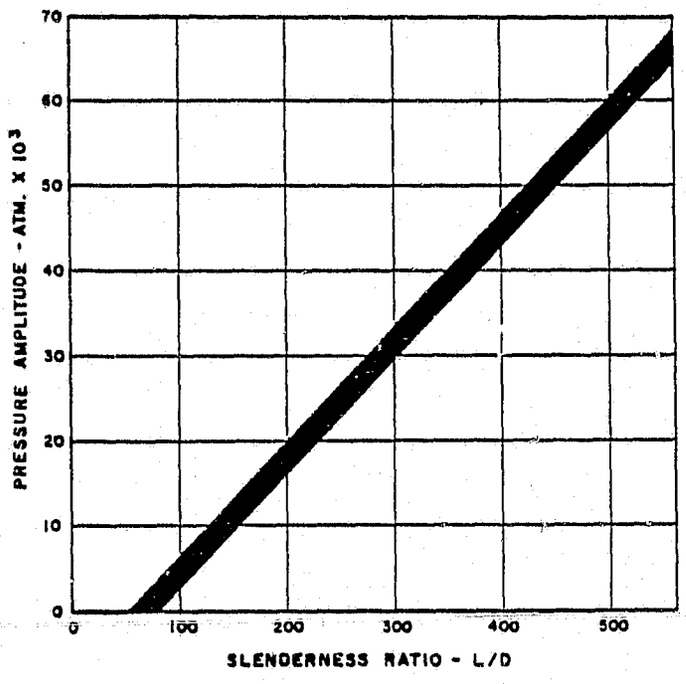

Figure 4-1 THERMAL ACOUSTIC OSCILLATION PRESSURE AMPLITUDE VERSUS LENGTH-TO-DIAMETER RATIO FOR A TUBE IN LIQUID HELIUM (Reference 10)

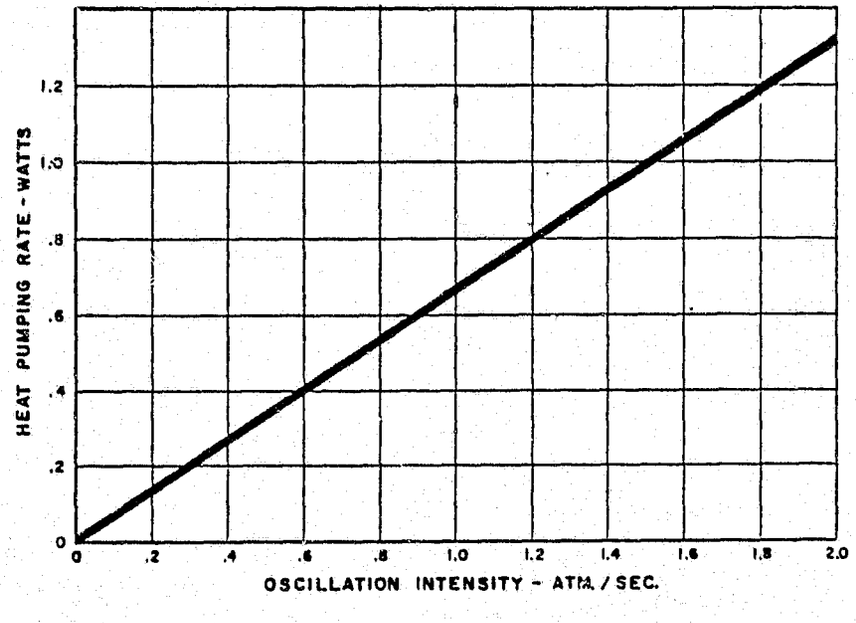

Figure 4-2 THERMAL ACOUSTIC OSCILLATION HEAT RATE VERSUS INTENSITY (AMPLITUDE TIMES FREQUENCY) FOR A TUBE IN LIQUID HELIUM

M. T. Norton and R. C. Muhlenhaupt (1967) (Reference 11). Norton and Muhlenhaupt developed a computer program to determine solutions for thermal acoustic oscilations in gas-filled pipes. For a specified temperature gradient along the tube length, the program calculates frequencies, overpressure amplitudes and the effects of changes in heat transfer coefficient and friction factor on the oscillation amplitude. The heat transfer is computed using unmodified heat transfer coefficients from McAdams (1954) and the friction factor is input as a constant.

To determine the oscillation frequency, the program divides the tube into constant temperature gas elements such that each element has an equal sonic traverse time.

With a temperature gradient and an arbitrary initial pressure pulse as inputs, the program calculates the gas velocity and pressures for each of the elements. These calculations consider not only the sonic velocity in each element, which is a function of temperature, but also consider the reflections of the sonic fronts at the interfaces of adjacent elements of different densities (temperatures). Therefore, the peak pressure at any point is the summation of multitudinous reflections and advances at something less than sonic velocity. The program calculates the period between each of the first ten pressure minimums thereby obtaining nine periods, and nine corresponding frequencies. The average of these nine frequencies is then considered to be the true frequency.

During the pressure rise portion of an oscillation cycle there is movement of gas from the open cold end towards the closed warm end. As the gas pressure increases, its temperature increases from adiabatic compression and heat transfer from the wall to the gas. After the pressure in the gas has peaked the process is reversed, the pressure drops, and heat is transferred out of the gas. When plotted on a temperature-entropy diagram this sequence of events traces out a positive work area, see Figure 4-3.

For the amplitude calculation the assumptions were made of a sinusoidal pressure variation at the closed end that that all peak pressures tend to occur at the same time. These assumptions were supported by oscilloscope observations. The gas in the tube was divided into a large number of equal length elements with additional elements in the dewar (N elements in the tube and M elements altogether). The period of a cycle was divided into 360 degrees and the compute time interval was taken as 5 degrees. Initial approximate temperatures and densities were assumed and the heat transfer was calculated for one complete cycle per each gas element. Conditions after the first cycle

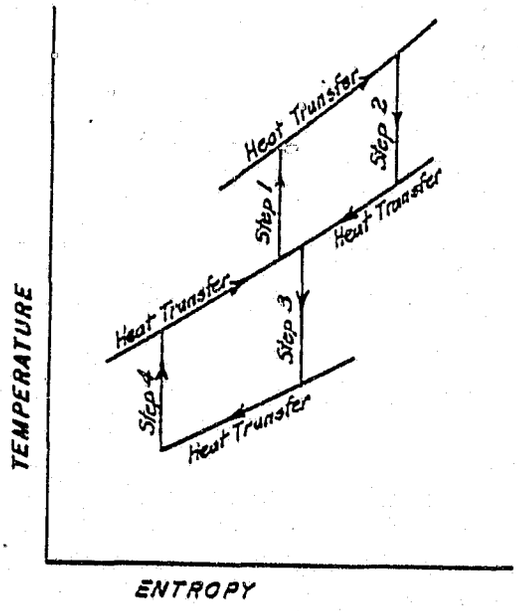

Figure 4-3 SIMPLIFIED TEMPERATURE-ENTROPY DIAGRAM FOR THERMAL ACOUSTIC OSCILLATION CYCLE

were different than the initially assumed conditions but, after a number of calculation cycles, an equilibrium condition was obtained. These calculations were performed for each of the M elements and the heat transferred, and the infinitesimal work done was also computed. The program then sums all the heat transferred and work done in one cycle for all the gas elements in the tube; this summation gives the net heat transferred into and the net work done by the gas. If there is positive work (net heat greater than net work), the conditions for the existence of thermal oscillations are present. If the work summation is negative, any accidental oscillations will quickly damp out. In the case where the work summation was positive, at equilibrium it must exactly balance the losses which are friction and kinetic energy ejected into the dewar.

P. Thullen and J. L. Smith, Jr. (1968) (Reference 12). Thullen and Smith developed an analysis for determining the parameters and stability regions for thermal oscillations associated with liquid helium. They used a lumped parameter model consisting of the following components:

1. A lumped isothermal inertial element, representing the inertia of the oscillating gas column.

2. Two adiabatic volumes, representing warm and cold void volumes.

3. Two ideal heat exchangers a distance ℓ apart, at temperature T_1 and T_2, representing the hot and cold portions of the tube wall.

4. A viscous damper whose force is proportional to the velocity of the inertial.

The equations of motion were linearized and solved in terms of dimensionless parameters. It was assumed that the system oscillated at the Helmholtz frequency; this was calculated by assuming that the adiabatic spring volume consisted of the warm portion of the tube and the warm void volume, and that the mass is concentrated in the cold portion of the tube. This equation was a function of the average pressure, the density and the cold length-to-total length ratio.

J. D. Rogers (1968) (Reference 13). Rogers examined subcritical fluid hydrogen oscillations during forced convection heating in a vertical test section with various heat inputs. The stability limit heat rates were correlated to a dimensionless boiling number. The threshold was identified with the formation of small amounts of vapor during the low pressure portion of the oscillation cycle.

N. Rott (1969) (Reference 14). Rott presented an analysis of the oscillations of a gas column in a tube with a nonuniform temperature distribution along its axis in general, and the stability limits of cryogenic oscillations of helium in particular. His analysis was based upon the theoretical work done by Kramers (1949). Kramers' results had yielded very large temperature ratios for the stability limits of helium which was contrary to experience; consequently, Kramers concluded that his linear stability theory did not lead to any useful results. Rott pointed out that, "For helium, however, the theory fails due to a 'quirk of nature': the material constants of helium are such that Kramers' asymptotes lie at practically infinite temperature ratios." He demonstrated that the linear theory had failed because of the restrictive assumptions placed upon the extent of the viscous region of the gas motion. Upon including second order viscous effects in the linear stability theory, Rott was able to obtain one branch of the stability curve. The entire stability curve was later worked out by Rott and published in his 1973 paper.

N. Rott (1973) (Reference 15). This analysis, an extension of Rott's previous work, presented theory and numerical calculations which determined the entire stability curve for helium. A reprint of one of these stability curves is given in Figure 4-4.

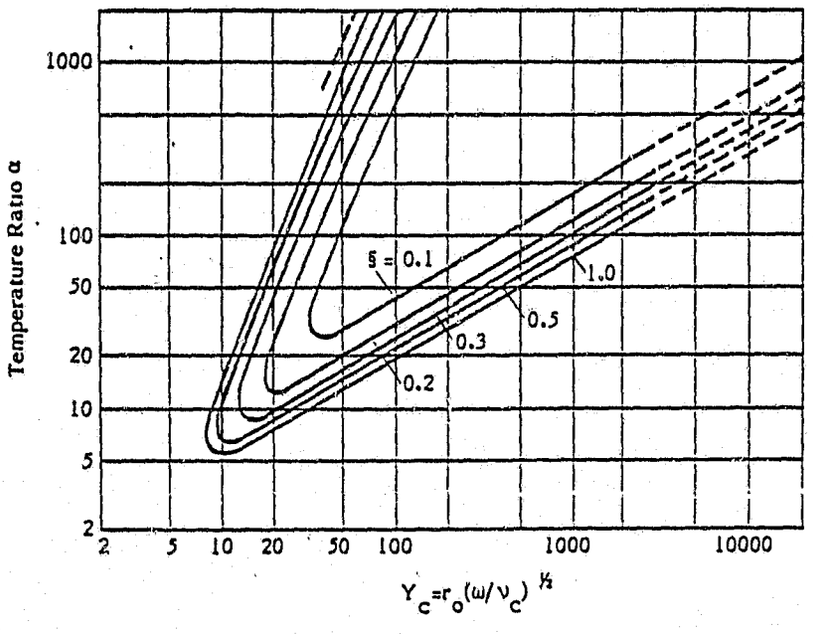

Figure 4-4 STABILITY CURVE FOR HELIUM (Reference 15)

α = Hot-to-cold temperature ratio

§ = Hot-to-cold length ratio

$Y_c = r_o (\omega/\nu_c)^{1/2}$ = tube radius-to-Stokes boundary layer thickness ratio

r_o = Tube radius

ω = Angular frequency

ν_c = Kinematic viscosity

In his first paper, Rott assumed that the viscous boundary layer was small compared to the tube radius; thus, yielding the lower branch of the stability curve. The second branch was found to exist for the case where the viscous region fills the whole tube in the hot part, but is small compared to the tube radius in the cold part.

T. Von Hoffmann, V. Lienert and H. Quack (1973) (Reference 16). Von Hoffmann, Lienert and Quack presented results of an experimental study to verify the stability limit of Rott. Tubes of various sizes were inserted into a double glass dewar containing helium. A brass vessel filled with liquid nitrogen was used to control the temperature of the warm end of the tube in order to vary the hot-to-cold temperature ratio. A piezoelectric pressure

sensor at the closed upper end of the tube was connected to an oscilloscope so that the oscillations could be observed. A plot of the results, compared to the theory of Rott, is given in Figure 4-5.

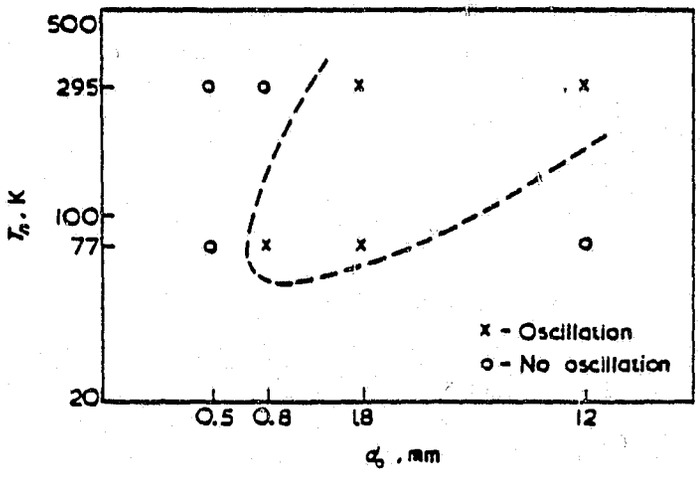

Figure 4-5 DATA OF VON HOFFMAN, et al., COMPARED WITH ROTT'S STABILITY THEORY

This figure demonstrated some qualitative agreement with Rott's theory; however, the stability curve of Rott should lie somewhat more to the left than indicated in Figure 4-5. This discrepancy was attributed to inaccuracies in the experimental setup and difficulty in obtaining reproducible results for the pressure amplitude.

L. W. Spradley (1974) (Reference 17). Spradley developed a numerical method for the solution of a nonsteady, viscous, heat conducting, compressible flow program using a nonlinear formulation. In his model, helium gas, initially at a uniform temperature, T_o, was confined between two parallel boundaries. At time t = 0, the temperature of the lower plate is suddenly raised to $T_w = 2\ T_o$, while the upper plate is kept at the constant value T_o. Because of heat transfer and compressibility effects, thermal acoustic waves are set up in the system which greatly increase the heat transfer rate into the system. Typical results of this solution, obtained from the computer program, are shown in Figure 4-6.

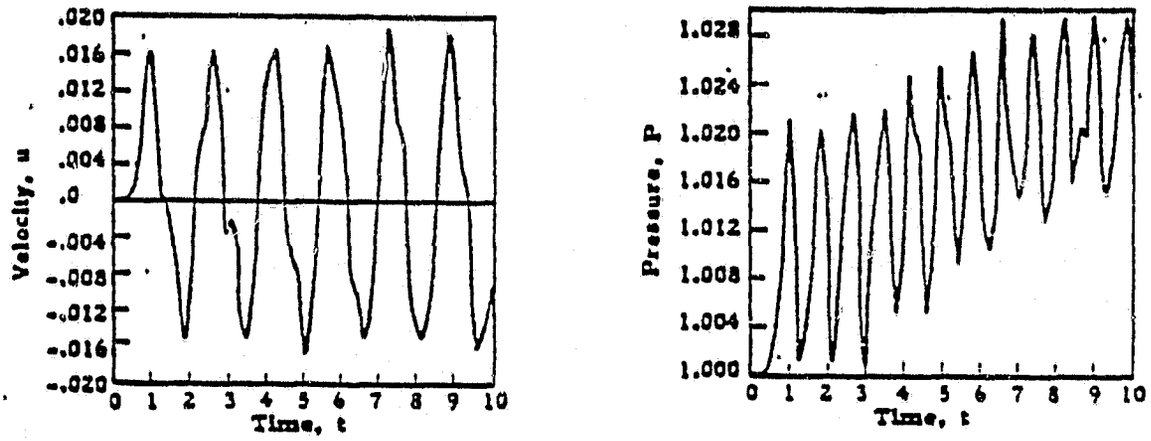

Figure 4-6 VELOCITY AND PRESSURE PROFILES OF THERMAL ACOUSTIC OSCILLATIONS (SPRADLEY)

This figure shows the calculated dimensionless velocity and pressure profiles as a function of time at the center between the two plates. This figure also shows the oscillatory nature of the wave motion. The period of the calculated wave is 1.55 units of dimensionless time which corresponds to the acoustic wave period in this system (which is $2/\sqrt{\gamma}$ or 1.55); thus, the calculated waves are acoustical. This analysis also shows that thermally induced wave motion can greatly increase the heat transfer over the pure conduction mode. A general numerical technique and computer program was developed for solving the nonlinear conservation equations governing the thermally induced waves. Complete profiles of temperature, pressure, gas velocity and heating rate can be obtained. This work formed the basis for the following Lockheed study of thermal acoustic oscillation in tubes connected to low temperature apparatus.

L. W. Spradley, W. H. Sims and C. Fan (1975) (Reference 18). This study was conducted by Lockheed-Huntsville Research and Engineering Center for NASA/MSFC.

A thermal acoustic oscillation program (TAO) based upon the numerical solution of the Navier-Stokes equations was developed as the principal analytical tool for this study.

An experimental verification program was conducted in conjunction with the analytical model development. A liquid helium research dewar was used for the experimentation. Stainless steel and aluminum tubes having length-to-diameter ratios from 100 to 1,000 were used as the test penetrations. Measurements were made for oscillation frequency,

amplitude and boil-off rate for a matrix of tube sizes, materials and distances of the tube in the dewar. The data were reduced and compared with results of the analytical predictions.

The oscillating system modeled consisted of a cylindrical tube closed at the warm end and open at the cold end. The tube was filled with helium gas whose cold end was at liquid helium temperatures.

A stability diagram for helium was constructed by processing many cases with the TAO Program in which the T_h/T_c ratio and the Δ parameter were varied (Figure 4-7). The Δ parameter is based upon the acoustic Reynolds number which was evaluated at the cold end temperature, and may be correlated with dimensionless parameters used in Rott's stability analysis. For comparative purposes, the stability curve generated from Rott's analysis is superimposed on Figure 4-7 (solid line).

Other theoretical correlations derived from the TAO Computer Program were:

1. Pressure amplitude versus L/D and T_h/T_c
2. Oscillation frequency versus L/D.
3. Oscillation intensity versus L/D.
4. Heat leak ratio versus L/D and pressure amplitude.

Figure 4-8 is the plot of peak-to-peak pressure amplitude versus L/D for parametric values of l_c/L. The pressure amplitude is shown to increase linearly with increasing L/D for all values of l_c/L. The effect of temperature ratio (T_h/T_c) on the pressure amplitude is illustrated in Figure 4-9. This shows that the amplitude decreases with decreasing T_h/T_c for all values of L/D, going to zero at the critical T_h/T_c.

The oscillation frequency is shown in Figure 4-10 for the parametric variations of L/D and l_c/L. The frequency decreases with L/D as would be expected since the longer tubes produce lower frequency oscillation than the shorter ones. The frequency was found to be nearly independent of the temperature ratio, T_h/T_c.

The oscillation intensity (defined as the product of the frequency and the amplitude) is shown as a function of L/D and l_c/L in Figure 4-11. The pressure amplitude always

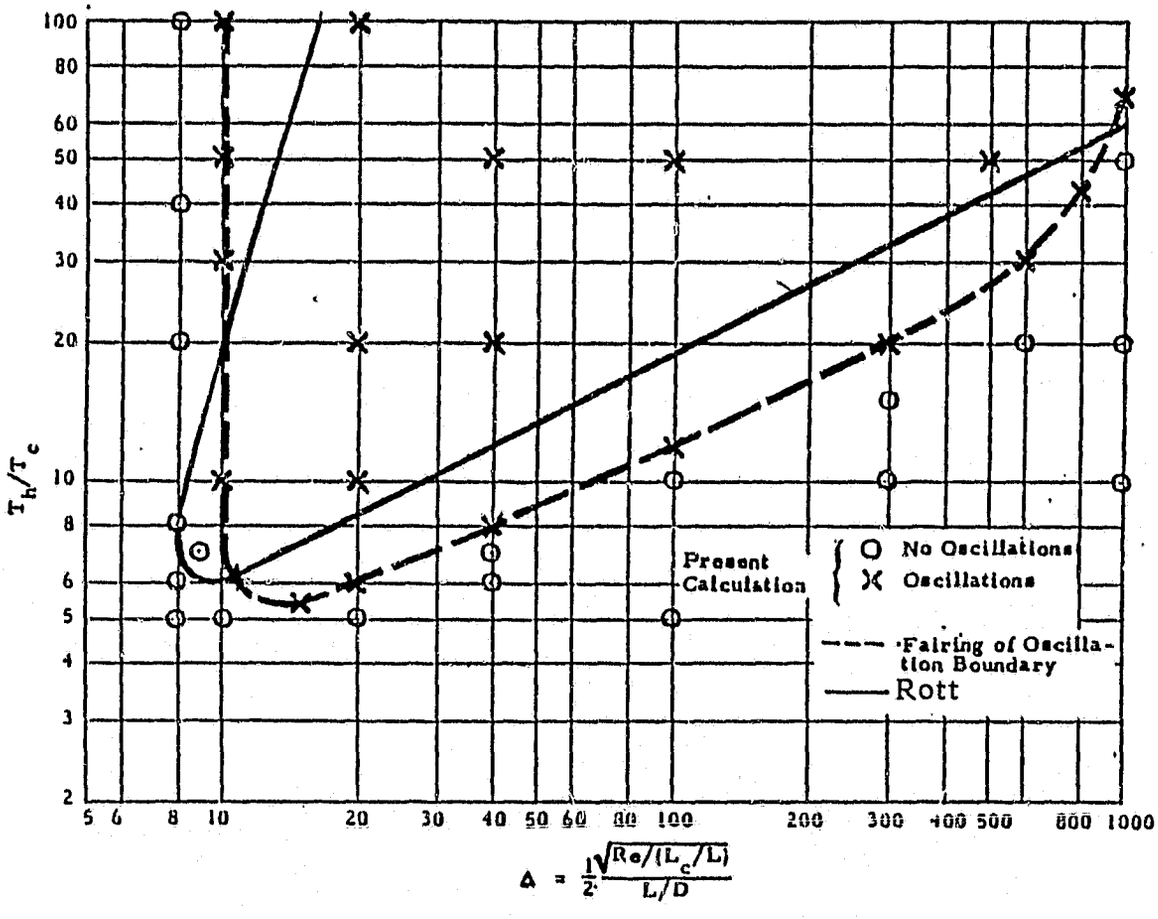

Figure 4-7 STABILITY LIMIT FOR HELIUM, COMPARISON OF SPRADLEY (Reference 18) AND ROTT (Reference 15)

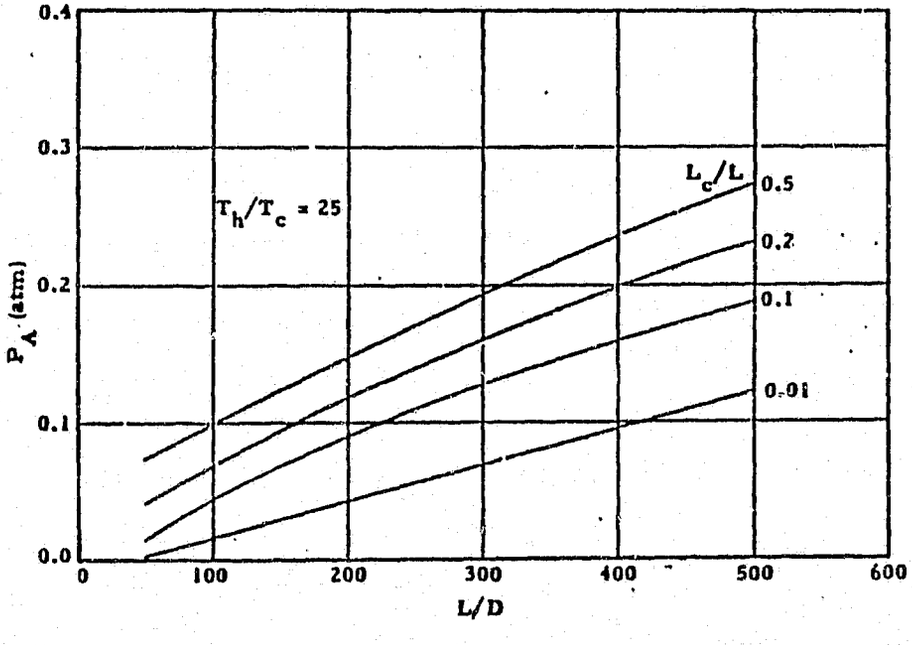

Figure 4-8 PRESSURE AMPLITUDE VERSUS LENGTH-TO-DIAMETER RATIO FOR VARIOUS COLD LENGTH-TO-TOTAL LENGTH RATIOS

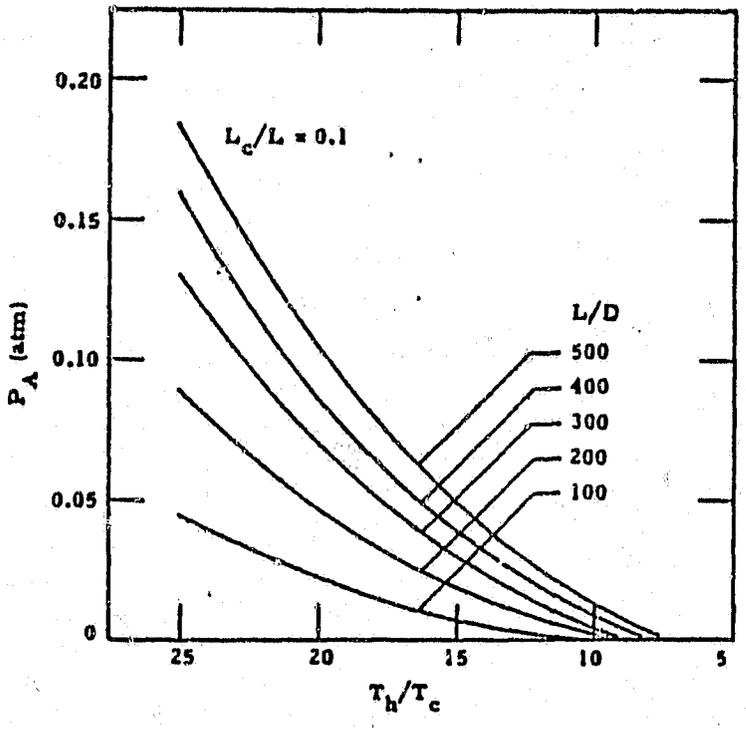

Figure 4-9 PRESSURE AMPLITUDE VERSUS T_n/T_c FOR VARIOUS L/D RATIOS

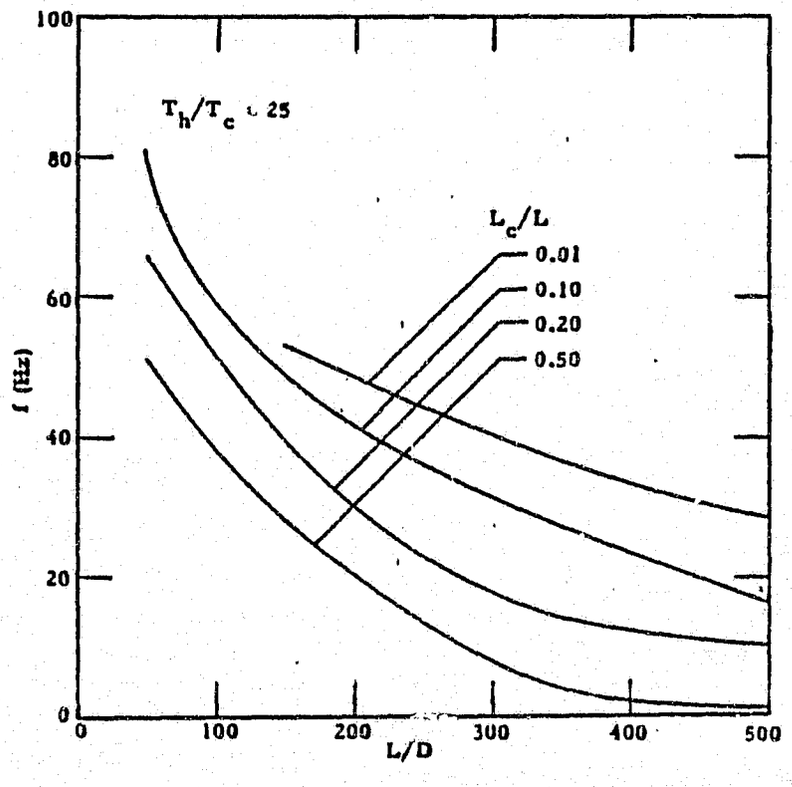

Figure 4-10 OSCILLATION FREQUENCY VERSUS L/D RATIO FOR VARIOUS l_c/L RATIOS

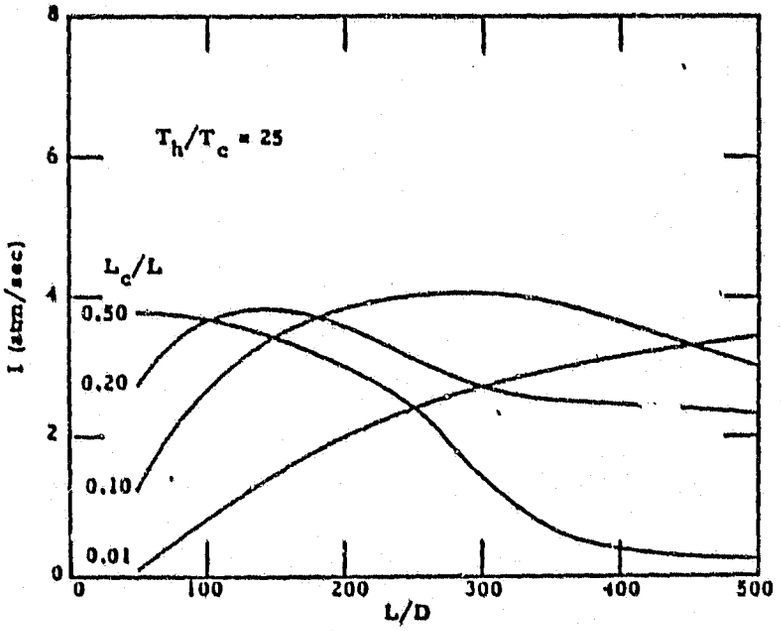

Figure 4-11 OSCILLATION INTENSITY VERSUS L/D RATIO FOR VARIOUS l_c/L

increases with increasing L/D and the frequency decreases with increasing L/D. The product will then either increase or decrease, depending on the slope of the frequency and amplitude variations. If the pressure amplitude increases faster than the frequency decreases, the intensity will increase (and vice versa).

Figures 4-12 and 4-13 relate the increased heat transfer due to thermal oscillations with the L/D ratio and the pressure amplitude. The quantity Q is the total heat pumped by the oscillations plus the conduction in the tube wall. The Q_t is simply the conduction heat leak down the tube wall.

Figure 4-12 shows that no additional heat leak was present for L/D less than about 75. If oscillations exist at an L/D of 75, the amplitude is so small that the additional heat transfer is negligible. However, the Q/Q_t ratio rises rapidly when tube L/D's exceed 100 with as much as an order of magnitude increase for L/D = 200 and over 2 orders of magnitude above L/D = 450.

Figure 4-13 is a cross plot of the Q/Q_t ratio versus pressure amplitude for $l_c/L = 0.1$. The curve was typical for all parametric values of l_c/L. The increase in Q/Q_t with increasing

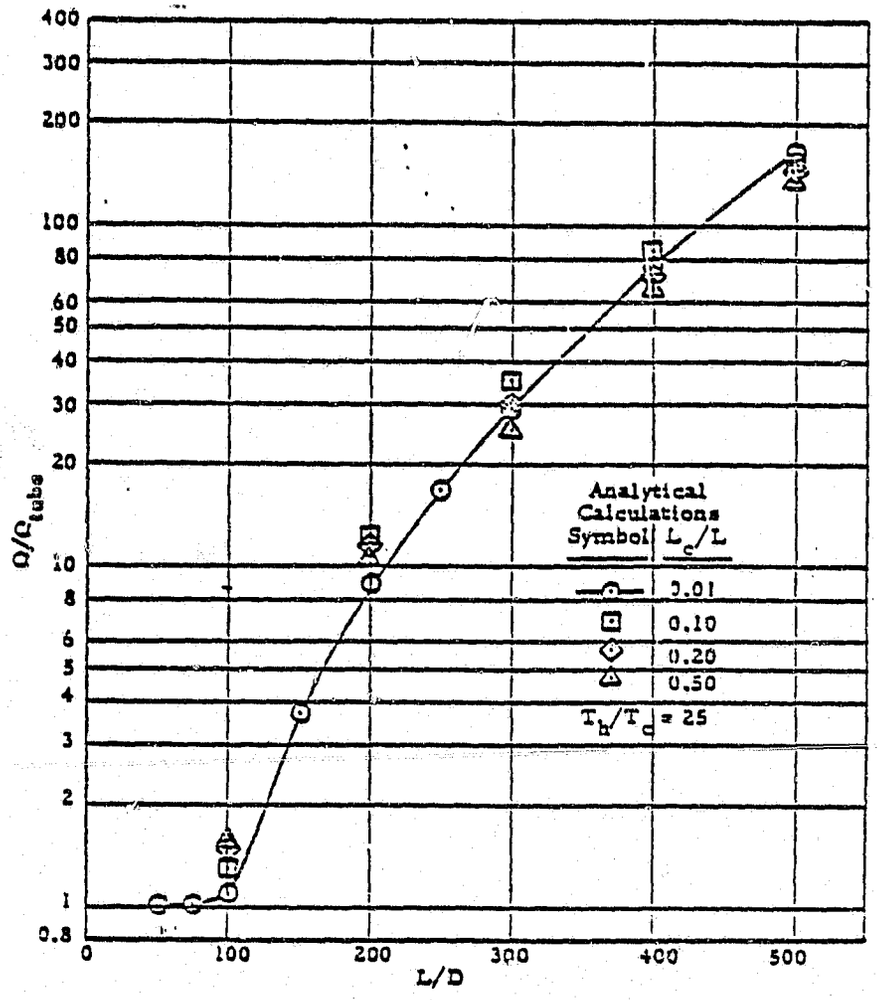

Figure 4-12 RATIO OF TOTAL HEAT LEAK (OSCILLATING) TO CONDUCTION HEAT LEAK VERSUS L/D RATIO

amplitude is due to the larger amount of mass pumped out of the tube by the larger amplitude pressure waves.

N. Rott (1975) (Reference 19). Rott presented a paper in which he calculated the second-order heat flux (thermo-acoustic streaming) for thermally driven acoustic oscillations. By using a generalization of his basic theory of thermal acoustic oscillations to the case of variable wall temperature, he was able to obtain the second-order energy equation without the restriction to thin boundary layers. From this theory, Rott was able to calculate the maximum heat flow carried by the oscillations into the dewar. Calculation

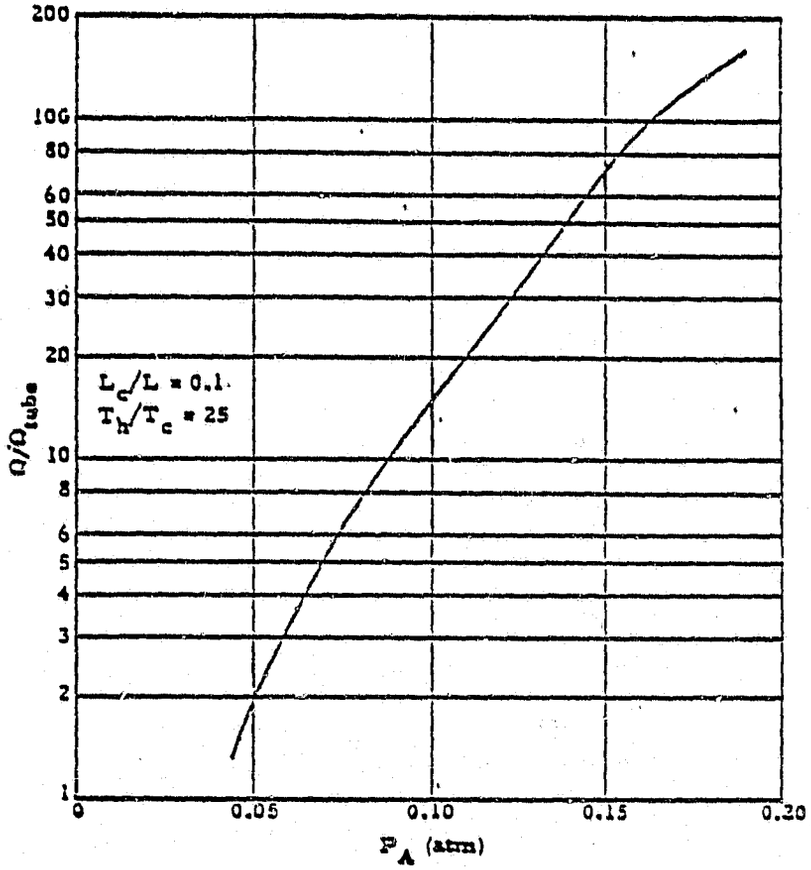

Figure 4-13 RATIO OF TOTAL HEAT LEAK (OSCILLATING) TO CONDUCTION HEAT LEAK VERSUS PRESSURE AMPLITUDE

of the thermo-acoustic streaming appeared to be satisfactory when conducted up to the second order of the temperature gradients used; it was doubtful whether the theory would converge in the limit of very sharp temperature gradients.

Yu. P. Dmitreoskiy and Yu. M. Melnik (1976) (Reference 20). The authors presented experimental data on the dependence of the thermal acoustic oscillation frequency upon the height of a liquid column in tubes dipped into nitrogen, oxygen, argon and hydrogen. The conditions under which these oscillations occur were found and the oscillation amplitudes were measured. They made attempts to observe thermal-acoustic oscillations with a gas column of nitrogen and oxygen with the help of sensitive equipment.

N. Rott (1976) (Reference 21). In his initial publications, Rott derived the stability limit for thermally driven acoustic oscillations in tubes of constant cross-section.

The applications were restricted to the case of tubes filled with helium gas. It was found that for "optimal" conditions, excited oscillations of He in a tube of constant cross-section need a minimum ratio of the absolute temperatures between the hot and the cold end of about 5.5. In this paper, Rott investigated the problem of thermally driven acoustic oscillations for tubes with variable cross-section, with particular emphasis on the possible reduction of the necessary temperature ratio for excitation. Tubes with optimal conditions in the vicinity of the temperature jump, and with large cross-sections in parts with constant temperature are found to give the best performance in this respect. Included in the family of devices which were treated is the classical Sondhauss tube. Experiments which give a striking confirmation of the theory were reported. The treatment of the different gases in tubes of constant cross-section as a special case was a by-product of this work.

D. E. Daney, P. R. Ludtke and M. C. Jones (1977) (Reference 22). This study was undertaken as an exploratory study for the design of leads for superconducting power transition line terminations. These current leads were cooled with supercritical helium. Four distinct lead designs were studied encompassing a wide variation in flow characteristics. The effects of the thermodynamic state of the helium and the hydraulic diameter of each lead were in agreement with the theoretical predictions of Rott for simple tubes.

T. Yazaki, A. Tominaga and Y. Narahara (1979) (Reference 23). In this paper, the authors determined experimentally the stability limit for thermally driven acoustic oscillations for helium gas. Instead of a half open tube, two stainless steel U-shaped tubes of different lengths and diameters closed at their top ends were used. The warm end reservoir was controlled with heaters at either 77.3°K or 300°K; temperatures at the cold end could be varied from 4.2°K to 45°K. The Stokes boundary thickness could be varied by changing the density (pressure) in the closed tubes. The theoretical stability curves predicted by N. Rott are shown in Figures 4-14 and 4-15 by the solid lines. Superimposed upon these figures are the experimentally determined stability limits determined by the authors confirming the existence of the two branches of Rott's stability curve. The solid and open circles represent warm end temperatures of 77.3°K and room temperature, respectively.

J. A. Liburdy (1979) (References 24, 25 and 26). Liburdy presented an analysis for the occurrence of thermal acoustic oscillations in gaseous helium, laminar tube flow. The analysis is based upon Rott's first two papers to which the author added a net flow term.

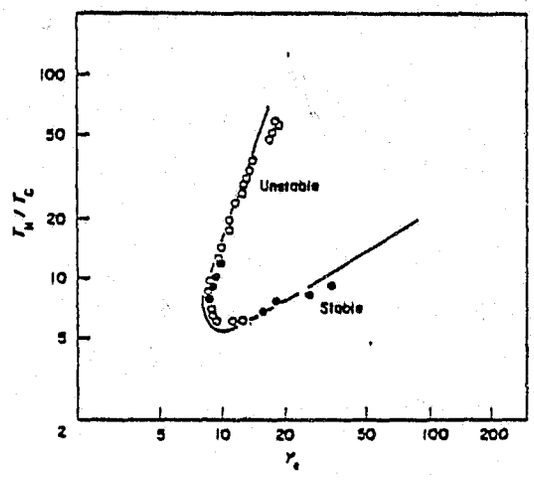

Figure 4-14 DATA OF T. YAZAKI, et al., COMPARED WITH ROTT'S STABILITY LIMIT FOR 2.4-mm ID TUBE

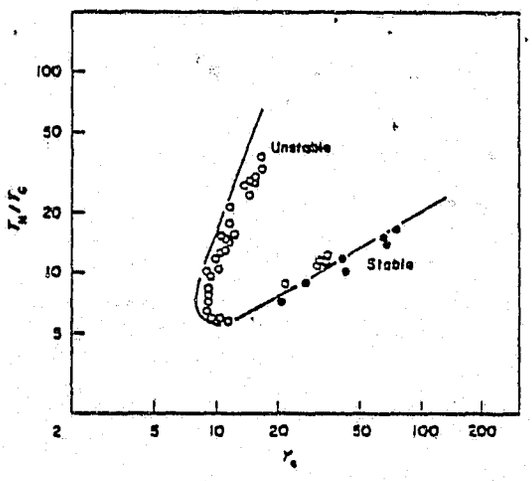

Figure 4-15 DATA OF T. YAZAKI, et al., COMPARED WITH ROTT'S STABILITY LIMIT FOR 4.4-mm ID TUBE

His results are shown by Figure 4-16 where the parameter Γ_c is the ratio of the mean flow velocity to the cold end acoustic velocity. These results indicate that even a substantial flow rate has no effect on the stability curve, except in the region of the upper branch in which the temperature ratios are not normally experienced.

4.2 Analytical Model Discussion. The work presented by Liburdy (References 24, 25 and 26) is essentially the analytical method developed by Rott (References 14 and 15) with the inclusion of a mean flow term. Figure 4-17 is the stability limit, developed by Liburdy, for $\S=1$ for various nondimensional flow velocities. Γ is defined as the ratio of the mean flow velocity to the cold end acoustic velocity $\left(\frac{\dot{m}}{2\pi r_o^2 a_c \rho}\right)$. A quick calculation of the nondimensional velocity for this study reveals that Γ ranges from 0 (no flow) to approximately 28. For the relatively low values of α ranging from 7 to 12, and values of Y_c of 38 to 254 indicate that the effect of Liburdy's mean flow term is negligible. These curves were developed for subcritical helium; however, discussions with Dr. Liburdy indicate that the same negligible effect of low flow rates should exist for hydrogen. Based upon these observations, a decision was made to use the analysis

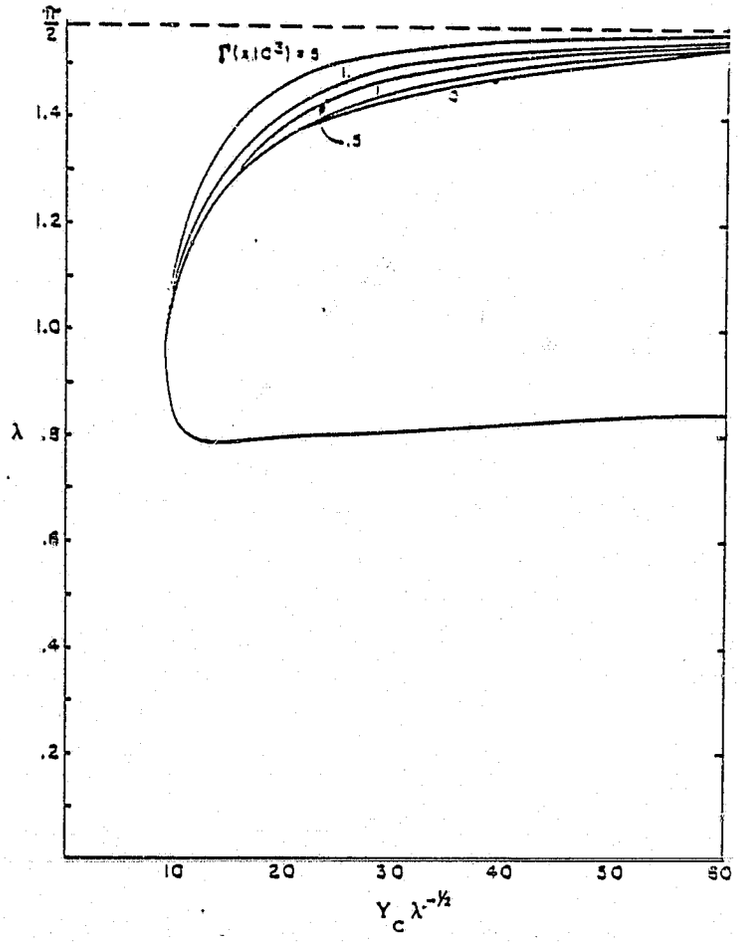

Figure 4-16 FREQUENCY PARAMETERS λ_c AND $Y_c \lambda_c^{-1/2}$ FOR HELIUM AT LOW MACH NUMBERS

developed by Rott. Inasmuch as the mean flow term has negligible effect, any correlation of the data with Rott's analysis should also apply to Liburdy's model. The following paragraphs contain a discussion of Rott's method as it applies to this study.

As mentioned in Section 4.1, Rott examined thermally driven oscillations and presented an analysis which makes use of linear nature of the governing equations with the inclusion of second order viscous effects. Previous works were based on boundary layer assumptions for flow in a pipe, whereas Rott based his analysis on the long tube constraint which, simply stated, requires the tube length to be much larger than the tube radius. The long tube assumption is met with considerable ease for the PRSA Hydrogen Tank lines with effective length-to-diameter (L/D) ratios of approximately 50, 130 and 150 for the vent, fill and supply lines, respectively. The models presented by Rott and Liburdy consist of piecewise approximate solutions of the governing equations for two constant temperature tube sections. The tube sections are assumed to exist at the cold or hot temperature. The solutions are then matched by requiring the hot and cold pressures and pressure

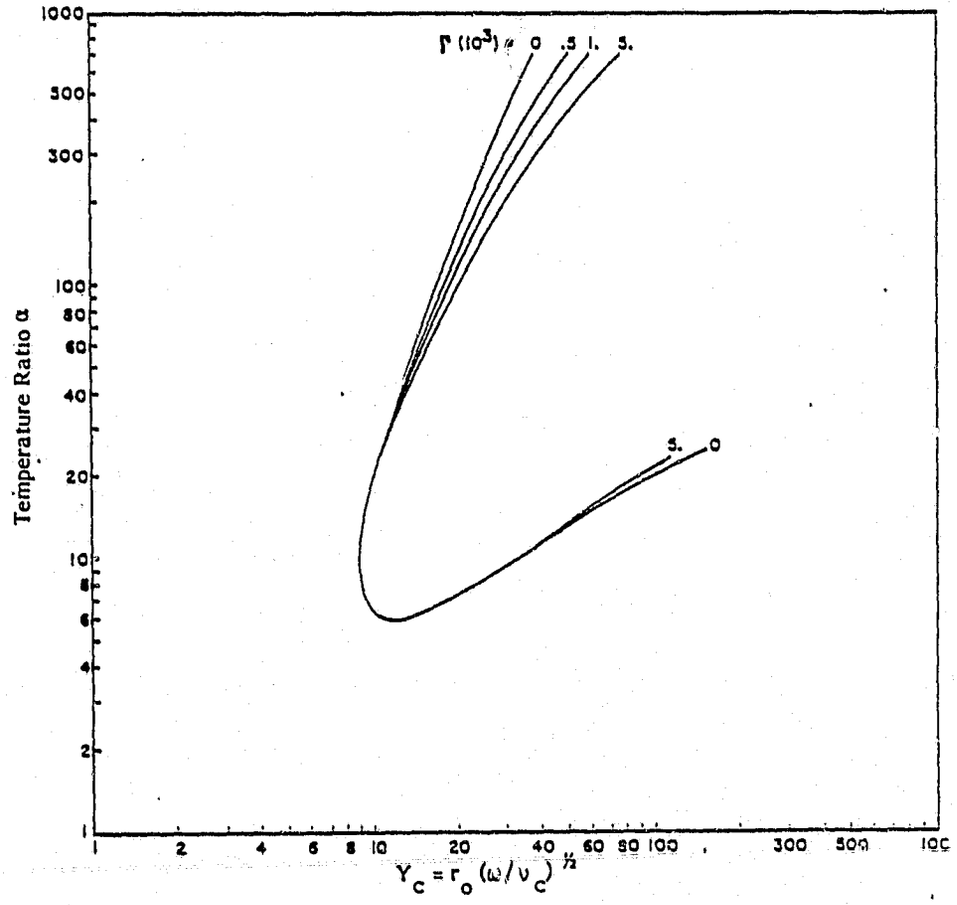

Figure 4-17 TEMPERATURE RATIOS VERSUS Y_c AT THE STABILITY LIMIT FOR LOW VELOCITY FLOW

gradient to be equal at the temperature jump. Figure 4-18 illustrates the "idealized temperature jump" for the PRSA Hydrogen Tank conditions. This figure also contains sketches of the temperature profile for the fill and supply lines. Note the supply line forms the VCS which explains the long sloping section to its temperature profile. The cold tube length of l and the hot tube length of L-l are also shown in Figure 4-18.

While the supply and fill line temperature profiles are not similar to the idealized profile, Rott (Reference 15) examined the application of his analysis to nonideal temperature profiles. He defined the steepness which is given in Equation 4-1.

$$S = \frac{2l}{T_h - T_c} \left(\frac{dT}{dx}\right)_{x=l} \qquad \text{Equation 4-1}$$

He indicates that the effect of steepness on the temperature ratio of stability limit is not very large. He based his conclusion on calculations made for steepness values ranging from 5 to ∞, where the effect on the temperature ratio was from 24 to 21.

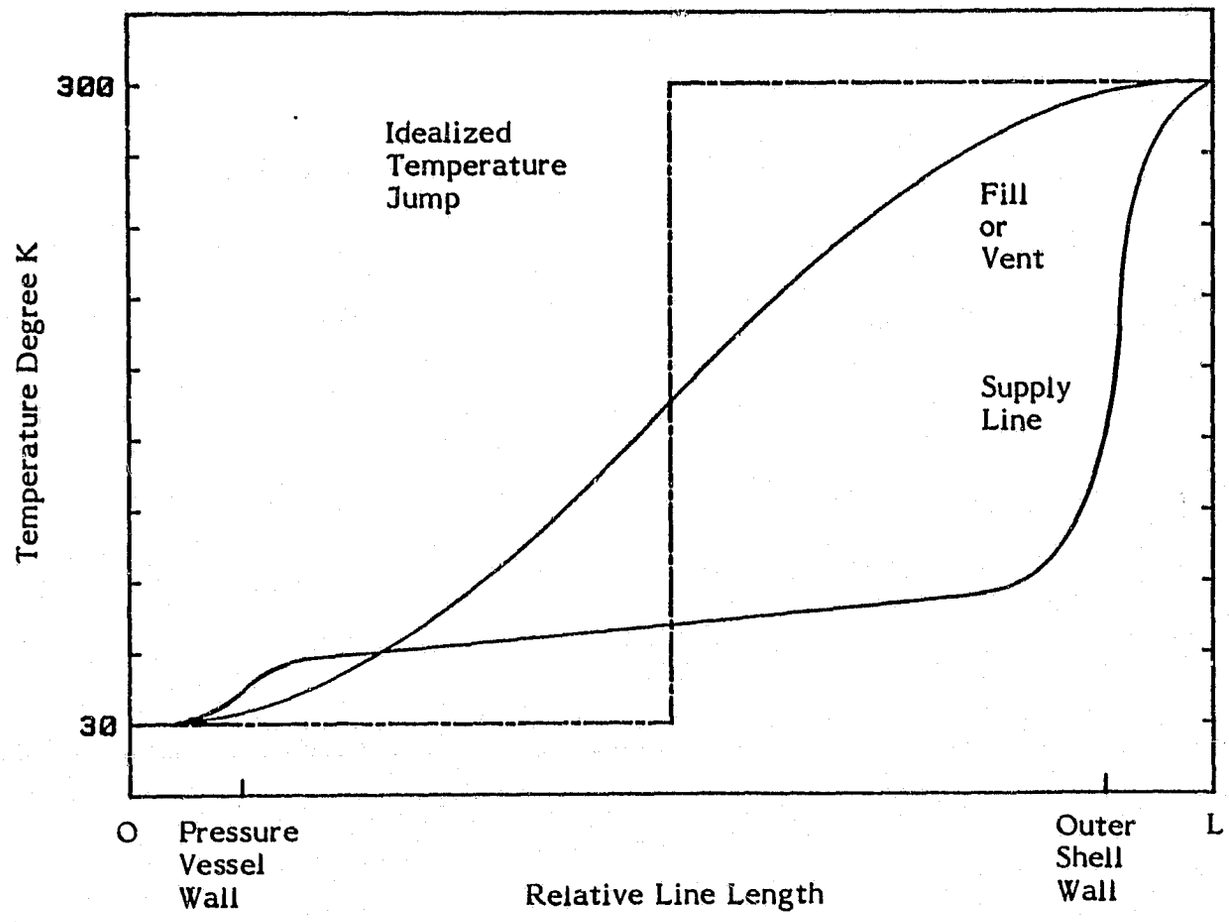

Figure 4-18 FLOW LINE REPRESENTATIVE TEMPERATURE PROFILES

The work by Rott and Liburdy makes use of a power-law kinematic viscosity curve given by Equation 4-2.

$$\nu = \frac{\mu}{\rho} = T^{(1+\beta)} \qquad \text{Equation 4-2}$$

For helium, the work conducted by Rott, this relationship fits very well; however, for hydrogen and, in particular hydrogen at the PRSA operating conditions, some difficulty is involved in determining the appropriate value of β. In addition to β, the analysis utilizes a constant ratio of specific heat (γ) and Prandtl number (Pr). Again for hydrogen at the PRSA tank operating conditions, the appropriate value is difficult to determine. This problem is best shown by examining Figure 4-19, which contains plots of the kinematic viscosity, ratio of specific heats, acoustic velocity and Pr number for 1.9 M Pa (280 psia),

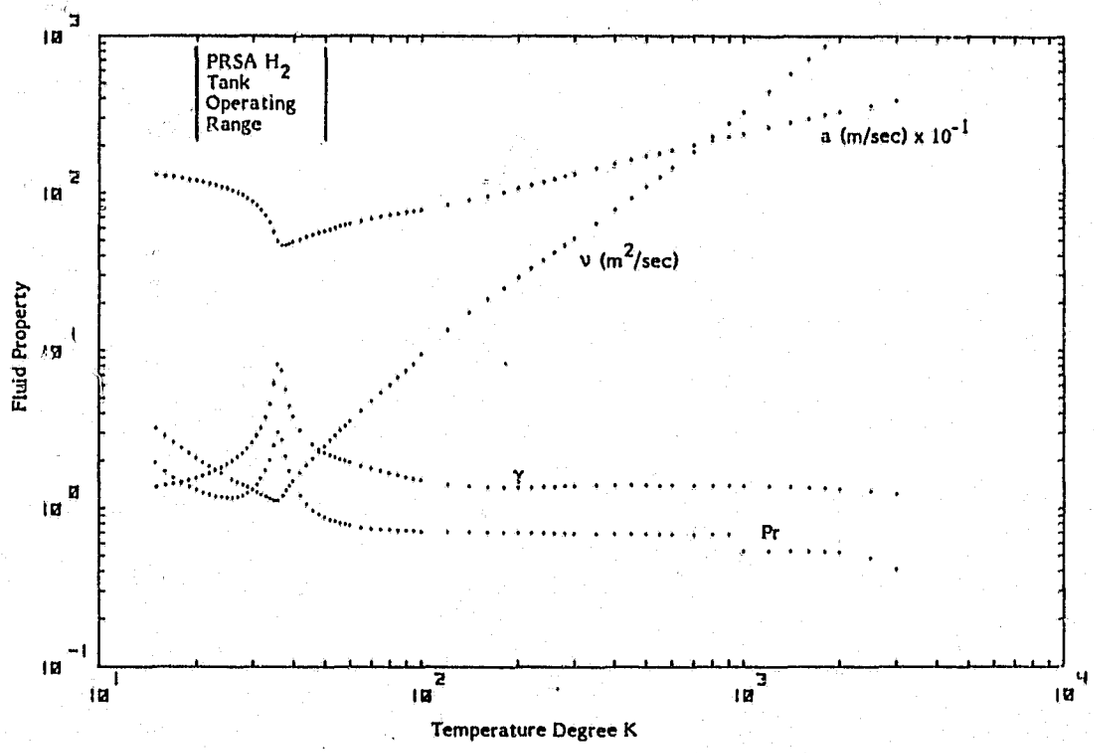

Figure 4-19 HYDROGEN PROPERTIES FOR 1.9 MPa (280 psia)

the PRSA tank operating pressure. This figure also indicates the PRSA Hydrogen Tank operating temperature range. Note the behavior of properties in this range; in particular the viscosity curve as it applies to the power-law equation. For this study, the following values of $\beta = .823$, $\gamma = 1.42$ and $Pr = .71$ were used for hydrogen at 1.9 M Pa.

With the use of the power-law viscosity curve and the linearized governing equations, Rott proceeded to solve for the stability limit. Figures 4-20 and 4-21 represent the stability curves developed by Rott (Reference 15). The curves are plotted for the temperature ratio versus the dimensionless parameter Y_c. Figure 4-20 contains the stability limit for small values of $\S = (L - l)/l$, ratio of hot-to-cold length ranging from .1 to 1. The stability curves for larger values of § are contained in Figure 4-21, where § ranges from 2 to 50. The dotted lines in Figures 4-20 and 4-21 represent the asymptotic curves. The agreement for moderate values of § is quite good, while for larger values of §, the agreement is poor. The asymptotic values were determined by Rott (Reference 15) for the lower or right-hand branch of Figure 4-20. Equation 4-3 produces the lower branch asymptotic curves.

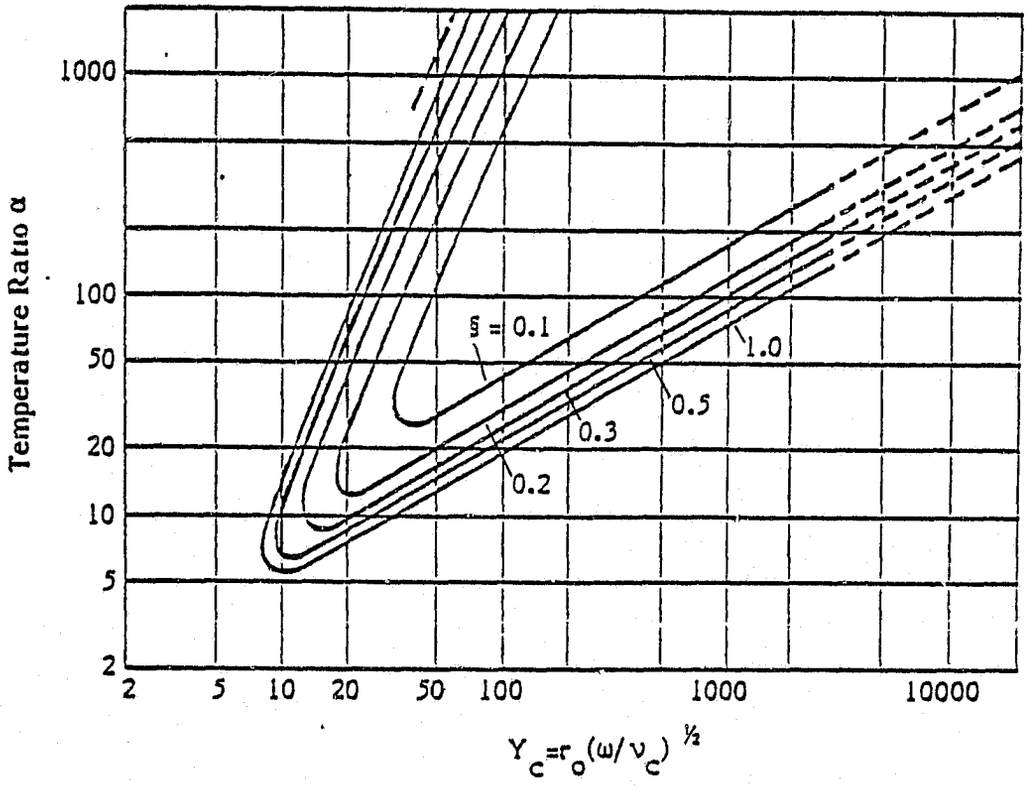

Figure 4-20 STABILITY LIMIT FOR HELIUM, TEMPERATURE RATIO VERSUS Y_c FOR SMALL §

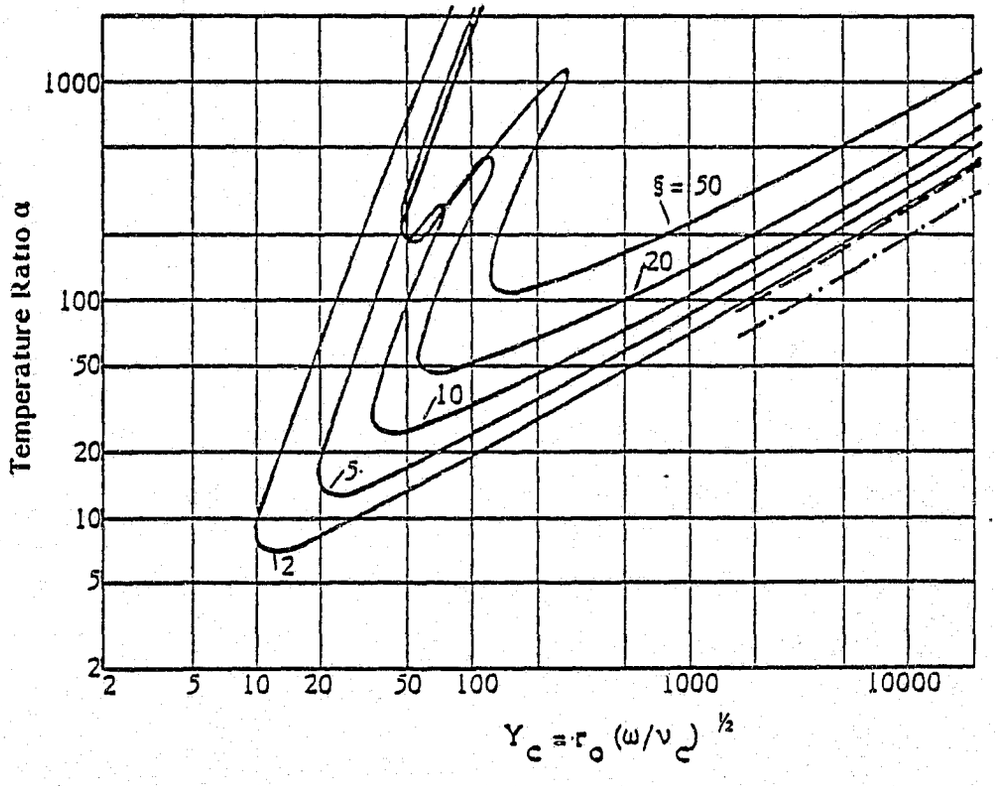

Figure 4-21 STABILITY LIMIT FOR HELIUM, TEMPERATURE RATIO VERSUS Y_c FOR LARGE §

$$Y_c = 2D\,(1 + \S^{-1} + \lambda_c^2\,\S)^{-1}\,\alpha(1+\beta) \qquad \text{Equation 4-3}$$

where:

$$D = d^*\sqrt{2/C}$$

$$C = 1/2\,(1 + \frac{\gamma-1}{\sqrt{Pr}})$$

$$d^* = 2C^2 - C + 1/2\,(d - d^2) + d'$$

$$d = (\frac{1}{1+\beta})(\frac{2}{Pr+\sqrt{Pr}}) - \frac{\gamma-1}{\sqrt{Pr}}$$

$$d' = \frac{1}{4\,Pr}\,(\gamma - 1 - \frac{1}{1+\beta})$$

The significance of the earlier discussion on hydrogen properties becomes more apparent as the stability criteria is dependent on γ, β and Pr. The dotted lines on the lower branch of Figures 4-20 and 4-21 were determined by the use of Equation 4-3 with the values for helium of .647, 5/3 and 2/3 used for β, γ and Pr, respectively. For this study, the lower branch is the section of the stability curve of interest since it corresponds to the lower values of Y_c and α which the PRSA Hydrogen Tank exhibits. The asymptotic stability limit was determined for hydrogen by use of Equation 4-3 by evaluating it with the values of β, γ and Pr, as previously mentioned in this section, of .823, 1.42 and .71, respectively. In order to evaluate Equation 4-3, a relationship between λ_c and $\S$ must be known for the stability limit. Rott (Reference 15) presents just such a relationship in Equation 16 of Reference 15 which is given in Equation 4-4.

$$\S\,\lambda_c \tan \lambda_c = 1 \qquad \text{Equation 4-4}$$

The solution to this transcendental equation is determined numerically and the results are given in Figure 4-22. This figure represents the relationship between λ and $\S$ for the lower branch when Y_c is large. Rott (Reference 15) presented the more complete frequency relationship by plotting λ_c versus a new dimensionless parameter $Y_c\,\lambda_c^{-1/2}$ which is defined by $r_o\,(a_c/\nu_c l)^{1/2}$. This parameter has the advantage of not requiring previous knowledge of frequency; this plot is reproduced in Figure 4-23. It should be noted that Equation 4-4 and its resulting solution, Figure 4-22, determine the lower branches of Figure 4-23, while the upper branch has a limit on λ of $\pi/2$. The lower branch of Figure 4-23 corresponds to the right-hand branch of Figures 4-20 and 4-21.

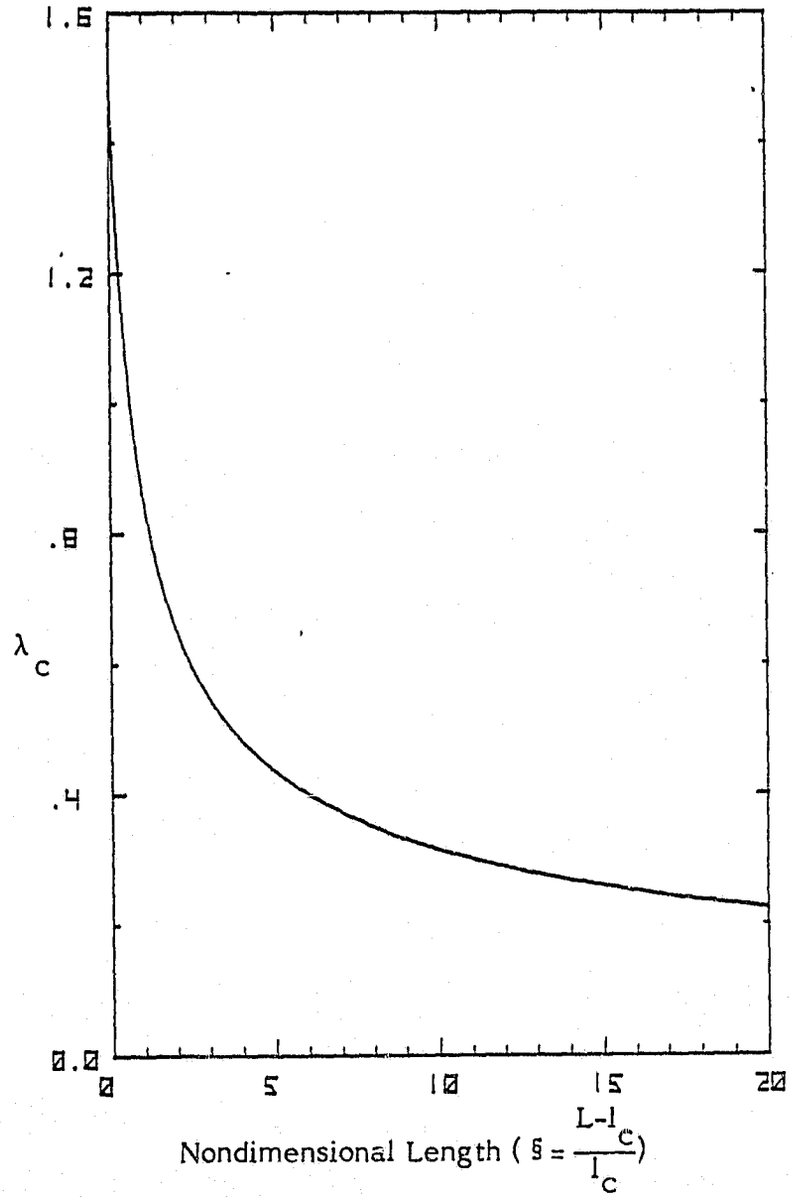

Figure 4-22 LOWER BRANCH ASYMPTOTIC VALUES OF NONDIMENSIONAL FREQUENCY VERSUS LENGTH

The asymptotic stability curves for hydrogen at 1.9 M Pa, the operating condition of the PRSA tank, are given in Figure 4-24 for values of § ranging from .5 to 10. By combining Equations 4-4 and 4-3, it is possible to create a stability criteria independent of frequency. The result of just such a combination is shown in Figure 4-25.

Figures 4-24 and 4-25 will make up the essential stability curves required for the PRSA data correlation.

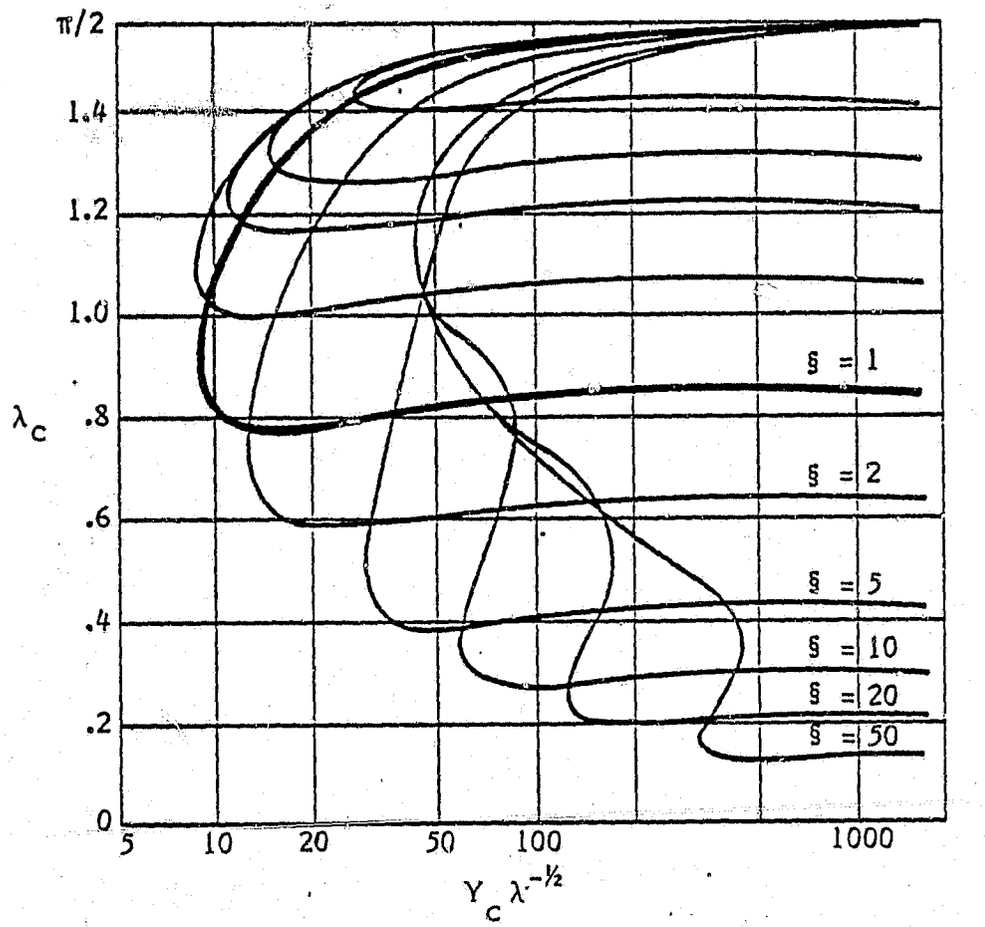

Figure 4-23 DIMENSIONLESS FREQUENCY PARAMETER l_c VERSUS $Y_c \lambda_c^{-1/2}$

4.3 Data Correlation. This section presents the comparison of PRSA supercritical Hydrogen Tank test data with the analytical models by Rott and Liburdy. As mentioned in Section 4.2, the work by Rott will be used due to the lack of effect of flow on the stability limit predicted by Liburdy. The data presented in Table 3-I and the stability curve presented in Figure 4-24 will be used for the test data and model comparison.

Figure 4-26 contains a plot of the stability curve produced in Figure 4-24 and selected oscillating data points from the PRSA test data. Only selected data points were included due to the number of points clustered on a small section of the plot. While, in general, the agreement with the predictions based on the work by Rott is poor, by far the most successful correlation appears for the supply line.

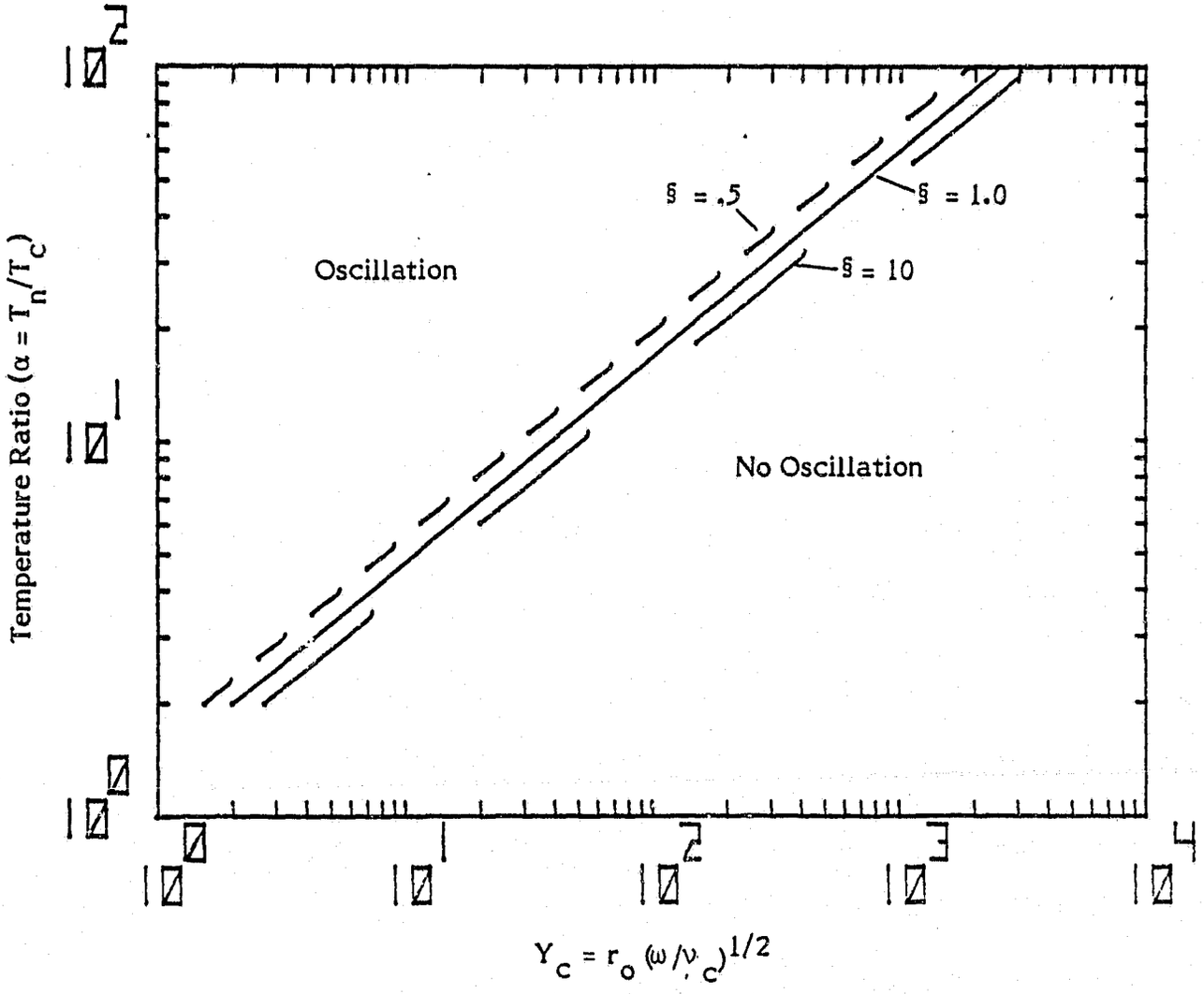

Figure 4-24 RIGHT-HAND BRANCH ASYMPTOTIC STABILITY CURVES FOR HYDROGEN, TEMPERATURE RATIO VERSUS Y_c

The selection of which curve (value of §) the correlation should be made on warrants some discussion. Since § represents the hot-to-cold length ratio of the fluid line in question, it becomes necessary to attempt to determine these lengths. No test data is available to supply the temperature profile of the liquid lines; however, some limiting values are possible. If the fluid line interface with the outer shell is assumed to be a thermal short, a reasonable assumption, then the maximum cold length, which is the length of line to the mid point of the temperature gradient, is one-half the effective line length from the pressure vessel to the outer shell. For the fill and vent lines, this is 1.9 m and .9 m, respectively. The supply line presents a more interesting case. Figure 4-18 illustrates conceptually the temperature profile for the supply line. The temperatures shown are

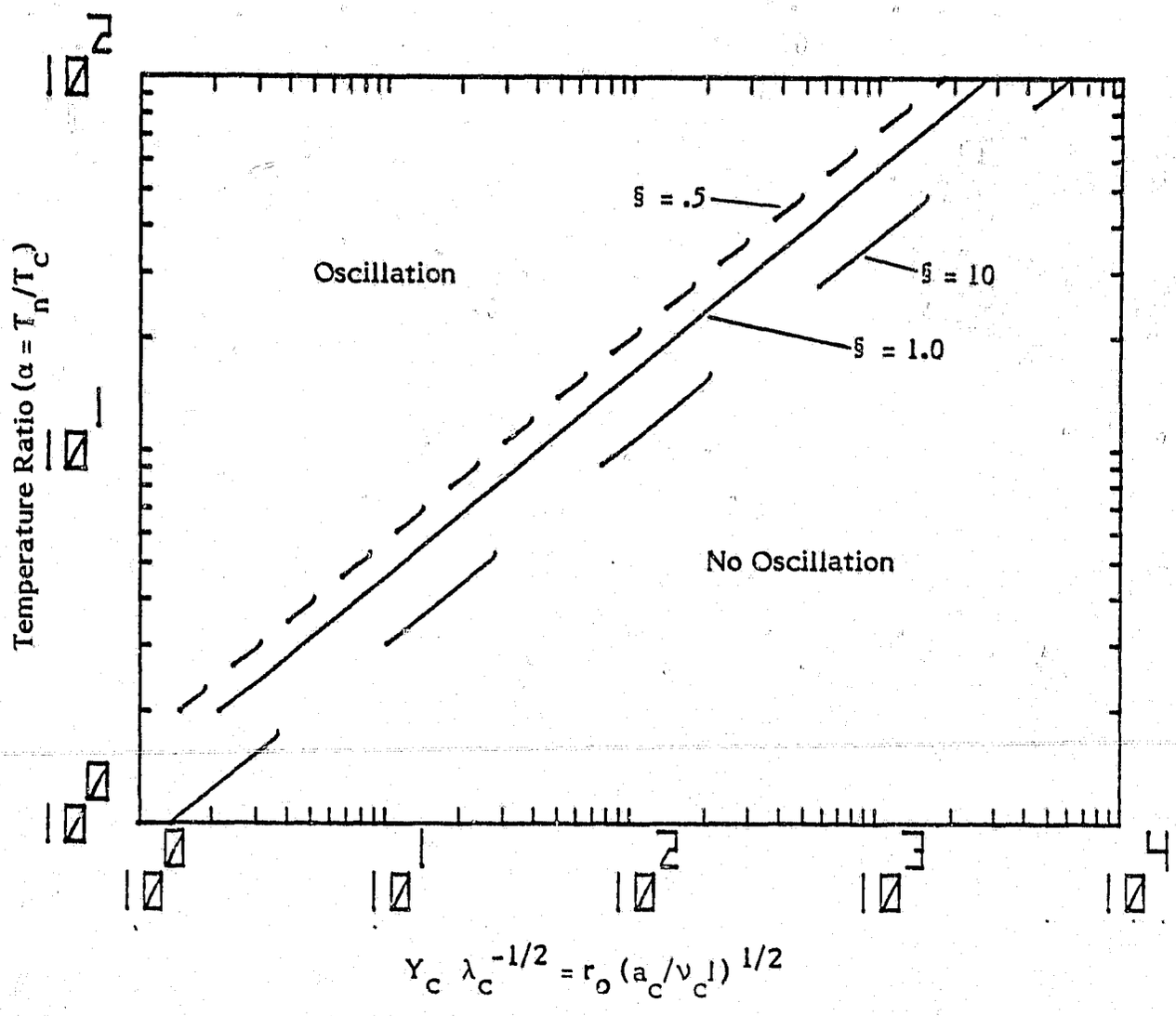

Figure 4-25 RIGHT-HAND BRANCH OF STABILITY CURVE FOR HYDROGEN, INDEPENDENT OF FREQUENCY

typical operating conditions for the PRSA Hydrogen Tank. Based upon these temperatures, a temperature ratio of approximately three exists for both temperature jumps. This presents a difficulty in determining whether one jump is dominant or the effect is compounded. The determination was made that the effect was one of a net temperature ratio of six; i.e., treat the double jump as a single temperature jump. This decision is verified by the prediction that, for helium, a temperature ratio of at least 5.5 was required to sustain oscillations. A similar value of approximately five is required for hydrogen as well. With this, the supply line cold length can be approximated as one-half the line length of the VCS, plus the line length internal to the pressure vessel. This results in an approximate cold length of 8.0 m for the supply line.

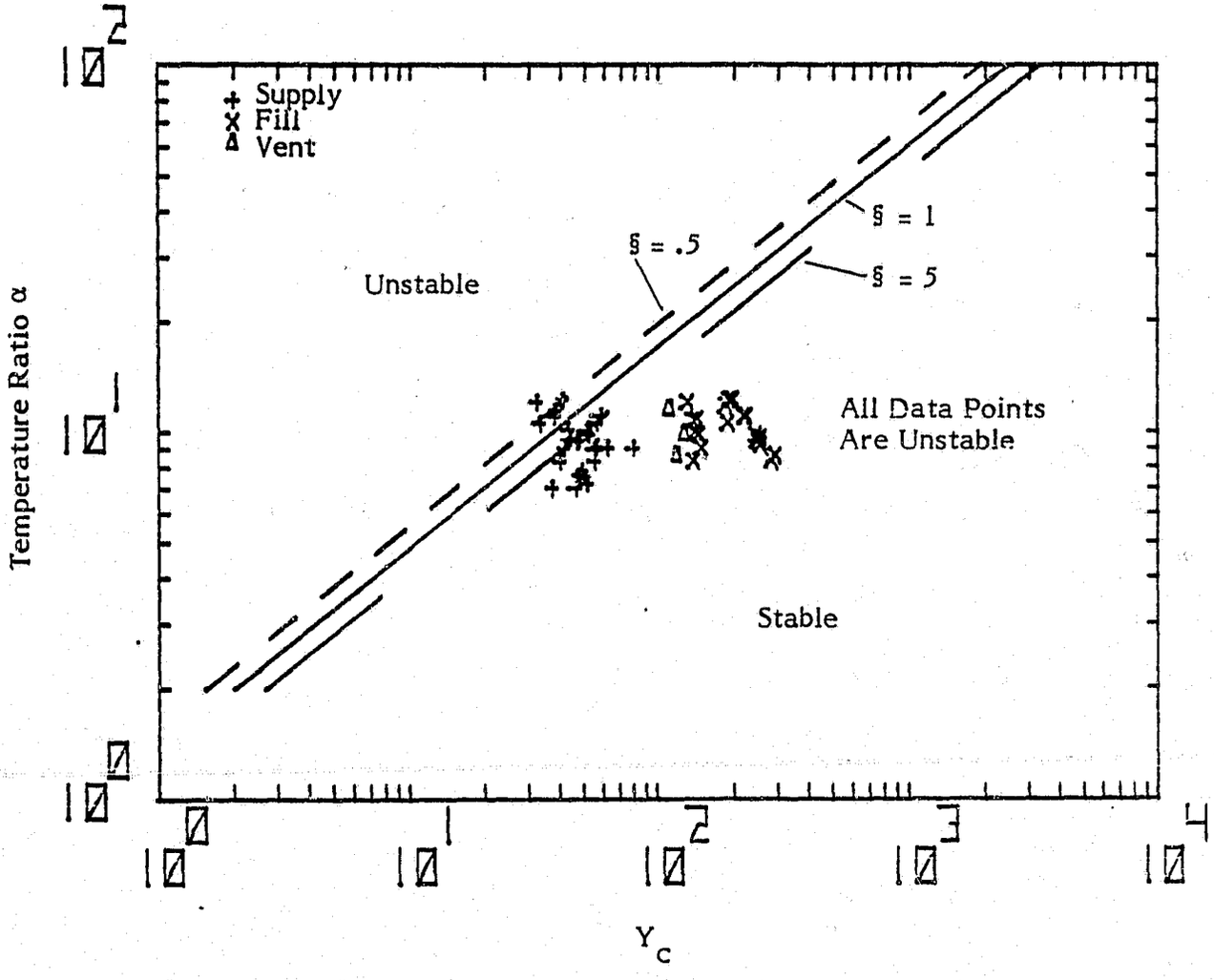

Figure 4-26 COMPARISON OF PRSA HYDROGEN TANK TEST DATA WITH THE ANALYTICAL PREDICTIONS BY ROTT

With the cold lengths presented here and the external line lengths presented in Figures 2-1 through 2-17, the values of § between 1 and 10 are reasonable.

5.0 CONCLUSIONS AND RECOMMENDATIONS

The correlation between the PRSA Hydrogen Tank test data and the analytical model by Rott must be examined in light of the following comments:

1. Supercritical hydrogen properties result in poor agreement with constant Pr number, and a power-law kinematic viscosity law.

2. Determination of actual cold fluid line lengths was prevented by a lack of instrumentation. This presents uncertainties in evaluating the proper stability curve.

3. The relatively small steepness ratio raises the question as to the validity of the discontinuous temperature jump where the temperatures are assumed constant on both sides of the jump. As the length of the temperature gradient increases, validity of this assumption decreases.

The small variation in temperature ratios and other critical oscillation parameters makes any conclusions as to the verification of the analytical models impossible. The difficulty in applying the model by Rott or Liburdy to an existing production PRSA Hydrogen Tank suggests more intensive study of the thermal acoustic oscillation phenomena is warranted.

Future work must include not only work dealing with subcritical hydrogen, but also supercritical hydrogen. It is suggested that work be initiated in a test dewar instrumented for the study of thermal acoustic oscillations. This should result in sufficient data to initiate a study of oscillations in production cryogenic tanks. Where the effect of nonidealized conditions may be studied, this would provide useful design information for future cryogenic storage facilities.

6.0 REFERENCES

1. Sondhauss, C., "Uber die Schallschwingunzen der Luft in erhitzten Glasrohren and in gedeckten Pfeifen von ungleicher Weite," Ann. Phys., Volume 79, 1980, Page 1.

2. Helmoltz, H. v., Verhandlungen des naturhistorisch-medizinischen Vereins zu Heidelberg vom Juhre, Bd. III, S. 16, 1863.

3. Kirchoff, G., Uber den Einfluss der Warmeleitung in einem Gas auf die Schalbewegumg, Pogg. Aun., Volume 134, Page 177, 1868.

4. Rayleigh, L., Theory of Sound, Volume II, MacMillan, London, 1940.

5. Taconis, K. W., et al., "Measurements Concerning Vapor-Liquid Equilibrium of Solutions of He^3 in He^4 Below 2.19°K, Physica, Volume 15, No. 8-9, Page 733, 1949.

6. Kramers, H. A., "Vibrations of a Gas Column, Physica, Volume 15, Page 971, 1949.

7. Clement, J. R., and Gaffney, J., "Thermal Oscillations in Low-Temperature Apparatus," Adv. Cryogen. Eng., Volume 1, 1954, Page 302.

8. Trilling, L., "On Thermally Induced Sound Fields," J. Acoustical Soc. Am., Volume 27, 1955.

9. Feldman, K. T., Jr., "A Study of Heat Generated Pressure Oscillations in a Closed End Pipe," PhD Dissertation, University of Missouri, Columbia, February 1966.

10. Bannister, J. D., "Spontaneous Pressure Oscillations in Tubes Connecting Liquid Helium Reservoirs to 300°K Environments, Bulletin Int. Institute Refrigeration, 1966-5, Page 127.

11. Norton, M. T. and Muhlenhaupt, R. C., NBS Technical Note 363, 1967.

12. Thullen, P. and Smith, J. L., Jr., "Model for Thermally Sustained Pressure Oscillations Associated with Liquid Helium," Advances in Cryogenic Engineering, Volume 13, Plenum Press, New York, 1968, Page 215.

13. Rogers, J., "Oscillations in Flowing and Heated Subcritical Hydrogen," Advances in Cryogenic Engineering, Volume 13, 1968.

14. Rott, N., "Damped and Thermally Driven Acoustic Oscillations in Wide and Narrow Tubes," ZAMP, Volume 20, 1969, Page 230.

15. Rott, N., "Thermally Driven Acoustic Oscillations, Part II: Stability Limit for Helium," ZAMP, Volume 24, 1973, Page 54.

16. Von Hoffmann, T., Lienert, T. and Quack, H., "Experiments on Thermally Driven Gas Oscillations," Cryogenics, 1973.

17. Spradley, L. W., "Thermoacoustic Convection of Fluids in Low Gravity," AIAA Paper No. 74-76, AIAA 12th Aerospace Sciences Meeting, Washington, DC, January 1974.

18. Spradley, L. W., et al., "Thermal Acoustic Oscillations," NASA CR-102776, March 1975.

19. Rott, N., "Thermally Driven Acoustic Oscillations, Part III: Second-Order Heat Flux," ZAMP, Volume 26, 1975.

20. Dmitreoskiy, Yu. P. and Melnik, Yu. M.

21. Rott, N. and Zouzoulas, G., "Thermally Driven Acoustic Oscillations, Part IV: Tubes with Variable Cross-Section, ZAMP, Volume 27, 1976.

22. Daney, D., et al., "Thermal Acoustic Oscillations in Current Leads Cooled with Supercritical Helium," IEEE Transactions on Magnetics, Volume MAG-13, No. 1, January 1977.

23. Yazaki, T., et al., "Stability Limit for Thermally Driven Acoustic Oscillation," Cryogenics, July 1979.

24. Liburdy, J. and Wofford, J., "Stability Criteria Governing Vent/Fill Lines of Cryogenic Storage Vessels," Final Report NASA Grant No. NS6-2272, June 1979.

25. Liburdy, J. and Wofford, J., "A Stability Criterion for the Occurrence of Thermally Induced Oscillations in Steady Laminar Flow," ASME Heat Transfer Division, 79-HT-74, August 1979.

26. Liburdy, J. and Wofford, J., "Acoustic Oscillation Phenomena in Low Velocity Steady Flow with Heating," Presented at Cryogenic Engineering Conference, August 1979.

27. McCarty, R. and Weber, L., "Thermodynamic Properties of Parahydrogen from Freezing Liquid Line to 5000°R for Pressures to 10,000 Psia," NBS Technical Note 617, April 1972.